

TECHNISCHE UNIVERSITÄT MÜNCHEN

Lehrstuhl für Ernährungsmedizin

The human metabolome under nutritional challenges in young men and subjects  
carrying risk alleles for obesity and diabetes mellitus type 2

Susanne Gabriele Krug

Vollständiger Abdruck der von der Fakultät Wissenschaftszentrum Weihenstephan für Ernährung,  
Landnutzung und Umwelt der Technischen Universität München zur Erlangung des akademischen  
Grades eines

Doktors der Naturwissenschaften

genehmigten Dissertation.

Vorsitzender: Univ.-Prof. Dr. M. Klingenspor

Prüfer der Dissertation: 1. Univ.-Prof. Dr. J. J. Hauner

2. Univ.-Prof. Dr. H. Daniel

Die Dissertation wurde am 08.05.2013 bei der Technischen Universität München eingereicht und  
durch die Fakultät Wissenschaftszentrum Weihenstephan für Ernährung, Landnutzung und Umwelt  
am 24.07.2013 angenommen.

*Meinen lieben Eltern*

# ACKNOWLEDGEMENT

The discoveries about my topic and the personal experiences made throughout the years of my dissertation could have never been achieved alone. Hence, I take the first page to thank those who helped me along the way.

This dissertation was accomplished at the Chair for Nutritional Medicine (TU München, Freising-Weihenstephan). First of all I want to thank Professor Hans Hauner for providing the opportunity to undertake this project and for the constant and valuable support I received over the years. I want to thank Professor Hannelore Daniel for sharing her expert knowledge and her enthusiasm for human metabolism with me. My deepest thanks go to my supervisors Helmut Laumen and Thomas Skurk: I am very grateful for your support, advice, guidance and help throughout the experiments, the data-analysing and the process of manuscript- and thesis-writing. I extend my gratefulness to Gabi Kastenmüller and Simone Wahl for their excellent contributions, regarding the statistics of this work. I deeply thank my dear friend Marie Standl for explaining the basics of R-Programming to me. I thank Andrea Bierschneider for the great work she contributed during her master thesis. Furthermore, I wish to thank Sylvia Heinrich, my colleagues and my office mates. I am grateful for your help, your support and especially for the enjoyable time I spent with you. I will take with me a whole bunch of memories and hopefully some friends. I also want to express my appreciation to all volunteers for their participation.

Last but not least I do thank those who are closest to me: My parents Irmgard and Wilhelm Krug, Alex and my brother with his family. I count myself very lucky to have you all in my life.

## ABSTRACT

The recent development of metabolomics technologies allow the simultaneous measurement of multiple metabolites produced along various interconnected pathways of the human metabolism.

This thesis addresses the dynamics of metabolite concentrations, divided into two major topics:

1.) The investigation of the dynamics of multiple metabolites in response to altered substrate availability or demand. 15 young and healthy male volunteers underwent 6 highly controlled physiological challenges, such as a 36 hour-fast or an oral glucose tolerance test. Blood, urine, exhaled air and breath condensate were collected at up to 56 time-points and analyzed by MS- and NMR-based methods yielding 274 metabolic traits. The analysis revealed: a) physiological challenges increased inter-individual variation, revealing metabolic phenotypes (metabotypes) not observable at baseline; b) metabolite quantities were consistently volunteer-specific over all analyzed sample types, as shown for acetone or acetylcarnitine; and c) a systematic model of  $\beta$ -oxidation derived parameters, like the acetylcarnitine/palmitoylcarnitine-ratio, which were significantly ( $p < 0.05$ ) and more strongly associated with physiological parameters, than absolute metabolite concentrations, indicating that such a modeling approach may aid in the understanding of inter-individual variations.

2.) The impact of two common genetic variants, associated with obesity (*FTO*) or diabetes type 2 (*TCF7L2*), on baseline metabolite profiles and metabolite changes in response to nutritional interventions. 19 men homozygous for *FTO* risk allele (rs9939609), 16 homo- or heterozygous for the *TCF7L2* risk allele (7903146) and 20 controls (negative for both risk alleles) underwent an oral glucose-, a western diet- and an oral lipid test. Pre- and post-challenge metabolite analyses revealed that the oral glucose test showed stronger genotype-specific differences during metabolite regulation than the other challenges. Compared to controls, the *FTO* risk allele significantly ( $p < 0.05$ ) altered lactate and phosphatidylcholine output after glucose intake, whereas the *TCF7L2* risk allele altered amino acid and phosphatidylcholine regulation. These results show that intervention tests may help deepen our understanding of gene function and may help to estimate disease risk and progression.

# ZUSAMMENFASSUNG

Neue technologische Fortschritte ermöglichen die simultane Messung einer Vielzahl von Metaboliten, welche entlang verschiedener ineinandergreifender Stoffwechselwege entstehen. Diese Dissertation befasst sich mit der Dynamik von Metabolitenkonzentrationen, gegliedert in zwei Hauptforschungsziele:

1.) Die Untersuchung der Dynamik von Metabolitkonzentrationen als Reaktion auf veränderte Verfügbarkeit von Energie. 15 junge, gesunde Männer absolvierten sechs standardisierte Interventionen, z.B. 24-stündiges Fasten. Mithilfe MS- und NMR- basierter Methoden wurden, an bis zu 56 Zeitpunkten in Blut-, Urin-, Atemgas- und Atemgaskondensatproben 274 Metabolite gemessen. Die Ergebnisse zeigten: a) physiologische Interventionstests verstärkten die inter-individuelle Variation, so dass im Gegensatz zum Basalzustand metabolische Phenotypen erkennbar wurden; b) Metabolitenkonzentrationen waren über alle analysierten Probenarten konsistent probandenspezifisch, hier gezeigt für Aceton und Acetylcarnitin; und c) Parameter eines  $\beta$ -Oxidations-Model wie die Acetylcarnitin/Palmitylcarnitin-Ratio waren signifikant ( $p < 0.05$ ) und stärker mit physiologischen Parametern assoziiert als absolute Metabolitkonzentrationen. Solche Modelle können daher das Verständnis für inter-individuelle Unterschiede verbessern.

2.) Die Auswirkungen zweier gängiger genetischer Varianten, assoziiert mit Adipositas (*FTO*) oder Diabetes Typ 2 (*TCF7L2*), auf das basale Metabolitprofil und die -dynamik unter Ernährungsintervention. 19 Männer, homozygot für das *FTO* Risikoallel (rs9939609), 16 Männer homo- oder heterozygot für das *TCF7L2* Risikoallel (rs7903146) und 20 Kontrollpersonen (negativ für beide Risikovarianten), absolvierten orale Glukose-, Fast Food- und Lipidtests. In vor- und nach-interventionellen Analysen zeigte der orale Glukosetoleranztest stärkere genotyp-spezifische Unterschiede in der Metabolitenregulation als die anderen Tests. Das *FTO* Risikoallel veränderte signifikant ( $p < 0.05$ ) den Laktatanstieg und die Phosphatidylcholinabnahme nach Glukoseaufnahme, wohingegen das *TCF7L2* Risikoallel die Aminosäuren- und Phosphatidylcholinregulation beeinflusste. Somit können Interventionstests helfen Genfunktionen besser zu verstehen oder Krankheitsrisiken und -verläufe abzuschätzen.

# CONTENTS

ACKNOWLEDGEMENT .....	I
ABSTRACT .....	II
ZUSAMMENFASSUNG .....	III
CONTENTS .....	IV
1 INTRODUCTION.....	1
2 DYNAMICS OF THE HUMAN METABOLOME.....	5
2.1 Introduction.....	5
2.2 Research design and methods.....	7
2.2.1 Study participants and study design .....	7
2.2.2 Sample collection .....	10
2.2.3 Standard biochemistry parameters .....	11
2.2.4 Metabolomics analyses .....	12
2.2.5 Statistical analysis.....	14
2.2.6 Mathematical modeling of fatty acid $\beta$ -oxidation .....	15
2.3 Results.....	17
2.3.1 Time dependent metabolite changes reflect the metabolic conditions induced by the challenges. ....	17
2.3.2 Metabolite correlations .....	29
2.3.3 Metabolites to classify the metabolic condition.....	31
2.3.4 Inter-individual metabolite variation during challenges.....	32
2.3.5 Read-outs from a $\beta$ -oxidation model provide stronger associations with phenotypic data than absolute metabolite concentrations .....	35
2.4 Discussion .....	38
2.5 Conclusion .....	42

3 THE IMPACT OF TWO COMMON GENETIC VARIANTS ON METABOLITE RESPONSE TO NUTRITIONAL INTERVENTIONS .....	44
3.1 Introduction .....	44
3.2 Research Design and Methods .....	45
3.2.1 Study participants and study design .....	45
3.2.2 Biochemical analyses.....	49
3.2.3 Metabolomics analyses .....	49
3.2.4 Statistical analysis.....	50
3.3 The impact of a common <i>FTO</i> gene variant on plasma metabolite profiles during nutritional challenges .....	51
3.3.1 <i>FTO</i> – Fat Mass and Obesity Associated Gene .....	51
3.3.2 Results .....	53
3.3.2.1 Genotype-specific differences in baseline measures .....	53
3.3.2.2 Genotype-specific differences in challenge-induced metabolite dynamics.....	54
3.3.3 Discussion .....	59
3.3.4 Conclusion .....	64
3.4 The impact of the T risk variant in rs7903146 of the <i>TCF7L2</i> gene on plasma metabolite profiles during nutritional challenges.....	65
3.4.1 Transcription factor 7 like 2 - <i>TCF7L2</i> .....	65
3.4.2 Results .....	67
3.4.2.1 Genotype-specific differences in baseline measures .....	67
3.4.2.2 Genotype-specific differences in challenge-induced metabolite dynamics.....	70
3.4.3 Discussion .....	75
3.4.4 Conclusion .....	81
LIST OF FIGURES .....	82
LIST OF TABLES .....	84
ABBREVIATIONS .....	85
REFERENCES .....	88
PUBLICATIONS AND PRESENTATIONS.....	98
CURRICULUM VITAE .....	100

# 1 INTRODUCTION

The term energy metabolism stands for the collection of all interconnected chemical processes by which a system or cell meets its energy demands. Centuries of research uncovered the fundamental principles of energy extraction from nutrients, its storage and expenditure and yielded integrated molecular knowledge on the components (enzymes, transporters, hormones etc.) necessary for the function and regulation of many metabolic processes. Dysfunctions or deregulations of one of those components cause metabolic diseases such as diabetes. Metabolites, the intermediates produced along the multiple pathways of metabolism provide a final read-out of the effective metabolic function and can be used to evaluate the present metabolic condition or the health status of an individual. The concept of using metabolites for diagnostic purposes is ancient: Already 3,500–4,000 years ago, traditional Chinese doctors used ants for the detection of sugar in urine of patients as an indicator for diabetes. In modern medicine metabolites are routinely used for disease diagnosis (for example, glucose for diabetes or cholesterol for vascular diseases). However, the number of metabolites presently used for disease diagnosis is small, compared to the number of metabolites existent in humans.

The study of metabolism always depended on the availability of methods to identify and quantify metabolites (1). As outlined above, since a long time various chemical methods for quantification of specific metabolites were developed. As a methodological challenge, metabolites are highly diverse in its chemical and physical properties and include a wide range of chemical species, from low molecular weight polar volatiles such as ethanol, to high molecular weight polar glucosides, non-polar lipids and anorganic species. Additionally, the range of metabolite concentrations can vary over nine orders of magnitude (pM–mM). Therefore, only with the technological advances derived over the last 100 years measurement of multiple metabolites in one assay became possible by NMR- and MS-based technologies. These advances rouse hopes to measure the entire collection of metabolites of an organism, which was termed "metabolome" in analogy to the genome. Nowadays, two detection technologies are in the focus of attention: Nuclear Magnetic Resonance (NMR) spectroscopy and Mass Spectrometry (MS).



**NMR spectroscopy** enables in theory the detection of any organic molecule possessing nuclei with spin. These nuclei possess different energies, depending on their orientation when placed inside a magnetic field and, depending on the chemical environment of the protons, an energetic fingerprint for that molecule can be detected (2). NMR spectroscopy using the resonance of proton nuclei, known as  $^1\text{H}$  (proton) NMR spectroscopy, is able to detect a wide spectrum of metabolites. Other magnetic nuclei have also been used for distinct applications, e.g.  $^{13}\text{C}$  spectra for labeled metabolites (3) or  $^{31}\text{P}$  spectroscopy suitable for phosphate-containing molecules such as ATP, ADP and phosphocreatine (4). NMR is less sensitive than MS approaches, despite the recent improvements like increases in field strengths and cryoprobe technology, improvements in probe and spectrometer design, and the development of microprobes. Nevertheless, NMR spectroscopy has its advantages, because it is rapid, cheap on a per sample basis, highly robust and allows non-destructive measurements (5).

**Mass Spectrometry** distinguishes molecules based on their mass:charge ( $m/z$ ) ratio. Therefore, molecules are ionized and placed into an electrical field. For metabolic profiling the triple quadrupole mass spectrometer, also known as a tandem mass spectrometer (or MS/MS), is widely used. Therefore, three quadrupoles are arranged in series and each quadrupole consists of 4 rods creating a controlled electrical field. The first quadrupole selects ions based on their  $m/z$  ratio, in the second ions are fragmented, and the third selects ion fragments based on  $m/z$  ratio (6). A key advantage of MS is its high sensitivity. Chromatography is often used in conjunction with MS. Chromatography separates molecular species within complex biological samples by their retention time, delivering them to the mass spectrometer in a time-resolved manner. Gas chromatography and liquid chromatography are the two main chromatographic technologies used for metabolic profiling.

Metabolic profiling based on these two technologies can be either targeted or untargeted. Targeted methods quantify pre-defined metabolites, which were characterized ahead of measurement. Targeted analysis can be achieved by MS and identifies each metabolite by a unique combination of chromatographic retention time, precursor ion  $m/z$  ratio and fragment ion  $m/z$  ratio. The known identity of the measured analytes allows biological interpretation of the data.

In contrast, untargeted methods acquire metabolite spectra. Subsequent data processing methods can extract distinct features of the metabolite fingerprint. Additionally, metabolite identification can be achieved by comparing the gathered NMR spectra of biological samples to reference spectra of individual metabolites. Potentially, non-targeted methods can detect metabolites not previously considered. Both, MS and NMR spectroscopy can be used in a non-targeted manner. Mass spectrometry technologies suitable to identify metabolites in an untargeted manner need a mass resolution high enough to determine an unequivocal chemical formula of an analyte, such as Fourier transform ion cyclotron resonance (FTICR) (6).

The overall function of metabolism is influenced by numerous factors such as genes, environment, diet, age or physical activity. Metabolites, the products or intermediates of metabolism provide a valuable read-out on the effects of those influencing factors.

In this thesis metabolite measurements were used (i) to gain fundamental knowledge on energy metabolism during defined metabolic challenges and (ii) to investigate metabolite alterations in individuals carrying gene variants associated with an increased risk for diabetes or obesity.

The first part of this thesis addresses the acute effects of defined stresses, like oral glucose intake or physical activity on the human metabolome. Such stresses immediately change energy availability or need, challenge and therefore evoke adaptive metabolic responses. Transitions from anabolic to catabolic states are accompanied by concentration changes in a multitude of metabolites. It is necessary to systematically investigate these changes to acquire detailed biochemical knowledge of the multiple metabolic processes and their interrelations. Such knowledge helps to classify the metabolic condition on multiple levels and therefore potentially improves the classification of abnormalities. However, so far only few studies systematically investigated acute metabolome changes under defined metabolic challenges. Currently, frequent sampling is still necessary to assess reliable time profiles, which help to define time points where excursions in the metabolic vocabulary define an individual reaction at best. In comparison to organ-specific metabolite profiles, blood plasma/serum or urinary profiles provide the best surrogates for systemic metabolism. Therefore, the Human Metabolome (HuMet) - study was designed to systematically investigate the dynamics of the human metabolome in response to environmental stimuli such as food-intake or fasting. 15 young and healthy male volunteers were

submitted to a highly controlled four-day-challenging protocol, including 36 hour-fasting, oral glucose and lipid tests, liquid test meals, physical exercise and cold-stress. Blood, urine, exhaled air and breath condensate were collected on up to 56 time-points. All samples were analyzed by MS- and NMR-based methods yielding 275 metabolic traits, mainly lipids and amino acids. Results of this investigation and therewith parts of this thesis were published by Krug et al. (7). Additionally, the dynamic changes in the panel of 163 metabolites quantified by LC-MS/MS using the AbsoluteIDQ kit (BIOCRATES Life Sciences AG) are described in more detail within this thesis, because this set of metabolites were also measured in the second part of this thesis.

The second part of the thesis addresses the question if early metabolite alterations occur in non-diabetic and non-obese individuals carrying gene variants associated with T2DM or obesity. Humans differ in many ways in their response to diet or other physiological stresses, which can be explained in parts by the individual genetic equipment. Many genes are implicated in the expression of enzymes, proteins or hormones involved in metabolism. In fact a small genetic defect can produce a large difference in metabolite levels, obvious for example in inborn errors of metabolism such as alkaptonuria. Such gene defects lead to absence or dysfunction of proteins essential for certain metabolic processes and result in a perilous deficiency or accumulation of intermediate metabolites in the human organism (8, 9). More common metabolic diseases such as T2DM or obesity also have a genetic component. However, in such multifactorial disorders, the occurring gene variations only result in minor metabolic alterations, which pose an additional risk factor upon today's obesogenic environment (10). Genome-wide association studies have identified various genetic polymorphisms associated with T2DM and obesity. The metabolic effects of the found variants are modest and often paired with a poor understanding about the gene function or disease causing mechanisms. Variants within the *TCF7L2* gene have been found to correlate strongly with T2DM and variants within the *FTO* gene with obesity (11, 12), however especially for *FTO*, the gene function and its relation to obesity remains elusive. In chapter 3, I introduce the VID-study, which aimed to analyze metabolite alterations, in individuals carrying the *TCF7L2* risk variant rs7903146 or in individuals carrying the *FTO* risk variant rs9939609. The study was designed to analyze metabolite differences in the fasting state but also under defined nutritional interventions. Such an approach can unmask early alterations not visible in the fasted state and possibly provides additional information on metabolic pathways affected by the selected gene variants.

## 2 DYNAMICS OF THE HUMAN METABOLOME

### 2.1 Introduction

“In bio fluids or tissues, metabolomics identifies and quantifies the final entities of the reaction chain along the paradigm of biology; from genes to transcripts to proteins to the metabolic intermediates. In contrast to the other profiling technologies, such as transcriptomics or proteomics, metabolomics data can be better interpreted on the basis of biochemical knowledge gained over almost a century. For diagnostic purposes, metabolic analysis of body fluids was first established for inborn errors of metabolism based on the pioneering work of A. Garrod on “Incidence of alkaptonuria: a study in chemical individuality” published in 1902 (13) and is now standard in newborn screenings (14). More recent developments propose metabolomics as a biomarker discovery tool for a variety of diseases including Crohn’s disease, Parkinson or cancer (15-17). While markers that associate with a manifest disease are often readily detected, it is far more difficult to determine the status of health and define the border between health and disease. Early alterations in metabolism however might be unmasked by challenging metabolic regulatory processes, testing the individual capacity and flexibility to cope with environmental stressors such as physical activity or dietary components. However, most metabolomics studies to date are limited to the analysis of samples obtained in a fasted state and only very few studies reported time-resolved changes of the human metabolome in response to a challenge (18-20). Using an LC-MS/MS method with detection of 191 metabolites in plasma samples derived during an oral glucose tolerance test (OGTT) in healthy and pre-diabetic volunteers, Shaham *et al.* identified metabolites with significant changes not previously described in the context of glucose homeostasis, such as bile acids or urea cycle intermediates (18). Rubio *et al.* could reveal numerous new fasting markers by analyzing metabolite profiles of plasma and urine sampled during extended fasting in human volunteers with multivariate statistics (20). Wopereis *et al.* analyzed metabolome changes during an OGTT in overweight human volunteers during a 9 week intervention with a mild acting anti-inflammatory drug and demonstrated that the OGTT increased the statistical power for detecting differences by treatment (19).

In order to extend the knowledge on the dynamics of the human metabolome in response to diverse challenges, we performed a study, in which 15 healthy male volunteers underwent six different challenges over four study days: a prolonged fasting period of 36 hours (FASTING), a standard liquid diet (SLD), an oral glucose tolerance test (OGTT), an oral lipid tolerance test (OLTT), a physical activity test (PAT), and a cold pressure stress test (STRESS). Within this study, a variety of sample types (blood, urine, exhaled breath and exhaled breath condensate) were collected with high temporal resolution (on up to 56 time points) and were analyzed with NMR and different mass spectrometric techniques, mainly focusing on lipids and amino acids. The objectives of the present work are to describe the challenges and metabolic analysis protocols and to present examples of our data according to the three directions of our human metabolome (HuMet) study: the analytical depth (different methods), the breadth of the physiological challenges (different metabolic conditions) and the width of the sample coverage (different bio fluids and high sampling frequency). Additionally, we show an application of metabolome data for systems biology. To our knowledge, no other study has yet characterized the dynamics of the human metabolome in a more detailed manner. This study with >2100 individual samples provides a valuable data set of the metabolome under various physiological conditions, measured on different analytical platforms and in different bio fluids. The metabolomics data obtained within this study are freely and permanently available on <http://metabolomics.helmholtz-muenchen.de/humet>." (From: Krug et al. (7), pages 2607-2608)

## **2.2 Research design and methods**

### **2.2.1 Study participants and study design**

#### **Study participants**

“Volunteers were recruited into the human study center of the Else Kröner-Fresenius-Center for Nutritional Medicine of the Technische Universität München. After medical examination, 15 healthy, young and normal weight men were included into the study. They showed no metabolic abnormalities based on standard clinical chemistry, did not take any medication and gave their written informed consent. The study protocol was approved by the ethical committee of the Technische Universität München (#2087/08) and corresponds with the Declaration of Helsinki.

During a medical entrance examination standard clinical (blood lipids, blood pressure etc.) and anthropometric parameters, such as body mass index (BMI), waist-to-hip ratio etc. were determined. The resting metabolic rate (RMR) was measured by indirect calorimetry (Deltatrac™ Metabolic Monitor, Datex-Ohmeda, Helsinki, Finland). Body composition was assessed by Dual energy X-ray absorptiometry using Explorer™-Bone Densitometer (Hologic® Inc., Bedford, USA). Individual anaerobic threshold was assessed with an incremental bicycle ergometer test starting at 50 Watt at the Center for Prevention and Sports medicine of the Technische Universität München, Munich, Germany.

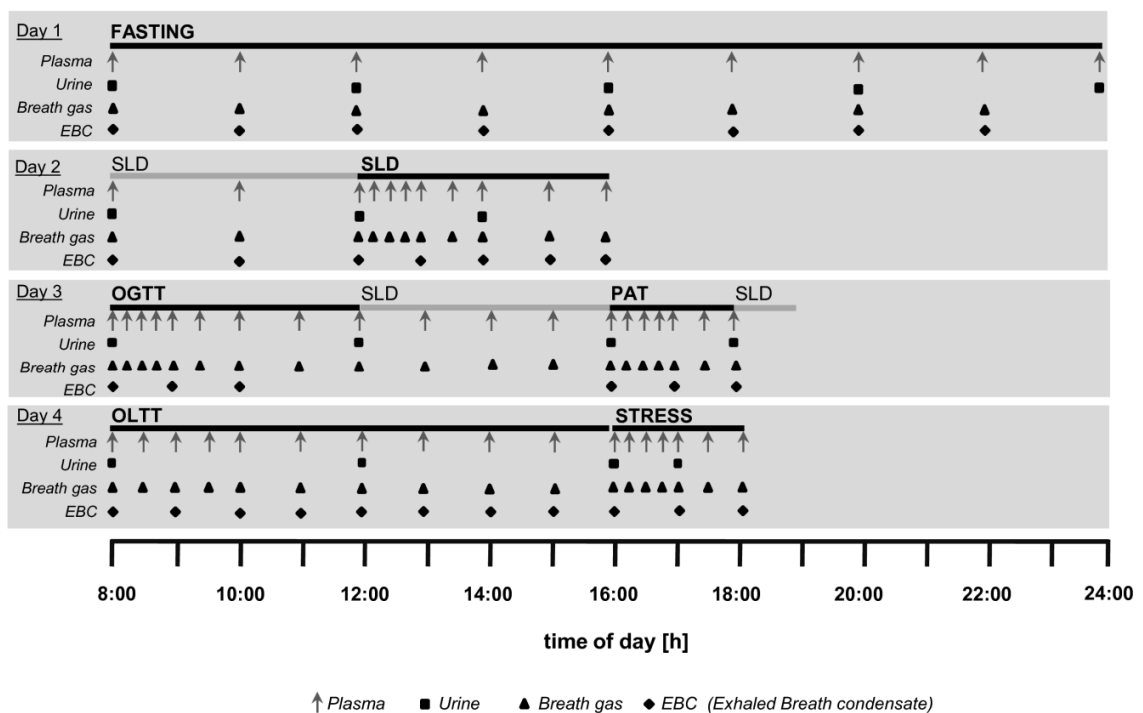
#### **Study design**

The study design showing the sequence of challenges is displayed in Figure 1. Volunteers underwent six challenges within two test periods, each lasting 2 days and 2 nights. In the 24 hours before each test period, subjects were asked not to consume alcohol or to undertake strenuous physical exercise. To minimize environmental influences on the metabolome, subjects stayed inside the study unit throughout both study periods under controlled food and fluid intake and physical activity. Volunteers were admitted to the study unit on the evening before each test period to consume a standardized balanced dinner at 7 pm, which consisted of a commercially available ready-to-serve meal with mineral water (nutrient composition per 100g: 502kJ, 28% protein, 29% fat, 48% carbohydrates). Besides the challenge meals, subjects received a standardized breakfast at

8 am (day 2), lunch at 12 pm (day 3), and dinner at 7 pm (day 3) which always consisted of a commercial fiber-free formula drink (Fresubin® Energy Drink chocolate, Fresenius Kabi, Bad Homburg, Germany). The amount of all standardized meals was individually calculated in order to maintain an energy content of 1/3 of the individual RMR multiplied with a factor of 1.3 for low physical activity for each volunteer. Samples were always taken shortly before each challenge test (= 0 min) and then at predefined time points.

**Figure 1: Study design of the HuMet-study**

Within 4 days volunteers underwent the six challenges: FASTING, SLD (Standard Liquid Diet), OGTT (Oral Glucose Tolerance Test), PAT (Physical Activity Test), OLTT (Oral Lipid Tolerance Test) and STRESS (Cold stress test). Duration of each challenge test is indicated by black bars. Time points of bio fluid collection are indicated by symbols.



**Fasting challenge (FASTING):** After the evening meal at 7 pm at day -1 the study participants fasted until the next morning 8 am, when the first samples were obtained and then continued fasting for another 24 hours. Plasma and breath air samples were collected every 2 hours between 8 am and midnight and again after a total fasting period of 36 hours. Urine was collected every 4 hours between 8 am and midnight and again after 36 hours of fasting. Exhaled breath condensate (EBC)

was collected every 2 hours between 8 am and 10 pm and again after a total fasting period of 36 hours. During the fasting period, subjects received 2.7 liters of mineral water according to a pre-defined drinking schedule.

Standardized liquid diet (SLD): To investigate the effects of a complex, balanced diet, subjects received a highly defined fiber-free formula drink (Fresubin® Energy Drink chocolate, Fresenius Kabi, Bad Homburg, Germany), providing 1/3 of the individual daily energy requirements, at 12 noon on day 2 for ingestion within 5 min. Plasma and exhaled air were collected at 0, 15, 30, 45, 60, 90, 120, 180, and 240 minutes. EBC was collected at 0 and after 60, 120, 180 and 240 min. Urine was collected at 0 min and 120 min after SLD intake.

Oral glucose tolerance test (OGTT): On day 3, an OGTT was carried out at 8.00 am after an overnight fast by ingesting a 75 g glucose drink (Dextro O.G.T., Roche Diagnostics, Mannheim, Germany). All subjects were asked to drink the 300 ml glucose solution within 3 min. Plasma and exhaled air samples were collected at 0, 15, 30, 45, 60, 90, 120, 180 and 240 min. EBC was collected at 0, 60 and 120 min. Urine was collected at 0 and 240 min.

Physical activity test (PAT): All subjects performed a 30 min bicycle ergometer training at a power level corresponding to their individual anaerobic threshold. Plasma and exhaled air was obtained before the PAT, during the PAT at 15 and 30 min and after the PAT at 45, 60, 90 and 120 min. EBC collections were performed at 0, 60 and 120 min. Urine was collected at 0 and 120 min.

Oral lipid tolerance test (OLTT): The lipid-rich liquid test diet consisted of 3 parts Fresubin® Energy Drink chocolate and 1 part Calogen® (Nutricia, Zoetemeer, Netherlands), a fat emulsion containing 50 g of long-chain triglycerides per 100 ml. The volume of the liquid meal was calculated for each volunteer to provide 35 g fat per m<sup>2</sup> body surface area. The test drink was served at room temperature for ingestion within 5 min. Plasma and exhaled air samples were collected at 0, 30, 60, 90 and 120 min and thereafter every hour until the 8th hours after lipid ingestion. EBC was sampled at 8 am (=0 min) and then every hour after the OLTT until 4 pm (= 480 min). Urine was collected at 0, 4 and 8 hours. The composition of all liquid diets is provided in Table 1.



Stress test (STRESS): To elicit a hormonal stress response and examine its effect on metabolism, volunteers underwent a cold pressure test by immersing one hand, up to wrist level, with fingers apart for maximal 3 minutes in ice water. Plasma and exhaled air was obtained at 0, 15, 30 45, 60, 90 and 120 minutes. Urine and EBC was collected at 0 and 60 minutes.

**Table 1: Nutrient composition of the SLD and the OLTT**

SFA, saturated fatty acids; MUFA, monounsaturated fatty acids; PUFA, polyunsaturated fatty acids

	SLD		OLTT	
	per 100ml	per subject (mean±SEM)	per 100ml	per subject (mean±SEM)
<b>Amount</b>	100	482 ± 20.3	100	415 ± 6.3
<b>Energy (kJ)</b>	630	3041 ± 127.6	935.50	3877± 57.6
<b>Energy (kcal)</b>	150	724 ± 30.4	225.00	932.4±13.9
<b>Protein (%)</b>	15	15	7.5	7.5
<b>Carbohydrates (%)</b>	50	50	25.1	25.1
<b>Fat (% energy)</b>	35	35	67.4	67.4
<b>Protein (g)</b>	5.6	27 ± 1.1	4.20	17.4 ± 0.3
<b>Carbohydrates (g)</b>	18.8	90.8 ± 3.8	14.10	58.4 ± 0.9
<b>Fat (g)</b>	5.8	28 ± 1.2	16.85	69 ± 1
<b>SFA (g)</b>	0.5	2.4 ± 0.1	1.70	7.1 ± 0.1
<b>MUFA (g)</b>	3.7	17.9 ± 0.8	10.38	43 ± 0.6
<b>PUFA (g)</b>	1.6	7.7 ± 0.3	4.78	19.8 ± 0.3
<b>Water (ml)</b>	78	353 ± 27.8	58.50	242.4 ± 3.6

## 2.2.2 Sample collection

Plasma: During the study, a total of 56 blood samples per subject were collected into 9 ml EDTA K<sub>2</sub>-Gel tubes (Sarstedt, Nümbrecht, Germany) through a venous cannula (18 G 1 ¼, Vasofix Braunüle, Braun, Germany) inserted into an antecubital vein. Tubes were mixed and centrifuged immediately (Centrifuge 5702 R, Eppendorf AG, Hamburg, Germany) at 3.000 g for 10 min at 20°C. Plasma was immediately aliquoted, frozen on dry ice and subsequently stored at -80°C until further analysis.

Urine: Spot urine samples were collected into 125 ml-polypropylene-beakers (Ratiolab, Dreieich, Germany), immediately aliquoted, frozen on dry ice and then stored at -80°C until analysis.

Breath air: The exhaled breath samples were collected into reusable 3 l FEP (Teflon) bags (SKC, Pennsylvania, USA) using the mixed expired sampling technique. Subjects filled the bag in a single exhalation. Breath gas collection was scheduled immediately before each blood collection. Room air was drawn contemporaneously. Breath and room air were sampled at the test location and analyzed immediately by proton transfer reaction (PTR)-MS. Before PTR-MS analysis the filled bags were heated up in an oven for at least 5 min at 40°C in order to evaporate the condensed humidity.

Exhaled Breath condensate (EBC): EBC was sampled using an ECO Screen II condenser (Jaeger GmbH, Hoechberg, Germany). Therefore, subjects respired into the device for approximately 10 min to collect 150 l breath volume. EBC was collected into two cooled (-20°C) disposable PTFE plastic bags. The exhaled air is fractioned into bronchial and alveolar breath partitions, each collected into one of the two cooled bags. Samples were immediately transferred into 1.5 ml storage tubes, frozen on dry ice and stored at -80°C until measurement.

### **2.2.3 Standard biochemistry parameters**

Venous plasma glucose and lactate concentrations were determined by an enzymatic amperometric technique (Super GL easy<sup>+</sup>, Dr. Müller Gerätebau, Freital, Germany). Insulin was measured by an enzyme-linked immunosorbent assay (ELISA) (Dako #K6219, Glostrup, Denmark). Non-esterified fatty acids (NEFAs) were quantified in plasma by an enzymatic colorimetric method (NEFA-HR, Wako Chemicals GmbH, Neuss, Germany) according to the manufacturer's recommendations.

## 2.2.4 Metabolomics analyses

### Targeted metabolomics in plasma

FIA-MS/MS based analysis using the Absolute/DQ Kit (BIOCRATES Life Sciences AG, Innsbruck, Austria) was performed as previously described (21-23) by using a 4000 QTRAP system (AB Sciex, Darmstadt, Germany) at the German Research Center for Environmental Health GmbH (Helmholtz Zentrum München, Munich, Germany). The metabolomics data set contains 14 amino acids, hexose, free carnitine (C0), 40 acylcarnitines, hydroxylacylcarnitines and dicarboxylacylcarnitines, 15 sphingomyelins, 77 phosphatidylcholines and 15 *lyso*-phosphatidylcholines. Data quality was assessed by repeated measurements of the same sample (5x) on different days. Metabolites showing a coefficient of variation (CV) greater than 25% as well as metabolites with CV >20% and a significant correlation (Kendall) to the day of the measurement were excluded from further analysis. 31 metabolites did not pass the quality control criteria and were excluded from statistical analysis.

### NMR metabolomics in plasma

Lipoproteins were analyzed by NMR spectroscopy at the LipoFIT Analytic GmbH (Regensburg, Germany). The technology was patented (US7,927,878; AU2005250571; DE 10 2004 026 903 B4). Briefly, diffusion-weighted NMR spectra of blood plasma were recorded on a Bruker 600 MHz spectrometer Avance II<sup>plus</sup>, which revealed characteristic overall profiles of the lipoprotein signals. The spectral regions of the spectra ranging from 1.5 to 0.7 ppm were modeled into a set of 15 lipoprotein subfractions. These 15 lipoprotein subfractions were used to calculate lipoprotein size and quantity (=number) in terms of the concentration of particle subclasses in [nmol/l] and the average particle size in [nm].

### NMR metabolomics in urine

NMR spectroscopy was carried out at LipoFIT Analytic GmbH (Regensburg, Germany) on a Bruker 600 MHz spectrometer Avance IIplus. We recorded one-dimensional <sup>1</sup>H-NMR NOESY experiments from the urine specimen in phosphate buffer at pH 7.4 with TSP (1,1,2,2-tetra-deutero-3-trimethylsilylpropionic acid) for reference at a frequency of 600.30 MHz. Metabolites in these NMR spectra were annotated using the Chenomx NMR Suite 7.0 (Chenomx Inc., Edmonton, Canada) (24).

Metabolite assignment was done manually since varying sample conditions affect the chemical shift of the metabolite resonances. The signal of a reference compound added to the specimen (TSP, 0.5 mM) was used to determine absolute metabolite concentrations. We normalized these concentrations by urinary creatinine levels and report them as mmol per mol of creatinine.

### **Nominal mass PTR-MS metabolomics in breath air**

From every breath sample five mass scans in the mass range between 20-200 amu were recorded with a standard PTR-MS (Ionicon, Innsbruck, Austria). The recorded counts of every mass were normalized to the count rate of the primaries and water clusters to compensate for fluctuations in the primaries concentrations and for consumption of the primary ions in saturated breath gas compared to the dryer room air. Because of the extraordinary high increase of the acetone count rate during the elongated fasting period, the acetone count rate was additionally factored into the normalization. The change of transmission of the PTR-MS over time was corrected and the conversion of the normalized count rate to ppbv (part per billions volume) used the standard formula for PTR-MS concentrations (25). Masses were excluded from comparison if normalized count rates were below 2 ncps in 80% of the data points of a challenge. Due to the unit mass resolution of the PTR-MS the assignment of a mass to a specific compound is rather tentative. However, in the selected cases the linear correlation between the isotope count rates supported the assignment (e.g. acetone).

### **FIESI-ICR-FT/MS non-targeted Metabolomics**

Samples were measured at the Helmholtz Zentrum München using a Bruker Solarix FT-ICR mass spectrometer (Bruker Daltonics, Bremen, Germany) with a 12 Tesla magnet and an Apollo II electrospray ionization source. Ionization was performed at positive mode and voltage of 4,500 V. Samples were flow-injected at 2 $\mu$ l/min flow rate. In total, 420 time-domain transients were acquired and accumulated per sample. Each fourier-transformed mass spectrum consists of 2 Mega Word (MW) data points which resulted in a mass resolving power of 400 000 at m/z 200 and 200 000 at m/z 400. Prior to analysis, mass spectra were calibrated with an error of < 100 ppb using Arginine clusters. Further calibration and mass spectrum unification was performed as previously described (26). Masses were filtered with a signal to noise ratio of S/N = 4 and/or 10<sup>-6</sup> % of maximum intensity. Masses were annotated using the MassTRIX server (27) at 0.5 ppm accuracy.

Unified spectra were normalized on the sum of signal intensities per spectrum and then subject-wise on the sum of normalized signal intensities, to compensate for different ion strengths in samples and for inter-individual variation, respectively.

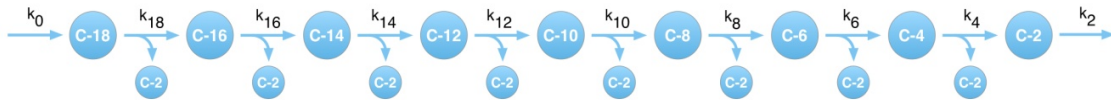
## 2.2.5 Statistical analysis

For unsupervised multivariate data analysis, we performed a PCA using the *prcomp* function as implemented in the R statistical software version 2.10.1 (<http://www.r-project.org>). On the one hand, we performed the analysis based on quantitative data for all metabolic traits with complete measurements (no missing values) in plasma (132 by MS/MS, 28 by NMR, 3 by standard biochemistry). On the other hand, we determined the principal components of the mean concentrations of the 15 subjects at the 56 plasma sampling time points. For the PCA, each metabolite quantity was scaled to a mean of 0 and a standard deviation of 1 in order to make the concentrations comparable.

Pearson correlation: For 275 metabolites (163 in plasma, 106 in breath air, 6 in urine), we calculated the mean concentrations of the 15 subjects at the 56 plasma sampling time points resulting in a mean time course for each metabolite. For metabolites quantified with the AbsoluteIDQ kit log-transformed values were used because most metabolite concentrations showed a log-normal distribution. Pearson correlations between metabolite mean time courses were calculated in order to uncover metabolites with similar or opposed time curves. The Pearson correlation coefficients were determined using the *cor.test* function in R. The matrix of pairwise Pearson correlation coefficients was hierarchically clustered and color-coded using the *heatmap* function with the default values for the clustering. Data is provided as mean $\pm$ SD.

## 2.2.6 Mathematical modeling of fatty acid $\beta$ -oxidation

The degradation of fatty acid chains in the beta-oxidation pathway can be seen as a linear cascade of subsequent reactions, such as



$M_1$  (e.g. fatty acid with 18 carbon atoms (C-18)) is supplied to the beta-oxidation pathway. During each reaction step the carbon chain is shortened by two carbon atoms. This results also in the production of  $M_9$  (e.g. acetyl-CoA). According to the law of mass action, we can describe each reaction with differential equations. The change of the first metabolite ( $\dot{M}_1$ ) at time  $t$  depends on the supply parameter  $k_0$  and the conversion of  $M_1$  to  $M_2$  with rate parameter  $k_1$ :

$$\dot{M}_1(t) = k_0(t) - k_1(t) \cdot M_1(t)$$

where  $\dot{M}_i$  represents the time derivative  $\frac{dM_i}{dt}$ .  $M_i(t)$  is the concentration of  $M_i$  at time  $t$ . Equations for intermediate metabolites  $M_2$  to  $M_8$  read

$$\dot{M}_i(t) = k_{i-1}(t) \cdot M_{i-1}(t) - k_i(t) \cdot M_i(t)$$

with  $i = 2, \dots, 8$ . The change of metabolite  $M_i$  at time  $t$  thus depends on the production of  $M_i$  by shortening of  $M_{i-1}$  (first part on the right hand side of the equation) and the conversion of  $M_i$  to  $M_{i+1}$  (second part). The last metabolite in the chain  $M_9$  (acetyl-CoA) is produced during each shortening of  $M_1, \dots, M_7$ , but also after splitting up  $M_8$ . The change of  $M_9$  can be described by the following differential equation:

$$\dot{M}_9(t) = \sum_{i=1}^8 (k_i(t) \cdot M_i(t)) + k_8(t) \cdot M_8(t) - k_9(t) \cdot M_9(t)$$

Under steady state conditions  $\dot{M}_i(t) = 0$ , i.e. metabolite concentrations do not change over time, solving of all coupled differential equations yields to

$$k_i(t) = \frac{M_9(t)}{M_i(t)} \cdot \frac{k_9(t)}{9}, \quad i = 1, \dots, 8.$$

Hence the rate  $k_i(t)$  of the conversion  $M_1 \rightarrow M_2$  (e.g. C-18  $\rightarrow$  C-16) can be deduced from the concentration ratio  $M_9(t) / M_i(t)$  (e.g. acetyl-CoA / C18-fatty acid) multiplied with a factor  $k_9(t) / 9$ , representing the removal rate of  $M_9$  from the system.

Accordingly, in our model, the fatty acid  $\beta$ -oxidation was described as a linear cascade of subsequent, irreversible first-order reactions like  $\dot{M}_i(t) = k_{i-1}(t) \cdot M_{i-1}(t) - k_i(t) \cdot M_i(t)$ , with  $\dot{M}_i$  being the time derivative  $\frac{dM_i}{dt}$  and  $k_i$  and  $k_{i-1}$  conversion rate parameters. The change of a metabolite  $M_i$  in the cascade at time  $t$  thus depends on the production of  $M_i$  by shortening of  $M_{i-1}$  (first part on the right hand side of the equation) and the conversion of  $M_i$  to  $M_{i+1}$  (second part). All reactions were described in this fashion and combined to a system of differential equations. Solving this system for steady state conditions, i.e. metabolite concentrations do not change over time, yields to conversion rates that are proportional to concentration ratios, also referred to as model-driven ratios. The correlations between anthropometric and biochemical parameters like BMI or plasma glucose with metabolite concentrations and model-driven ratios were calculated with Spearman's rank correlation statistics. Rank correlations for biochemical parameters were calculated using metabolite concentrations of the fasting test. Anthropometric parameters were correlated with averaged metabolite concentrations of the fasting period. P-values were corrected for multiple testing by controlling the false discovery rate at a global significance level of 0.05 (28). P-gain

statistic for metabolite ratios were calculated as: 
$$p\text{-gain}\left(\frac{M_1}{M_2}, X\right) = \frac{\min(p(M_1, X), p(M_2, X))}{p\left(\frac{M_1}{M_2}, X\right)}$$

with metabolites  $M_1$  and  $M_2$  and their respective model-driven ratio  $M_1/M_2$ , parameter  $X$  (e.g. BMI) and  $p(\text{variable A}, \text{variable B})$  being the corrected p-value of Spearman's rank correlation between variable A and variable B. For cases, where the model improves statistical correlations, p-gains will be bigger than 1. All analysis steps were performed using Matlab Version 7.11 (MathWorks, Natick, MA).

## 2.3 Results

### 2.3.1 Time dependent metabolite changes reflect the metabolic conditions induced by the challenges.

The challenges performed within this study induced either anabolic or catabolic states, resulting in reversible concentration changes of specific metabolites.” (From: Krug et al. (7), pages 2608-2611)

For each metabolite with complete measurements (no missing values) in plasma (132 by targeted MS/MS and 3 by standard biochemistry), p-values for time-dependent concentrations changes were calculated by the non-parametric Kruskal-Wallis test. Metabolites with Bonferroni corrected P-values of  $< 5.59E^{-06}$  were considered to show significant concentration changes over time. Table 2 lists all 47 metabolites with significant p-values. A more detailed description of these metabolites and their respective concentration changes is subject of the first part of this results section.



**Table 2: Presentation of all metabolites revealing significant concentration changes over time.**

P-values were calculated by non-parametric Kruskal-Wallis test for 135 metabolites with complete measurements (no missing values) in plasma (132 by targeted MS/MS and 3 by standard biochemistry). Table 2 lists all metabolites showing significant ( $p < 5.99 \times 10^{-6}$ ) concentration changes over time.

	Metabolite	Baseline			All timepoints			P
		Mean $\pm$ SD	Min	Max	Mean $\pm$ SD	Min	Max	
	Glucose [mg/dl]	85,97 $\pm$ 11,29	65,3	103	96,12 $\pm$ 22,6	50,7	195	1.02E <sup>-68</sup>
	H1 [ $\mu$ M]	4778,8 $\pm$ 491,74	3732	5981	4982,93 $\pm$ 1105,46	2670	11258	5.86E <sup>-63</sup>
	Insulin [ $\mu$ IU/ml]	5,8 $\pm$ 2,41	3,2	11,8	16,3 $\pm$ 21,52	0,87	125,66	5.86E <sup>-95</sup>
	Lactate [mg/dl]	9,56 $\pm$ 2,94	6,2	15,3	13,49 $\pm$ 11,02	4,5	127	1.17E <sup>-43</sup>
ACYLCARNITINES	C0 [ $\mu$ M]	39,65 $\pm$ 7,18	25,1	53,4	38,11 $\pm$ 7,9	15	63,7	1.77E <sup>-22</sup>
	C2 [ $\mu$ M]	5,44 $\pm$ 1,11	3,96	7,95	7,58 $\pm$ 3,32	2,51	25,8	2.17E <sup>-94</sup>
	C3 [ $\mu$ M]	0,4 $\pm$ 0,1	0,293	0,685	0,4 $\pm$ 0,14	0,093	1,12	3.44E <sup>-49</sup>
	C4 [ $\mu$ M]	0,19 $\pm$ 0,03	0,137	0,233	0,2 $\pm$ 0,05	0,101	0,411	4.56E <sup>-39</sup>
	C4.1.DC...C6 [ $\mu$ M]	0,05 $\pm$ 0,01	0,033	0,067	0,05 $\pm$ 0,02	0,02	0,128	2.09E <sup>-52</sup>
	C5 [ $\mu$ M]	0,15 $\pm$ 0,03	0,11	0,221	0,15 $\pm$ 0,04	0,065	0,334	4.45E <sup>-35</sup>
	C7.DC [ $\mu$ M]	0,04 $\pm$ 0,01	0,021	0,073	0,04 $\pm$ 0,02	0,011	0,102	6.88E <sup>-33</sup>
	C8 [ $\mu$ M]	0,14 $\pm$ 0,04	0,087	0,221	0,14 $\pm$ 0,05	0,053	0,399	1.02E <sup>-40</sup>
	C8.1 [ $\mu$ M]	0,07 $\pm$ 0,02	0,034	0,107	0,12 $\pm$ 0,07	0,02	0,389	6.37E <sup>-74</sup>
	C10 [ $\mu$ M]	0,22 $\pm$ 0,06	0,154	0,344	0,23 $\pm$ 0,1	0,068	0,676	8.12E <sup>-39</sup>
	C10.1 [ $\mu$ M]	0,11 $\pm$ 0,04	0,082	0,222	0,13 $\pm$ 0,05	0,042	0,418	1.19E <sup>-49</sup>
	C12 [ $\mu$ M]	0,08 $\pm$ 0,03	0,05	0,157	0,08 $\pm$ 0,01	0,027	0,266	9.61E <sup>-41</sup>
	C12.1 [ $\mu$ M]	0,1 $\pm$ 0,02	0,062	0,162	0,11 $\pm$ 0,04	0,033	0,31	1.22E <sup>-48</sup>
	C14 [ $\mu$ M]	0,03 $\pm$ 0,01	0,023	0,065	0,04 $\pm$ 0,01	0,018	0,122	9.56E <sup>-28</sup>
	C14.1 [ $\mu$ M]	0,09 $\pm$ 0,02	0,065	0,123	0,11 $\pm$ 0,05	0,023	0,382	4.41E <sup>-47</sup>
	C14.1.OH [ $\mu$ M]	0,01 $\pm$ 0	0,009	0,017	0,01 $\pm$ 0	0,004	0,031	8.09E <sup>-34</sup>
	C14.2 [ $\mu$ M]	0,02 $\pm$ 0,01	0,011	0,047	0,03 $\pm$ 0,02	0,005	0,126	4.37E <sup>-65</sup>
	C16 [ $\mu$ M]	0,09 $\pm$ 0,02	0,07	0,129	0,09 $\pm$ 0,03	0,039	0,248	2.76E <sup>-44</sup>
C16.2 [ $\mu$ M]	0,01 $\pm$ 0	0,003	0,008	0,01 $\pm$ 0	0,002	0,034	1.34E <sup>-51</sup>	
C18 [ $\mu$ M]	0,04 $\pm$ 0,01	0,03	0,05	0,04 $\pm$ 0,01	0,019	0,077	2.23E <sup>-13</sup>	
C18.1 [ $\mu$ M]	0,09 $\pm$ 0,02	0,05	0,124	0,12 $\pm$ 0,04	0,033	0,254	1.91E <sup>-52</sup>	
C18.2 [ $\mu$ M]	0,03 $\pm$ 0,01	0,02	0,059	0,04 $\pm$ 0,01	0,016	0,11	1.24E <sup>-41</sup>	
GLYCEROPHOSPHOLIPIDS	lysoPC.a.C14.0	2,89 $\pm$ 0,73	1,98	4,2	2,37 $\pm$ 0,71	1,27	5,74	4.87E <sup>-22</sup>
	lysoPC.a.C18.2	32,83 $\pm$ 6,98	20,7	48,8	33,77 $\pm$ 8,86	13,3	60,6	1.23E <sup>-48</sup>
	PC.aa.C30.0 [ $\mu$ M]	4,79 $\pm$ 1,7	2,51	7,76	3,63 $\pm$ 1,16	1,7	7,76	6.36E <sup>-20</sup>
	PC.aa.C32.1 [ $\mu$ M]	17,76 $\pm$ 9,44	5,72	35,9	13,25 $\pm$ 7	4,05	37,8	5.81E <sup>-11</sup>
	PC.aa.C32.2 [ $\mu$ M]	3,8 $\pm$ 1,38	1,98	6,25	2,46 $\pm$ 1,22	0,42	6,34	2.65E <sup>-50</sup>
	PC.aa.C34.4 [ $\mu$ M]	1,97 $\pm$ 0,77	1,14	3,57	1,48 $\pm$ 0,65	0,56	4,24	1.83E <sup>-27</sup>
	PC.aa.C36.2 [ $\mu$ M]	188,61 $\pm$ 19,99	156	229	188,36 $\pm$ 27,31	114	272	1.49E <sup>-18</sup>
	PC.aa.C36.6 [ $\mu$ M]	1,04 $\pm$ 0,28	0,57	1,53	0,9 $\pm$ 0,34	0,35	2,04	2.08E <sup>-14</sup>
	PC.ae.C34.0 [ $\mu$ M]	1,72 $\pm$ 0,54	0,79	2,67	1,51 $\pm$ 0,43	0,61	2,85	1.72E <sup>-09</sup>
PC.ae.C34.2 [ $\mu$ M]	10,84 $\pm$ 2,44	7,08	15,9	10,16 $\pm$ 2,21	5,83	16,8	7.37E <sup>-14</sup>	
AMINO ACIDS	Arg [ $\mu$ M]	93,04 $\pm$ 11,07	73,5	113	79,07 $\pm$ 16,03	34,6	131	1.40E <sup>-32</sup>
	Gly [ $\mu$ M]	286,94 $\pm$ 54,64	204,1	399	238 $\pm$ 48,94	122,2	438,1	1.20E <sup>-24</sup>
	His [ $\mu$ M]	100,94 $\pm$ 15,25	72,3	125	97,22 $\pm$ 14,39	56,4	146	2.06E <sup>-09</sup>
	Met [ $\mu$ M]	32,2 $\pm$ 5,59	22,4	44,2	29,23 $\pm$ 6,78	12,9	58,4	5.22E <sup>-31</sup>
	Orn [ $\mu$ M]	51,9 $\pm$ 8,67	36,3	68,4	46,01 $\pm$ 10,39	22,9	84,8	1.30E <sup>-21</sup>
	Phe [ $\mu$ M]	51,45 $\pm$ 7,55	31,9	64,9	53,84 $\pm$ 10,29	27,9	86,5	1.28E <sup>-48</sup>
	Pro [ $\mu$ M]	195,47 $\pm$ 30,1	151,1	248,6	188,05 $\pm$ 51,14	102,1	388,1	2.50E <sup>-45</sup>
	Trp [ $\mu$ M]	85,15 $\pm$ 11	71,1	107	78,21 $\pm$ 10,87	49,7	124	1.43E <sup>-14</sup>
	Tyr [ $\mu$ M]	74,87 $\pm$ 12,62	47,7	96,7	73,21 $\pm$ 15,74	30,3	125	2.06E <sup>-40</sup>
	Val [ $\mu$ M]	277,1 $\pm$ 60,23	209	444	283,49 $\pm$ 71,8	149	707	3.26E <sup>-41</sup>
	xLeu [ $\mu$ M]	223,62 $\pm$ 42,71	184	328	242,4 $\pm$ 69,57	89,1	632	3.76E <sup>-68</sup>

### **Glucose, insulin and lactate**

**Glucose** levels were measured at every time point. The courses of glucose are given in Figure 2A. As expected glucose levels were constantly low during fasting ( $85.9 \pm 11.3$ mg/dl) and increased 30 minutes after the OGT up to  $141.8 \pm 28.6$ mg/dl. Due to the high amount of fat, the elevation of plasma glucose levels induced by the OLT is delayed if compared with OGT and SLD. The glucose measurements proofed the compliance of the study subjects to follow the study protocol and validated the typical courses of glucose in accordance with the challenges/interventions. Hexose (Figure 2B) was measured with the LC-MS/MS and showed time courses, which absolutely paralleled the course of glucose.

**Insulin** measurements were also performed at every time point. Insulin levels revealed the expected curves over time (Figure 2C) with low values during fasting ( $4.6 \pm 1.5$  $\mu$ U/ml) and high values after carbohydrate intake. Highest insulin levels ( $62.1 \pm 20.3$  $\mu$ U/ml) appeared after the second SLT meal. This strong insulin response to the mixed meal is probably caused by superimposing effects of the previous SLD (“breakfast”).

**Lactate** levels did show a weak, but consistent dependency on the nutritional challenges and increased levels were seen 1h after the OGT (change: + 45%), 1.5h after the SLM (change: + 74%), (change: + 56%) and 2 hours after the OLT (change: + 56%). However, the most prominent change in lactate levels (from  $9.6 \pm 2.9$  to  $66.5 \pm 25.7$ , change = + 595%) occurred at 30 minutes of intensive cycling (Figure 2D) as a marker of increased lipolysis.

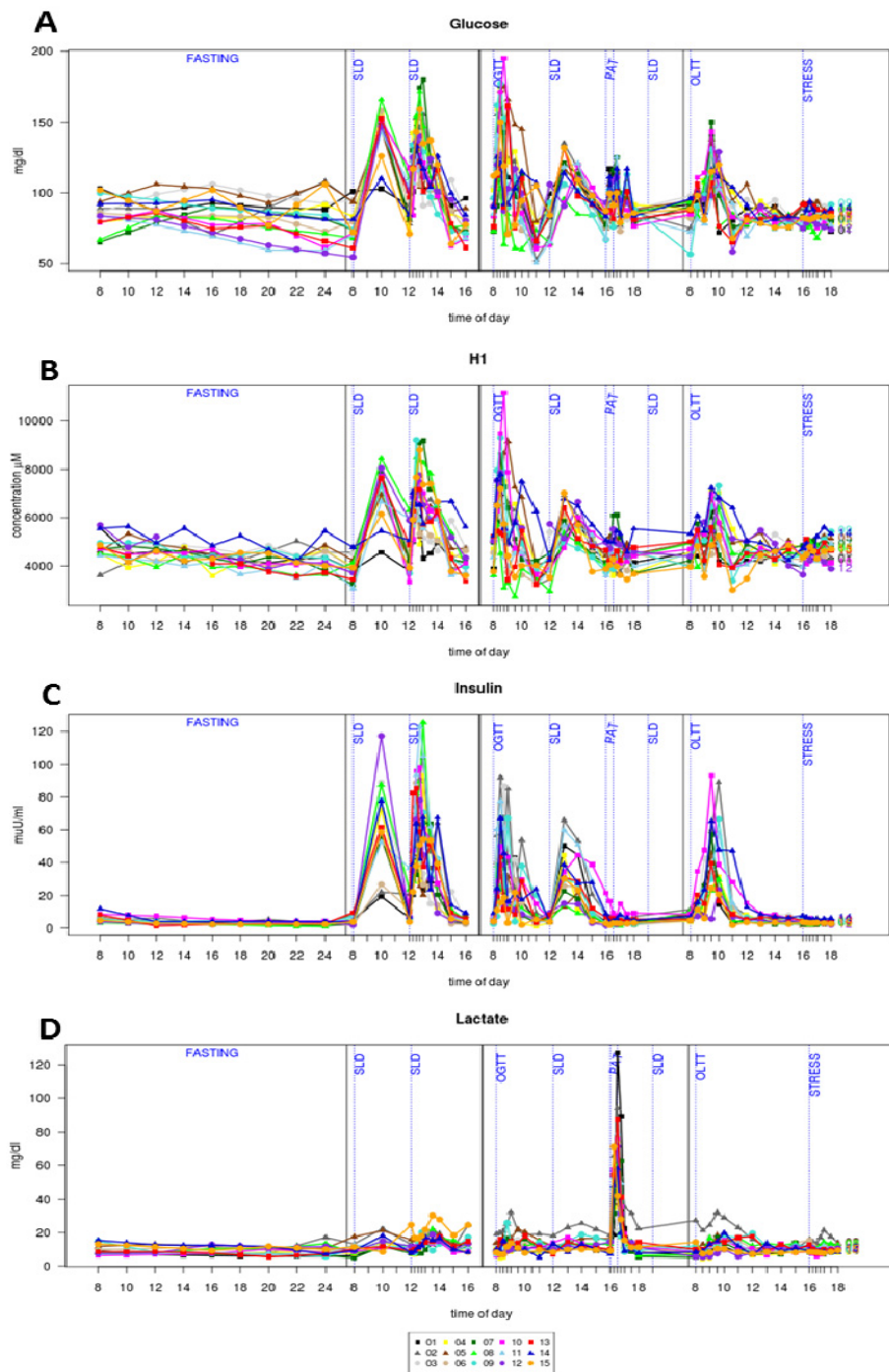


**Figure 2: Time courses of glucose (A), hexose (B), insulin (C) and lactate (D) concentrations over all 56 time-points measured within the HuMet-study.**

Time-concentration curves are color-coded for each volunteer.

### **Free carnitine and acylcarnitines**

Free carnitine (C0) and 30 acylcarnitines were quantified in plasma for all 56 time points and passed quality control criteria. Basal values of the carnitines showed that free carnitine is most abundant with an average concentration of 39.7  $\mu\text{M}$ , followed by acetylcarnitine (5.4  $\mu\text{M}$ ). All other measured acylcarnitines show very low plasma concentrations summing up to 2.42  $\mu\text{M}$ . In general, it can be noted, that the acylcarnitine plasma concentration is decreasing with decreasing chain length. Of the 31 carnitines included, plasma concentrations of 22 acylcarnitines were clearly affected by the challenges as evidenced by Kruskal-Wallis test (Table 2). Within the group of acylcarnitines a high amount (71%) was up- or down-regulated during anabolic or catabolic states.

A cluster analysis was performed in order to investigate, if all acylcarnitines show similar behavior (concentration changes) to the analyzed challenges. Neither label information nor previous data selection method was used to stratify the data. Cluster analysis clearly classified carnitines into two separate main clusters (Figure 3), according to their pattern of concentration changes over time. The bootstrap value (bp) indicates the percentage of times that this cluster was identified by cluster analysis performed on re-sampled data. A high bootstrap value indicates a high robustness of the cluster. The first main cluster combined free carnitine and the short-chain acylcarnitines propionyl-L-carnitine (C3) and isobutyryl-L-carnitine (C4) and isovaleryl-carnitine (C5). In contrast to the longer acyl-carnitines, these may be derived also from odd-chain fatty acids or branched-chain amino acid catabolism (e.g. isovaleryl-, and propionylcarnitine), whereas all other carnitines, including C2 are thought to be mainly lipid-derived and are combined in the second cluster. Inclusion of insulin and glucose values to the analysis assigned both parameters to Cluster 1. Based on these trees, we identified C0, C3, C4 and C5 as carnitines that show concentration profiles similar to insulin and glucose and were therefore elevated in the postprandial phase, whereas all other carnitines species increased postprandially. These differences in concentration profiles over time of the clusters were easily visible in simple time/concentration plots (Figure 4).

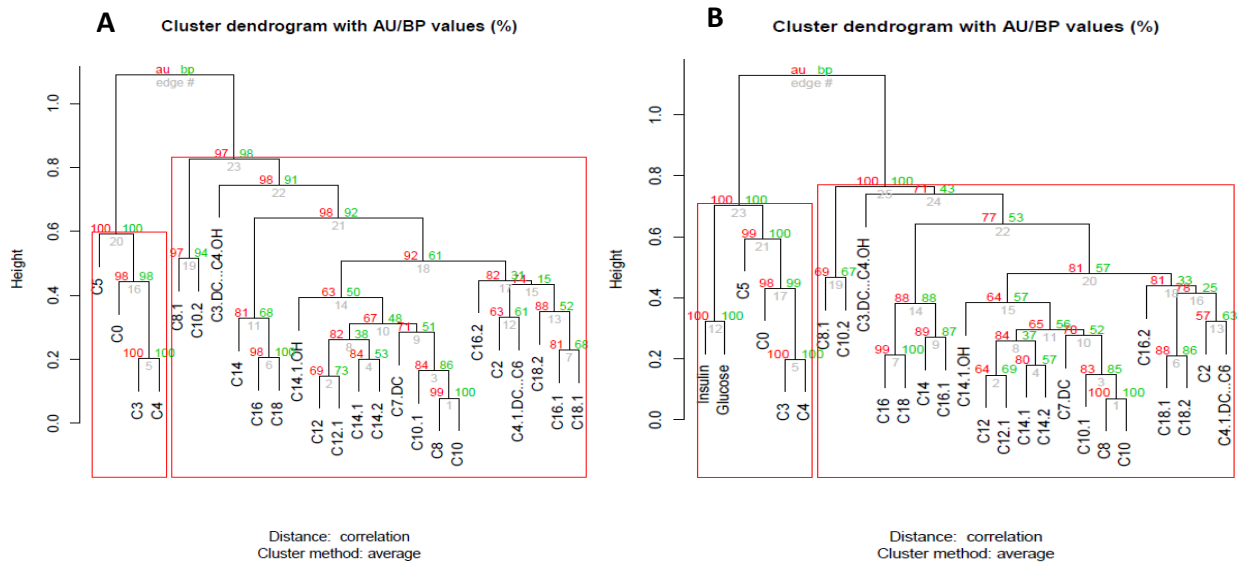


**Figure 3: Cluster analysis classifies plasma carnitines into two main clusters.**

Two p-values, AU (approximately unbiased, red) and BP (bootstrap probability, green) are shown in the cluster dendrogram. The clusters with an AU larger than 95% (highlighted by rectangles), are strongly supported by the data. Addition of insulin to the cluster analysis (B) assigns this parameter to the cluster containing free carnitine and the short-chain acylcarnitines (C3, C4 and C5).

The time profiling of the two clusters showed, that the clusters exhibited a mirror-like anti-correlation over all timepoints. This anti-correlation was mainly supported by the anti-correlation between C0 and C2 as visible in the time concentration curves in Figure 4. When comparing the relative increase of individual acylcarnitines during the whole experiment, a consistent pattern emerged: All acylcarnitines, except C0, C3, C4 and C5, tended to increase in plasma at time points of elevated  $\beta$ -oxidation (Figure 4), e.g. over the 36-hours fasting period and during/ after the ergometry test.

The C<sub>14</sub>-C<sub>16</sub> unsaturated species increased significantly (fold changes > 2), with C<sub>14:2</sub> reaching a 2.8-fold higher concentration after 36 hours of fasting. Palmitoyl- (C<sub>16</sub>), oleyl- (C<sub>18:1</sub>), linoleyl- (C<sub>18:2</sub>), and stearoylcarnitine (C<sub>18</sub>), corresponding to the carnitine esters of the most abundantly stored fatty acids, showed fold increases < 2 by the end of the fasting test.

Acetylcarnitine revealed the most pronounced absolute and relative increase. Its concentration increased significantly by 10.4 $\mu$ M and was therefore almost 2.9-fold higher by the end of the fasting test (15.9 $\pm$ 5.0 $\mu$ M). Free carnitine decreased from 39.6 $\pm$ 7.2 $\mu$ M at baseline to 33.4 $\pm$ 6.1 $\mu$ M

after 36 hours, resulting in an absolute decrease of  $5.7 \pm 1.1 \mu\text{M}$ . Therefore, the absolute increase of acetylcarnitine seems to be only partially derived by acetylation of free carnitine from plasma despite the perfect inverse regulation of both time profiles.

The ergometry test resulted in a stronger and faster decrease of C0 compared to fasting. Two hours after the cycling test, C0 levels were significantly ( $p < 5.59 \times 10^{-6}$ ) decreased by  $10.7 \mu\text{M}$  (to  $28.9 \pm 6.8 \mu\text{M}$ ) compared to baseline levels ( $39.7 \pm 7.2 \mu\text{M}$ ). On the other hand, concentration of C2 was changed stronger by fasting than cycling. Two hours after the cycling test C2 plasma concentration was significantly ( $p < 5.59 \times 10^{-6}$ ) increased by  $10.8 \pm 1.9 \mu\text{M}$ .

The suppression of  $\beta$ -oxidation by elevated plasma insulin levels resulted in an opposite effect on C0 and C2 plasma levels. 120 minutes after the oral glucose tolerance test, the C0 concentration was elevated to  $42.6 \pm 6.6 \mu\text{M}$  compared to basal levels of that day ( $39.7 \pm 9.1 \mu\text{M}$ ), whereas the concentration of C2 was decreased from  $5.8 \pm 1.5 \mu\text{M}$  to  $3.9 \pm 0.5 \mu\text{M}$ .

Overall, the inter-individual variation was augmented in the catabolic state (after the 36 hours fast, time point 10) as indicated by the increased coefficient of variation (24.0% for Cluster 1 and 29.1% for Cluster 2) if compared to baseline (17.9% for Cluster 1 and 17.6% for Cluster 2). Acetylcarnitine and acylcarnitines of Cluster 2 showed the highest dynamics during the fasting challenge as indicated by the fold-changes (Figure 4B).

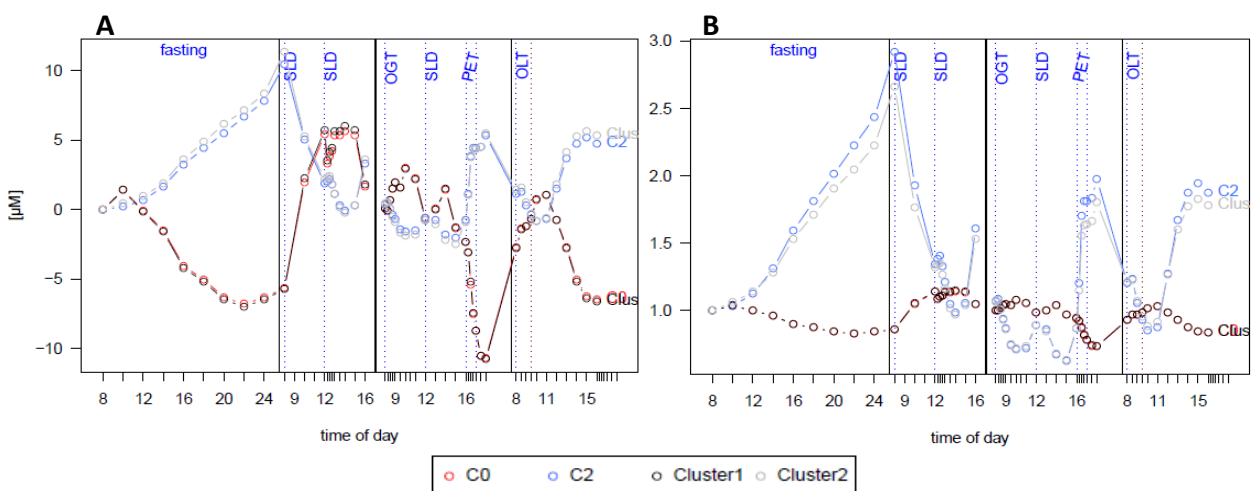


**Figure 4: Mean values of free carnitine, acetylcarnitine, cluster 1 and 2 over all time points.**

4A shows absolute changes centered on basal values and 4B illustrates the fold-changes from baseline.

### **Phospho- and Sphingolipids**

68 phosphatidylcholines (PC, aa = diacyl, ae = acyl-alkyl), 8 *lyso*-phosphatidylcholines and 13 were quantified for all time points and passed quality control. Table 2 displays the 8 PCs and 2 *lyso*-phosphatidylcholines, which showed significant time-dependent concentrations changes. Thus only 18% of the phospholipids were influenced by the challenges performed. Most of the PC species decreased during the fasting period, however, only PCs presented in Table 2 reached significant p-values for the concentration change over time. PC.aa.C32.2 revealed the lowest p-value ( $2.65E^{-50}$ ) of all phospholipids. PC.aa.C32.2 concentration decreased during the prolonged fasting challenge (Figure 5A). A similar trend was observed for some other PCs like PC.aa.32.1 (Figure 5B) and *lyso*-PC.a.C14 (Figure 5C). As illustrated in Figure 5, there were large differences in the individual volunteer-specific concentration curves. However, the trend of a decreasing plasma concentration was visible for almost all volunteers during the fasting challenge.

None of the 13 sphingomyelins revealed significant concentration changes over time upon the performed challenges. Furthermore, we observed a high heterogeneity between volunteers.

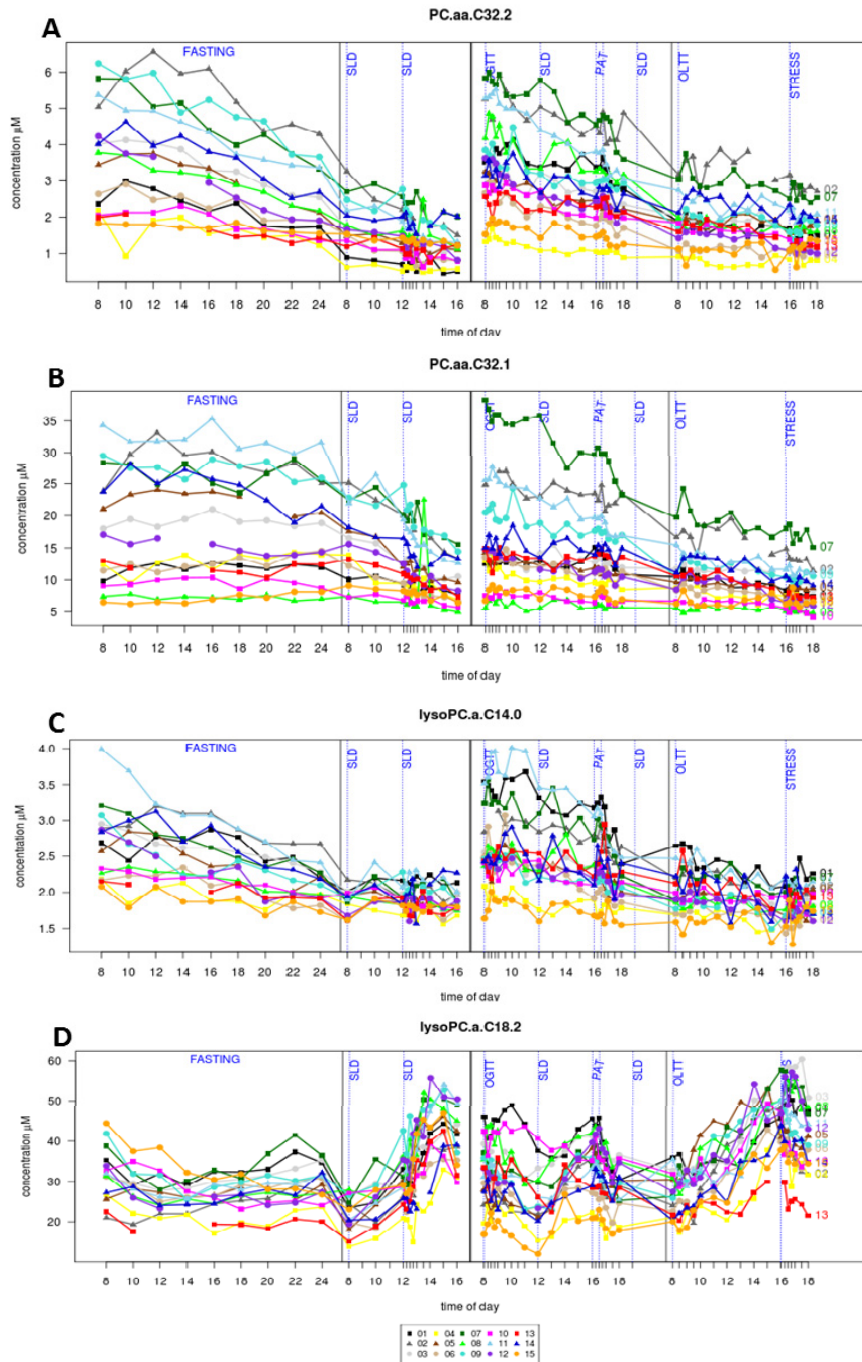


**Figure 5: Time courses of PC.aa.32.2 (A), PC.aa.32.1 (B), lysoPC.a.C14 (C) and (D) lysoPC.a.C18.2 concentrations over all 56 time -points measured within the HuMet-study. Time-concentration curves are color-coded for each volunteer.**



## **Amino acids**

11 out of 14 measured amino acids showed time-dependent concentration changes upon different challenges, pointing to the strong influence of catabolic and anabolic conditions on protein/amino acid metabolism. In detail, Arg, Gly, His, Met, Orn, Phe, Pro, Trp, Tyr, Val and xLeu (leucine and isoleucine are indistinguishable on this platform) were significantly affected by the challenges performed (detailed p-values, see Table 2). Insulin is the primary hormone known to regulate protein metabolism and is long known to lower plasma amino acid levels (29). Accordingly, in our study, plasma amino acid concentrations decreased consequently after the insulin peak induced by OGTT. Time-concentration-profiles over all time points revealed, that all of these amino acids decreased after the OGTT and increased after ingestion of amino acid containing liquid drinks such as the SLD. Therefore, the intake of pure carbohydrates reduced plasma amino acid levels (Figure 6), whereas oral uptake of amino acids resulted in a fast increase of plasma levels, with peak concentration after 2 hours. During our fasting challenge, the 11 individual amino acids showed a multidirectional pattern of their plasma concentration change: some amino acids showed no concentration change (e.g. His, Met), some decreased (e.g. Arg, Gly) and some showed an increase (e.g. Phe, Val, xLeu). At fasting states or during physical exercise protein degradation is enhanced and amino acid oxidation provides a contributing energy source.

Cluster analysis with these 11 amino acids, C2 and acylcarnitines classified time courses of all amino acids with C3, C4 and C5 into the first cluster and C2 with all other acylcarnitines into a separate cluster (Figure 7). C2 can be derived from carbohydrate catabolism,  $\beta$ -oxidation and amino acid degradation, whereas C3 and C5 are derived from amino acids and C4 from amino- or fatty acids. Accordingly, the here performed cluster analysis revealed that C3, C4 and C5 and the amino acids were similar in their respective time-concentration profiles.

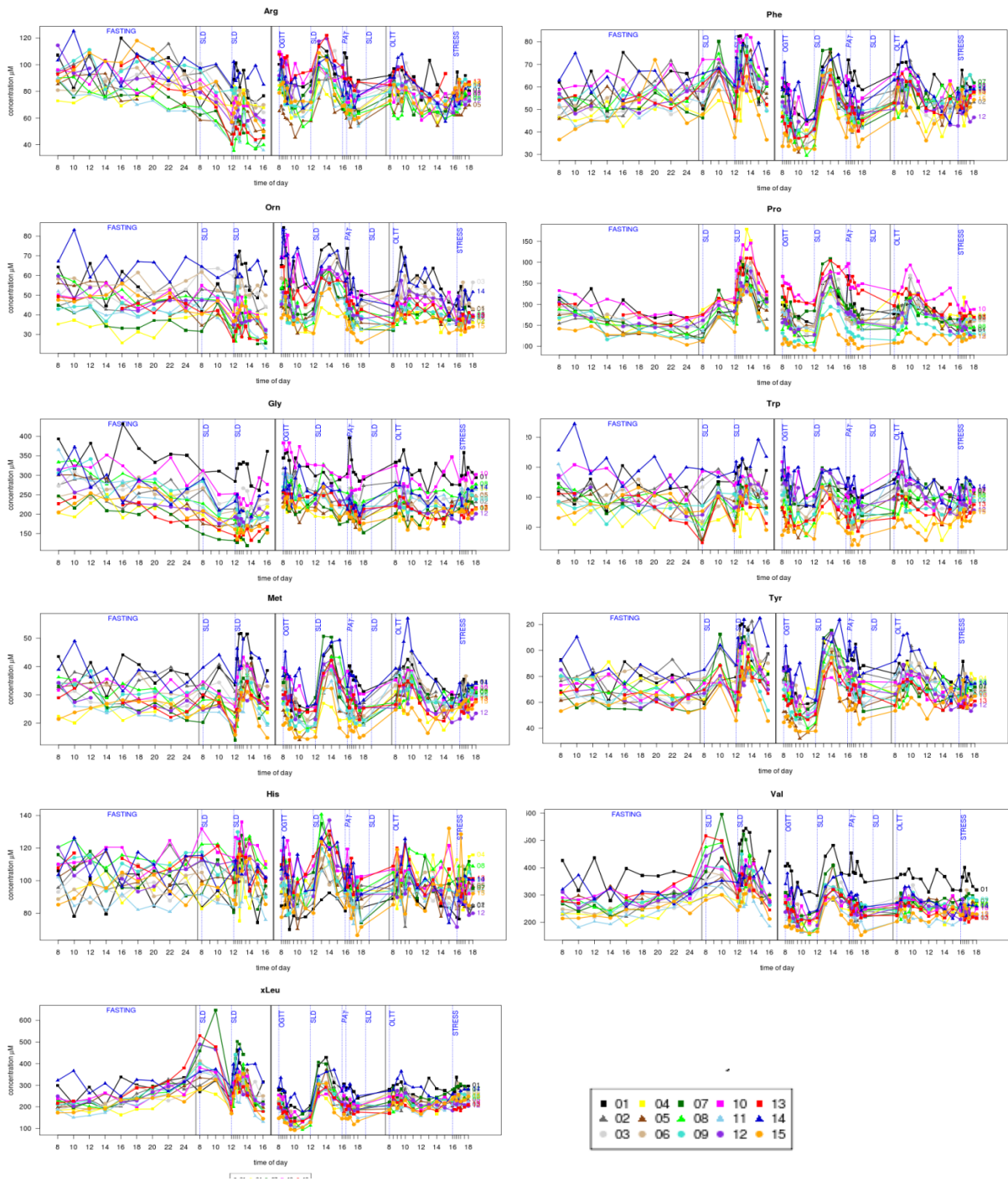


**Figure 6: Time courses of 11 amino acids, with significant concentration changes over all 56 time points measured within the HuMet-study.**

Time-concentration curves are color-coded for each volunteer.

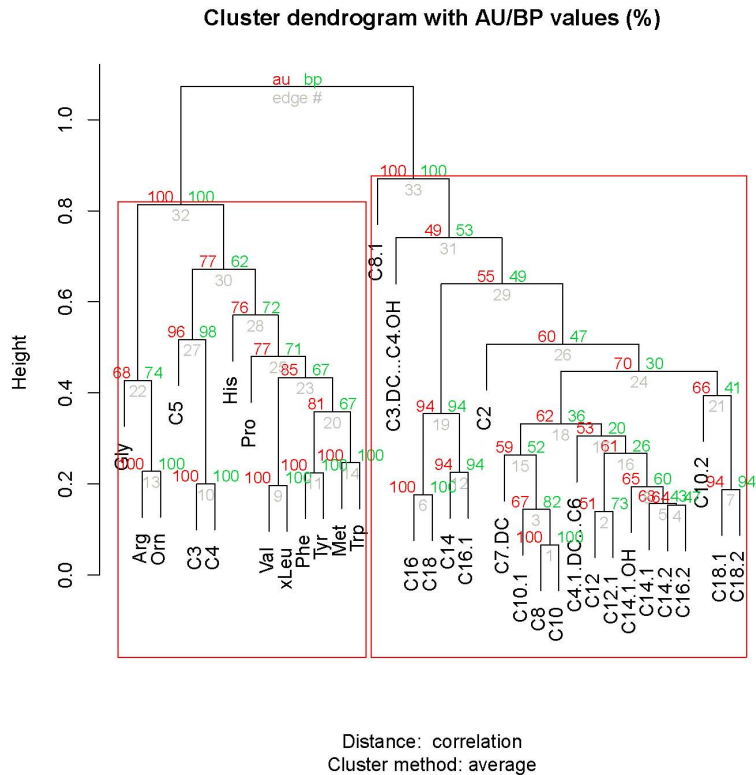


**Figure 7: Cluster dendrogram of 11 amino acids, C2 and acylcarnitines over all time points.**

Two p-values, AU (approximately unbiased, red) and BP (bootstrap probability, green) are shown in the cluster dendrogram. The clusters with an AU larger than 95% (highlighted by rectangles), are strongly supported by the data. The cluster analysis assigned C3, C4 and C5 and the 11 aminoacids into one cluster, indicating similarity in the time-concentration profile of these metabolites.

### Markers of catabolism

In parallel to branched chain amino acids (Ile/leu and valine), the 36 hours period of fasting increased non-esterified fatty acids (NEFAs) and in plasma, acetone in urine and breath and urinary excretion of  $\beta$ -aminoisobutyrate (Figure 8). “Complementarily exhaled breath condensate profiles of putatively annotated m/z peaks showed a decrease in medium oxoacid concentrations such as oxodecanoic acid ( $[C_{10}H_{18}O_3+Na]^+$ ,  $\Delta m/z = 0.024$ ppm) and oxododecanoic acid ( $[C_{12}H_{22}O_3+Na]^+$ ,  $\Delta m/z = -0.065$  ppm). Oxoacids are implicated in fatty acid biosynthesis.” (From: Krug et al. (7), page 2611)

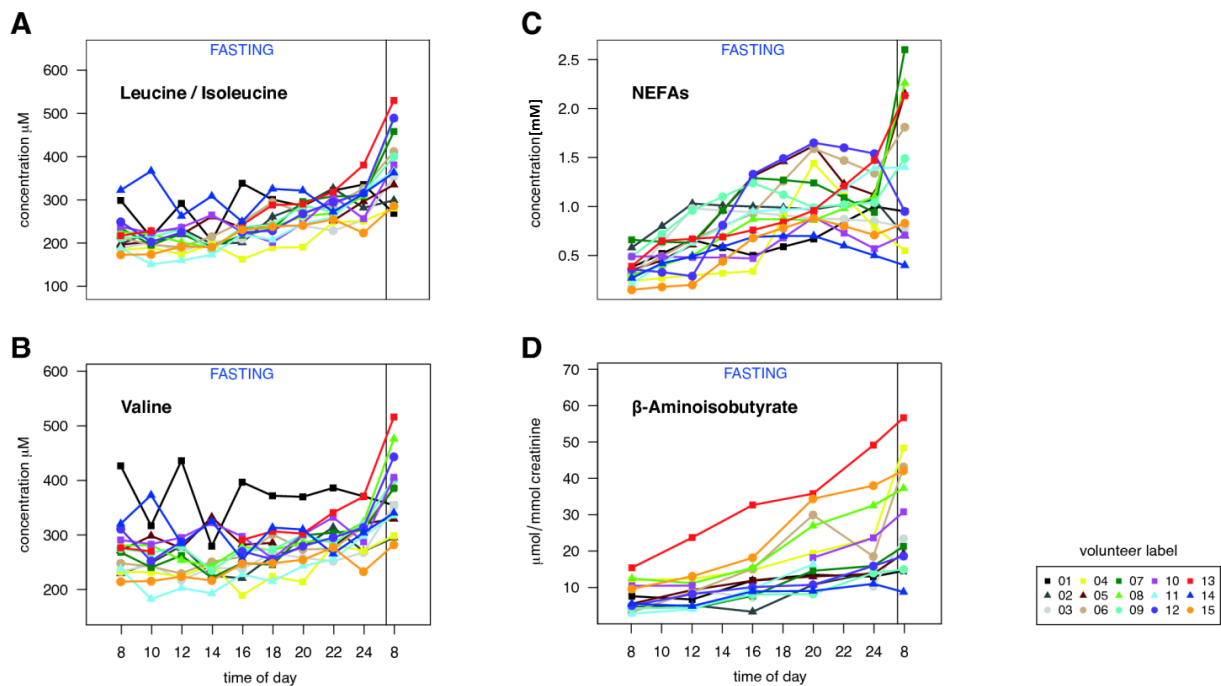


**Figure 8: Concentration changes of selected catabolic marker metabolites during the fasting period.**

Time-concentration curves are color-coded for each volunteer. Common catabolic parameters like branched-chain amino acids (Leucine/Isoleucine (A), Valine (B)) and non-esterified fatty acids (C) measured in plasma, but also less known metabolites like  $\beta$ -Aminoisobutyrate (D) measured in urine, indicate the metabolic alterations caused by strict fasting. Figure from Krug et al. (7), page 2612.

### 2.3.2 Metabolite correlations

“To investigate similarities in the time courses of metabolites we provide a pair-wise cross-correlation analysis of 275 metabolites quantified in plasma, urine and breath air in samples of all time points (Figure 9). High positive correlations shown in red indicate metabolites with coherent concentration changes over time. High positive correlations ( $r=0.94$ ,  $p<2\times 10^{-16}$ ) were found between metabolites like glucose and hexoses measured by different methods, or between metabolites which are known to be biochemically interconnected, such as chylomicron and VLDL quantity ( $r=0.9$ ,  $p<2\times 10^{-16}$ ). Insulin was positively correlated with ‘anabolic’ metabolites like glucose ( $r=0.88$ ,  $p<2\times 10^{-16}$ ) but also revealed high correlations with free carnitine ( $r=0.69$ ,  $p=5.1\times 10^{-9}$ ), propionylcarnitine (C3) ( $r=0.71$ ,  $p=1.0\times 10^{-9}$ ) and proline ( $r=0.68$ ,  $p=7.8\times 10^{-9}$ ). C0 was also positively correlated with the short chain acylcarnitines, especially C3 ( $r=0.71$ ,  $p=7.4\times 10^{-10}$ ) and

valerylcarnitine (C5) ( $r=0.67$ ,  $p= 1.4 \times 10^{-8}$ ), but negatively with longer acylcarnitines and acetylcarnitine (C2), which showed the strongest anti-correlation ( $r=-0.7$ ,  $p=2.1 \times 10^{-9}$ ).“ (From: Krug et al. (7), page 2611)

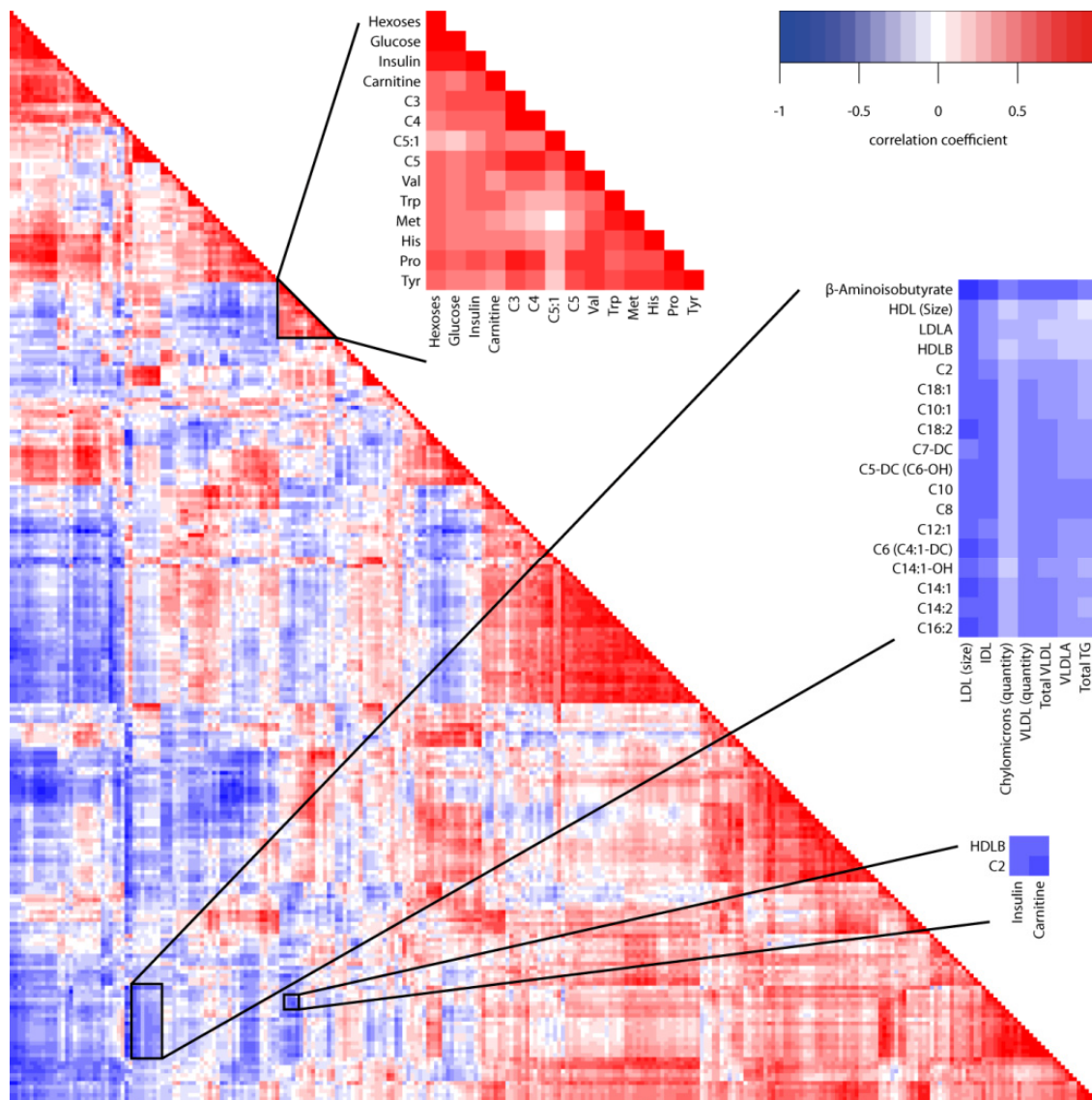


**Figure 9: Correlations in metabolite trends.**

Pearson’s correlations of 275 metabolites, measured in plasma (163), urine (6) and breath air (106). Cross-correlation of mean time courses of each metabolic trait reveals metabolites with a similar or opposite trend in their concentration curves. High positive correlations indicate similar behavior with regard to the direction of change induced by the challenge protocol. Zooming into panels reveals correlated (red) or anti-correlated (blue) metabolites. Figure from Krug et al. (7), page 2615.

### 2.3.3 Metabolites to classify the metabolic condition

The strong anti-correlation of C0 and the acylcarnitines (including C2) was evident over all time points and challenges. Figure 10A displays this mirror-like anti correlation ( $r=-0.66$ ,  $p=2.4 \times 10^{-8}$ ) of circulating plasma levels of C0 and the sum of acylcarnitines and illustrates that the C0/acylcarnitines-ratio is strongly depending on the metabolic condition.

“Read-outs for the metabolic condition were also derived by multivariate data analysis on the entire metabolite profiles in plasma. Principal component analysis (PCA) performed over all time points (Figure 10B) revealed distinct time-dependent trajectories of the metabolic profiles, reflecting the different metabolic conditions during the challenges. This was particularly apparent for the exercise challenge. As highlighted in Figure 10B, excursion of the metabolite profiles began immediately after starting the 30 min cycling exercise, and within only 2 hours the metabolite fingerprints returned almost to the original location.” (From: Krug et al. (7), page 2612)

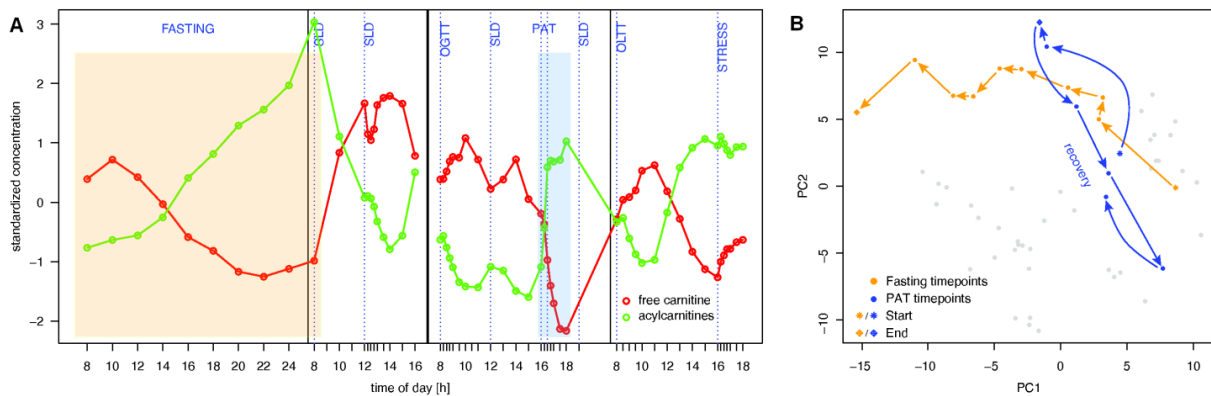


**Figure 10: Metabolic response to challenges.**

(A) The mean plasma concentrations of the 15 subjects at each sampling time point of C0 (red) and the sum of all acylcarnitines including C2 (green) are significantly anti-correlated ( $r=-0.66$ ,  $p=2.4 \times 10^{-8}$ ), reflecting switches between anabolic and catabolic metabolism induced by the various challenges. For better visualization, respective mean concentrations were scaled to a mean of 0 and a standard deviation of 1. (B) The PCA is based on mean concentrations over all 15 subjects at each time point for plasma metabolites with complete measurements (see Methods). PAT challenge time points (blue) started at 4 pm with sampling at 0, 15, 30 min during cycling and in the recovery phase at 15, 30, 60, 90 min after cycling. Time points of the FASTING challenge (orange) started with a sample taken at 8 am (after an overnight fast), followed by samples taken after further 2, 4, 6, 8, 10, 12, 14, 16, and 24 hours. According to the different challenges the samples are located in a time-dependent trajectory in the (metabolic) space spanned by the first two principal components. Figure from Krug et al. (7), page 2614.

### 2.3.4 Inter-individual metabolite variation during challenges

Baseline anthropometric and routine clinical data are presented in Table 3. Our study cohort consisted of 15 young, healthy, male Caucasians of similar BMI ( $23.1 \pm 1.8 \text{ kg/m}^2$ ) and age ( $27.8 \pm 2.9$  years). None of the 15 subjects suffered from a fatty acid  $\beta$ -oxidation disorder, as evidenced by the common diagnosis protocol of plasma acylcarnitine profiling before starting the study.

**Table 3: Baseline characteristics of the study cohort.**

All data are expressed as means  $\pm$  SD (n= 15 subjects). BMI, body mass index; BMR, basal metabolic rate; RQ, respiratory quotient; AUC, area under the curve, CV, coefficient of variation.

	Mean	Range	CV (%)
Age [y]	27.8 $\pm$ 2.9	22-33	10.7
Height [m]	1.8 $\pm$ 0.1	1.7-1.9	3.5
Weight [kg]	77.5 $\pm$ 7.1	63.5-90.4	9.1
BMI [kg/m <sup>2</sup> ]	23.1 $\pm$ 1.8	20.4-25.5	7.6
FM [kg]	14.4 $\pm$ 3.3	8.8-19	23.1
FFM [kg]	59.5 $\pm$ 5.9	47.7-70.4	9.9
Waist circumference [cm]	80.5 $\pm$ 4.6	70.5-87.5	5.7
Hip circumference [cm]	90.1 $\pm$ 4.7	84.1-98	5.2
Heart rate [1/min]	62 $\pm$ 11.4	44-84	18.4
Blood pressure syst. [mmHg]	121.5 $\pm$ 12.1	106-160	9.9
Blood pressure diast. [mmHg]	81.9 $\pm$ 5.9	70-93	7.3
24h-BMR [kcal]	1721.3 $\pm$ 223.6	1300-2160	13
RQ	0.85 $\pm$ 0.1	0.8-1.0	6.5
Total-Cholesterol [mg/dl]	169.8 $\pm$ 37.5	124-253	22.1
LDL-Cholesterol [mg/dl]	104.5 $\pm$ 33.3	59-165	31.9
HDL- Cholesterol [mg/dl]	60.2 $\pm$ 14.9	37-99	24.8
Triglycerides [mg/dl]	78.1 $\pm$ 26.2	50-125	26.2
Resting Plasma Lactate	0.9 $\pm$ 0.3	0.5-1.3	29
Fasting Plasma Glucose	84.9 $\pm$ 7.5	75.4-95.7	8.8
Plasma Glucose AUC [mg/dl]	339.9 $\pm$ 29.9	301.6-382.7	8.8
Fasting Plasma Insulin	5.7 $\pm$ 1.4	3.6-7.9	23.6
Plasma Insulin AUC [mg/dl]	22.9 $\pm$ 5.4	14.5-31.9	23.6

As visualized in Figure 11A, within this study the concentration difference in a metabolic parameter was markedly increased or decreased by a metabolic challenge. Insulin revealed highly diverse biological responses to the same oral glucose load in different subjects with some subjects showing a second insulin peak (Figure 11A). Nonetheless, we observed no obvious correlations between the

individual insulin response curves and basal anthropometric data or clinical parameters values (Kendall correlation).

“For anabolic parameters like glucose or insulin the between subject-distance was enlarged in postprandial states, e.g. after the OGTT, SLD and OLTT, whereas concentrations were very stable and showed little variation between the volunteers during the 36 hours fasting. In contrast, the fasting caused the most pronounced between-subject differences in catabolic metabolites. For example, the increase in plasma C2 after 36 hours fasting was accompanied by an elevated coefficient of variation (31.6%) when compared to baseline (20.5%). The increase of inter-individual variation in catabolic metabolites during fasting was observed in all sample types (Figure 11B). Figure 11B further shows, that volunteer 13 (V13=red) and volunteer 14 (V14=dark blue) mark the extremes of plasma C2 concentration changes within the study cohort. The plasma C2 concentration of V13 was more than three-fold higher (25.8  $\mu\text{M}$ ) at the end of the fasting period compared to the concentration observed in V14 (8.1  $\mu\text{M}$ ). Interestingly, this differential response to the fasting state spans across other catabolic marker metabolites like acetone in urine and breath, as evidenced by the consistent position of the subjects in the time-concentration profiles. V13 showed all indicators of a strong fasting response with enhanced levels of plasma non-esterified fatty acids and highest  $\beta$ -aminoisobutyrate in urine of our cohort (Figure 8D). In contrast, V14 showed the lowest levels in all these fasting state metabolites of different sample types. A PCA (Figure 11C) of plasma metabolites with samples colored by subject shows that the samples of each subject were grouped together. This grouping was evident over all time points and even more distinct if only samples of the 36 hours fasting period were included.



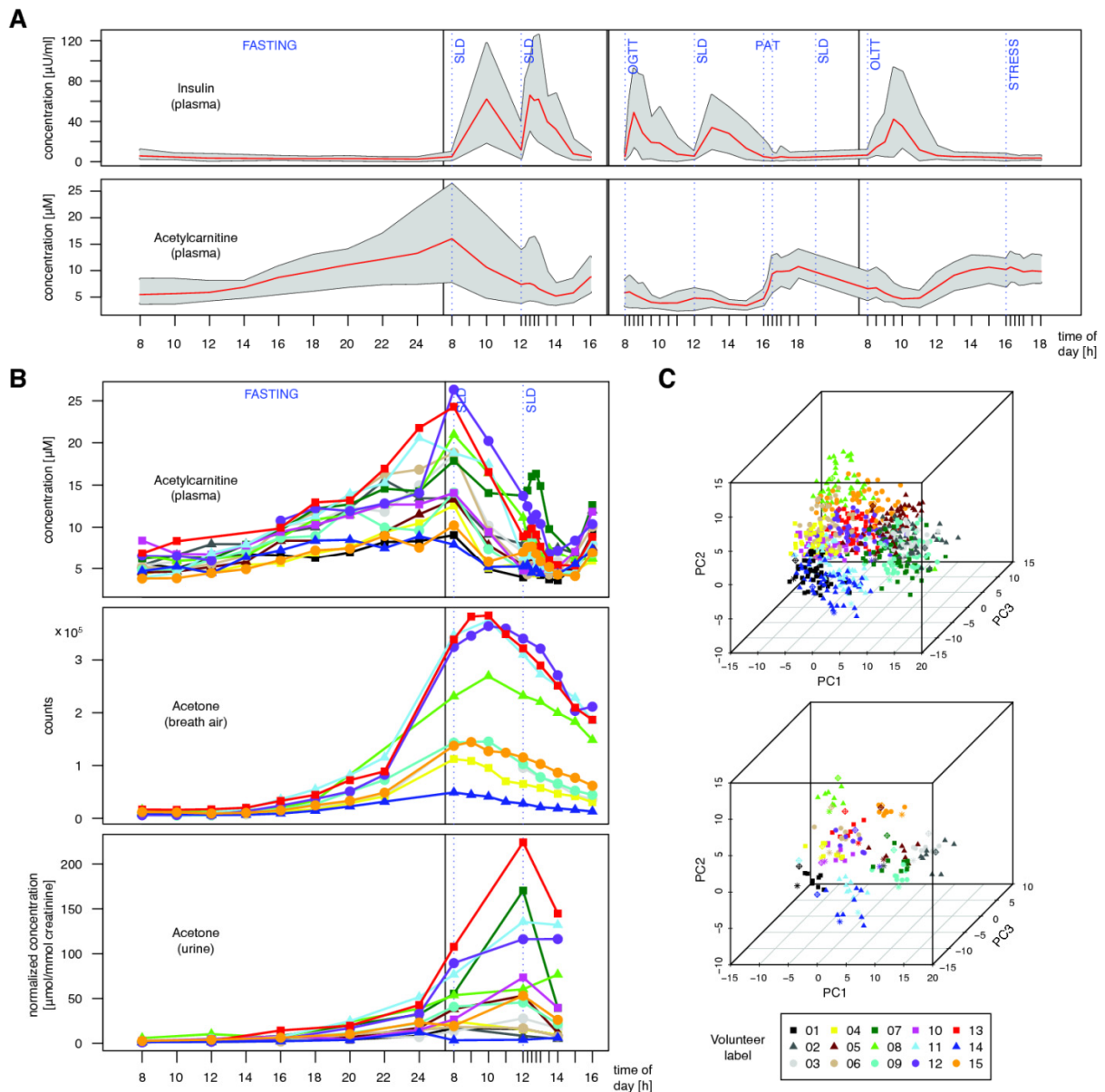


**Figure 11: Inter-individual variation of metabolite concentrations in the context of challenges and sample types.**

(A) Depending on the challenges, the inter-individual variation in the concentrations of metabolites increased or decreased. The mean plasma concentrations of insulin and C2 are shown as red curves. The grey area denotes the between subject-distance, i.e. the range between the minimal and the maximal concentration observed in any participant. (B) For day 1 and day 2, the individual C2 concentration curves in plasma are shown for each subject (top). The quantities of acetone in breath air (determined by PTR-MS) and urine (determined by NMR) (middle and bottom) match the observations seen for C2 (determined by MS/MS) in plasma. The large differences in the concentrations between subject 14 and subject 13 are consistent across the three sample types. (C) The upper plot shows the scores plot of a PCA based on the concentrations of all metabolites measured in plasma for all 15x56 samples. Beneath, only samples of the FASTING challenge are included in the PCA. In spite of intra-individual variations due to various challenges and sampling times, the samples of each subject are grouped together by the PCA. Figure from Krug et al. (7), page 2615.

### **2.3.5 Read-outs from a $\beta$ -oxidation model provide stronger associations with phenotypic data than absolute metabolite concentrations**

V13 and V14 showed marked differences in their responses to the fasting challenge. We assumed that those differences could be associated with the volunteers muscle or fat mass, expecting that higher fat mass should correspond with a higher plasma concentration of NEFAs, resulting in higher ketone body production in the catabolic condition. However, V13 and V14 were similar in their anthropometric measures like BMI (22.8 vs. 25.1kg/m<sup>2</sup>) or RMR (1,710 vs. 1,850 kcal). A correlation analysis revealed no correlation between diverse metabolite concentrations and anthropometric measures in our study cohort (Table 4). Therefore, we hypothesized that the individual's metabolic capacity in utilization of fatty acids might provide an explanation for the disparate responses to the fasting condition.

Consequently, we defined a mathematical model of fatty acid  $\beta$ -oxidation using plasma acylcarnitines of different chain lengths with their characteristic changes during 36 hours of fasting as input and output variables, and derived model driven ratios. In comparison with the metabolite levels these model driven ratios strongly increased correlations as shown for correlations of plasma glucose levels with C2, C16 or C2/C16 (Figure 12). As presented in Table 4 a series of model-derived metabolite ratios were significantly correlated with anthropometric or biochemical parameters. These model-derived ratios revealed far better correlations with anthropometric parameters than the metabolite-ratios, as indicated by the *p-gains*. Furthermore, in some cases solely the model-driven ratios were significantly correlated with anthropometric parameters (bold values in Table 4). As presented in Table 4, especially the ratio C2/C16 provides stronger correlations with anthropometric measures (e.g. BMI, fat mass or muscle-fat-ratio) than absolute plasma concentrations of C2 or C16. Therefore, this model-derived ratio strongly improved statistical correlations, expressed as *p-gains* larger than 1, yielding for example 8.8 for correlation with BMI, 7.3 for muscle to fat ratio and up to 18 for total fat mass. Similarly, biochemical parameters, such as fasting glucose or insulin levels, revealed higher correlation coefficients with model-derived ratios than with the absolute plasma levels for example of acylcarnitines (Table 4).“ (From: Krug et al. (7), page 2612-2614)

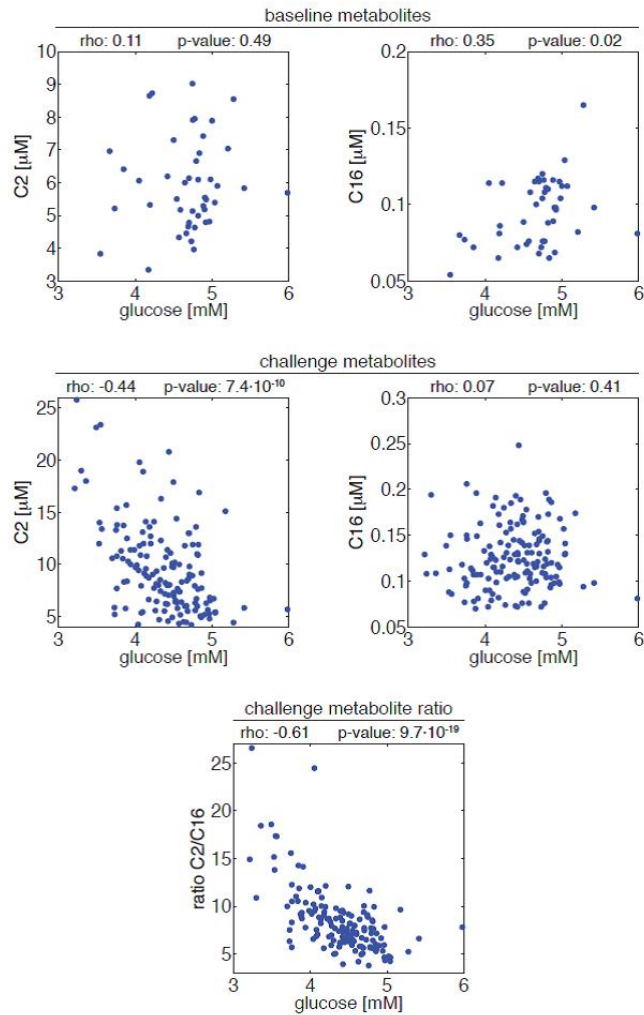


**Figure 12: Comparison of baseline metabolite, challenge metabolite and metabolite ratio levels with glucose concentration.**

Under non-challenging conditions (baseline) metabolites show no (acyl-carnitine, C2) or only weak (palmitoyl-carnitine, C16) correlation with glucose levels (top panels). Under challenge (fasting) conditions C2 is significantly correlated with glucose (middle panels). Taking metabolite ratio C2/C16 instead, greatly increases this correlation (p-gain of  $7.6 \times 10^6$ ). For comparing metabolite levels Spearman's rank correlation statistics (rho, p-value) was calculated. Figure from Krug et al. (7), supplemental data.

**Table 4: Model-derived metabolite ratios improve correlation with metabolic parameters.**

Correlations between anthropometric and/or biochemical parameters (ABP) with metabolite concentrations (C4, C6, C16, C18 and C2) and model-driven ratios derived from the  $\beta$ -oxidation model. Biochemical parameters, acylcarnitine and C2 concentrations were measured during the fasting period of study day 1. Rank correlation p-values were corrected for multiple testing using FDR at global significance level of 0.05. Bold values indicate cases for which only model-driven ratios, but not single metabolite levels, were significantly correlated with anthropometric or biochemical parameters. Model-driven ratios, reflecting biological processes, improve statistical correlations with anthropometric and biochemical parameters of energy metabolism when compared to the correlations with single metabolite concentrations, resulting in p-gains bigger than 1. Table from Krug et al. (7), page 2616.

			rank correlation					
			ratio C2/Cx vs. ABP		C2 vs. ABP		Cx vs. ABP	
p-gain	Cx	ABP	$p^{(2)}$	$\rho^{(3)}$	$p^{(2)}$	$\rho^{(3)}$	$p^{(2)}$	$\rho^{(3)}$
7.5x10 <sup>6</sup>	C16	sum of hexoses (p)	1.9x10 <sup>-15</sup>	-0.61	1.4x10 <sup>-8</sup>	-0.48	0.632	0.07
3.5x10 <sup>5</sup>	C16	$\beta$ -aminoiso-butyrate (u)	1.6x10 <sup>-16</sup>	0.77	5.7x10 <sup>-11</sup>	0.67	0.901	0.03
2.9x10 <sup>3</sup>	C6 <sup>(1)</sup>	free carnitine (p)	5.1x10 <sup>-7</sup>	-0.41	0.001	-0.29	0.918	0.02
221.5	C18	glucose (p)	1.4x10 <sup>-5</sup>	-0.46	0.003	-0.35	0.520	0.11
87.1	C4	free carnitine (p)	2.5x10 <sup>-6</sup>	-0.39	0.001	-0.29	2.1x10 <sup>-4</sup>	0.33
51.4	C18	hydroxyiso-butyrate (u)	4.1x10 <sup>-9</sup>	0.59	2.1x10 <sup>-7</sup>	0.55	0.914	0.03
18.1	C16	fat mass	0.015	-0.68	0.731	-0.19	0.267	0.44
10.9	C18	creatinine (p)	0.028	-0.62	0.405	-0.35	0.301	0.42
8.8	C16	BMI	0.002	-0.77	0.944	-0.04	0.014	0.70
8.5	C16	Body fat percentage	0.042	-0.58	0.798	-0.14	0.354	0.39
7.3	C16	muscle-fat-ratio	0.037	0.60	0.850	0.11	0.271	-0.43
5.3	C4	insulin (p)	0.018	-0.28	0.093	-0.23	0.200	0.19

Cx: acylcarnitine with chain length x

(1): detection methods cannot distinguish between C6 and C4:1-DC

(2): p-value corrected for multiple testing using FDR at global significance level of 0.05

(3): Spearman's rank correlation coefficient

(p): parameter concentration determined in blood plasma

(u): parameter concentration determined in urine

**bold:** significant correlation only between ratio and ABP

## 2.4 Discussion

### Metabolite changes reflect the challenges

“The human metabolome is subject to continuous changes. Anabolic conditions, as after food intake and catabolic states during fasting or physical exercise are an expression of the plasticity of metabolic control. Here, we present a study that conceptually explores the metabolic plasticity by analyzing metabolite changes in response to 6 metabolic challenges stimulating either catabolic conditions (fasting and cycling) or anabolic states (OGTT, OLTT and SLD). According to the catabolic to anabolic shifts and vice versa, the plasma concentrations of standard parameters like insulin, glucose and lactate revealed the expected alterations, demonstrating the validity of the applied challenges and the acquired data-set. .” (From: Krug et al. (7), pages 2612-2614)

The PC concentration changes of the volunteers showed no uniform or significant trend after the OGTT, in line with a previous report (30). However, we observed a significant reduction in phospholipid levels during the prolonged fasting. Phospholipids are important components of the cell membranes and lipoproteins and the reduced plasma levels during fasting might be a consequence of reduced lipoprotein levels during fasting. In this study, total cholesterol showed a tendency to decrease during fasting (data can be accessed under <http://metabolomics.helmholtz-muenchen.de/humet/metabolites>). Such a mechanism may be supported by the results of Wiesner et al., showing that many PC species associated with total cholesterol levels (31).

None of the 13 sphingomyelins revealed significant concentration changes over time upon the performed challenges. Furthermore, we observed a high heterogeneity between volunteers. Notably, Pietiläinen et al. reported that sphingomyelins are remarkably similar within twin pairs (32). This implies that the genetic component might be of higher importance for the determination of systemic sphingolipid levels than the effects of catabolic or anabolic states, and explains the here observed remarkably large individual differences.

“As insulin drives the transition from a fasting state to a fed state, its time-course was positively correlated with “anabolic” metabolites like glucose, but also revealed less known correlations over time with free carnitine and the short chain acylcarnitines C3, C4 and C5. During fasting, increased lipolysis and  $\beta$ -oxidation of fatty acids in mitochondria provides most of the energy needed. Fatty

acids enter the cytosol from plasma, are converted into CoA-thioesters and subsequently transferred into the mitochondria via the palmitoyl-CoA carnitine transferase II shuttle (33, 34). Since this acyl-CoA import requires C0, the here observed decline in plasma C0 concentrations during fasting may indicate that the cellular carnitine supply is increased by its uptake from plasma. Moreover, it has been hypothesized previously, that an intracellular accumulation of acetyl- and acyl- CoA, due to increased fatty acid flux through  $\beta$ -oxidation, is buffered by a release of the respective carnitines into plasma (35, 36). Our results are consistent with this view, as plasma levels of C2 and all acylcarnitines, except C3, C4 and C5, showed a strong increase in times of elevated  $\beta$ -oxidation, e.g. during fasting or exercise. When catabolism was reversed to an anabolic state with elevated plasma insulin levels, the exact opposite effect on the levels of C0 and C2, or the sum of acylcarnitines was observed. Therefore, the circulating plasma levels of C0 and the sum of acylcarnitines responded in an almost mirror-like anti-correlation to catabolic and anabolic challenges. The mirror-like anti-correlation of C0 versus C2 was observed over the entire 4 days of the trial and suggests that these two metabolites are the best markers for any shift from catabolic to anabolic state and *vice versa*.

Anabolic and catabolic states of metabolism were also obvious in a PCA performed over all time points that revealed distinct time-dependent trajectories of the metabolic profiles. These trajectories reflect the plasticity of the metabolite profile by illustrating metabolite alterations induced by the challenges and the return to the initial situation.

### **Inter-individual variation can be extended and compressed by metabolic challenges – the accordion effect**

Recognizing that the human metabolome is influenced by a number of factors, strict subject inclusion criteria were met in the presented study. As intended, the study participants consisted of a homogeneous group (Table 3) of 15 healthy, male Caucasians within a narrow BMI and age range. Sample collection, processing and subject treatment were also highly standardized to minimize variation. Despite best possible standardization, our metabolome data demonstrated between-subject variation, probably originating from environmental conditions (dietary habits, lifestyle, etc.) on the basis of a given genetic/epigenetic make-up. A PCA of all plasma metabolites showed that in spite of large intra-individual variation over the various challenges, the samples of each subject

were clustered together. This was even more pronounced after a strong metabolic challenge like a 36 hours fasting period. Regarding the individual time courses of the measured parameters, we observed that the inter-subject variation of a metabolic parameter was markedly increased or decreased by a metabolic challenge, even in volunteers of otherwise similar phenotypic appearance. For anabolic parameters like glucose or insulin the distance between subject concentrations was enlarged in postprandial states, e.g. after the OGTT, SLD and OLTT, whereas the concentrations were very stable and showed little variation between the volunteers during the 36 hours fasting. In contrast, the fasting caused the most pronounced between subject differences in catabolic metabolites, e.g. C2 in plasma or acetone in urine and breath. The elevation in inter-individual variation observed during the fasting challenge allowed the identification of two distinct metabotypes, namely V13 and V14. Those two volunteers marked the extremes of the study cohort as shown for the catabolic metabolites C2 in plasma or acetone in urine and breath (Figure 11B). V13 showed all indicators of a “classical fasting response” with enhanced concentrations of plasma non-esterified fatty acids as an indicator of enhanced lipolysis, increased ketone body production with increased urinary excretion and exhalation in breath, and also highest urinary excretion of  $\beta$ -aminoisobutyrate (Figure 8D).  $\beta$ -aminoisobutyrate is a thymine catabolite which was reported to increase fatty acid oxidation and reduce body fat in supplemented mice (37, 38). Our results indicate that  $\beta$ -aminoisobutyrate also provides a reliable marker for the degree of fatty acid oxidation in humans. In contrast, V14 appeared almost completely refractory to the catabolic condition with only small increases in fasting state metabolites and  $\beta$ -aminoisobutyrate of different sample types. This shows not only the high qualitative and quantitative consistency across samples from different body fluids and different analysis platforms, but also that we can identify distinct metabotypes even in our homogenous cohort by differences in the responsiveness to challenges, such as extended fasting.

**A model of  $\beta$ -oxidation provides parameters which correlate with the individual’s metabolic condition.**

In search of the origin of the inter-individual variation, especially in the fasting response, we performed a correlation analysis of metabolite concentrations and parameters derived from anthropometric measurements (body mass, fat and muscle mass, RMR etc.), expecting that, for

example, higher fat mass should correspond with higher non esterified fatty acid or ketone body production during catabolic conditions. However, in our healthy, young cohort the observed differences in metabolite concentrations during fasting provided no significant associations with anthropometric measures like body mass, fat and muscle mass or RMR (Table 4). Therefore, we hypothesized that the individual's metabolic capacity in utilization of fatty acids might provide an explanation for the disparate responses to the fasting condition. Consequently, we asked whether "apparent metabolic rates" from a biological process could provide a measure for metabolic capacity. To derive such "apparent metabolic rates" reflecting the capacity for fatty acid breakdown ( $\beta$ -oxidation), we developed a mathematical model of mitochondrial  $\beta$ -oxidation. Our model is based on the linearity and the irreversibility of the central reactions by which fatty acids from adipose tissue are subsequently degraded in mitochondria. We used plasma acylcarnitines of different chain lengths with their characteristic changes during 36 hours of fasting as input and output variables in our model, assuming that those provide a direct measure of overall  $\beta$ -oxidation function. This assumption was supported by findings in inherited diseases of  $\beta$ -oxidation which are associated with specific changes in plasma acylcarnitine levels (8, 39). Genome wide association studies also reported robust statistical associations between acyl-carnitines and genetic variants that are located in or near  $\beta$ -oxidation enzymes (22, 40). In our model, the intermediates of  $\beta$ -oxidation were therefore represented by C-2 shortened acylcarnitines (C<sub>n</sub>-2, C<sub>n</sub>-4 etc.) and the output trait by acetyl-CoA. With stearic acid (C18-acylcarnitine) as a starter and C2 as the final product, a series of acylcarnitine ratios were derived from the model which correlated significantly with anthropometric parameters such as BMI, total body fat mass, body fat content (%) or muscle to fat ratio (Table 4). Especially, the C2/C16 ratio showed strong anti-correlation with volunteer's fat mass, suggesting this ratio as an interesting target for metabolomics studies with overweight or obese subjects. In comparison to absolute plasma concentrations of C2 or C16, the model-derived ratio substantially improved statistical correlations. This suggests that models based on biochemical knowledge can help to explain associations and variations amongst metabolite patterns, body composition and metabolic state much better than absolute metabolite concentrations. Although, the  $\beta$ -oxidation model has proven its feasibility by the coherence of the derived ratios with parameters like fat mass, it has some caveats. For example, it was assumed that fatty acid import into cells as well as acylcarnitine efflux are not limiting and that the stepwise shortening of the fatty



acid is irreversible at least up to the last enzyme that mediates the thiolytic cleavage. The model also assumed steady state conditions with capacity limits determined only by the available redox-equivalents (FAD and NAD). When  $\beta$ -oxidation flux exceeds citric acid cycle and respiratory chain activity in muscle, hepatic ketone body production is increased. With a delay in time this can easily be followed by enhanced excretion of acetone in breath and urine as shown in our volunteers (Figure 11B). Extending the  $\beta$ -oxidation model to ketone body production could further improve analysis of coherent changes in metabolome data sets. Thus, it seems valuable to apply such quantitative modeling approaches also to other metabolite data sets to obtain parameters that better reflect pathway capacities. These may help in the characterization of human metabolotypes in genotype-phenotype association studies.

#### **Perspectives: from healthy to disease states.**

Recent biomarker discovery studies based on metabolomics have identified plasma free fatty acids, acylcarnitines and ketone-bodies, branched chain amino acids and amino acid degradation products to be significantly altered in states of insulin resistance or diabetes type 2 (41-43). These putative “metabolite biomarkers” of a pre-diabetic or diabetic state strongly resemble the signature of metabolite changes of a prolonged fasting state (>20 hours) in our healthy volunteers. In this respect, insulin-resistant or diabetic patients show metabolite profiles of a catabolic condition, even in an otherwise anabolic state. Increased keto-acid levels in urine or their volatile derivatives like acetone found in breath characterize an advanced fasting state in healthy humans and may in a postprandial condition report insulin resistance or diabetes specific metabolic impairments that can easily be detected in non-invasive samples like urine or breath.

## **2.5 Conclusion**

We have generated a large data set of time-dependent metabolite profiles representing normal and extreme metabolic conditions of young, healthy, male volunteers measured in different body compartments and by a variety of state-of-the-art NMR- and MS-based methods. To our knowledge, this is the first time that all biochemical processes related to extended fasting, glucose and lipid tolerance tests, controlled meals, physical exercise and physiological stress are explored in a single metabolome study. In an effort to describe the flexibility of the organismic response, we

demonstrated an “accordion effect” for metabolite profiles, showing that challenges increase metabolite variability between volunteers allowing discrete metabotypes to be identified that would not be seen under normal fasting conditions. Inter-individual variability of selected metabolites was consistent across the sample types studied and emphasizes the potential diagnostic use of non-invasive samples like urine or breath. Plasma free carnitine and acyl-carnitines were shown to define best any catabolic and anabolic conditions and their transitions, and their ratio could be useful as marker for the metabolic state. These metabolites used as input and output variables in a quantitative systems biology model of  $\beta$ -oxidation revealed parameters that provide more sensitive discriminators of the individual metabolic and anthropometric variation than absolute plasma concentrations, demonstrating that such modeling may aid in the interpretation of large metabolomics data-sets. The freely available data set of the HuMet-study provides a reference for future human studies and may also be used to develop and validate other metabolic models”. (From Krug et al. (7), pages 2614-2617)

# 3 THE IMPACT OF TWO COMMON GENETIC VARIANTS ON METABOLITE RESPONSE TO NUTRITIONAL INTERVENTIONS

## 3.1 Introduction

Twin studies in monozygotic or dizygotic twins (44–46) and human family studies of early-onset cardiovascular disease (47) have shown the heritability of metabolite profiles. Additionally, a targeted metabolite profiling approach combined with genome wide genotyping has revealed significant associations between common genetic polymorphisms and changes in specific metabolites (22, 48, 49). Gieger et. al. showed that common genetic variants in well-characterized genes (like *FADS1*, *LIPC*, *SCAD*, *MCAD*) altered metabolic traits of metabolic pathways in which the gene products are known to reside (48). These studies illustrate the power of novel metabolic analysis approaches as a tool to investigate the physiological or pathophysiological impact of gene variants on the metabolite profile. However, these genome-wide association studies have not described a metabolite profile for the variants in the *FTO* or the *TCF7L2* gene associated with obesity or T2DM respectively. One possible explanation is that GWAS generally rely on blood samples collected after an 8 hour overnight fasting period. This homeostatic type of sample might not be adequate to show small effects of genetic variants, after the necessary adjustments for BMI and T2DM. As shown within section 2 of this thesis, the analysis of metabolite time profiles during standardized metabolic challenges, might help to uncover metabolite profiles, not observable at baseline conditions.

Therefore, the VID (Virtual Institute for Diabetes)-study was performed. This study aimed to investigate the effects of a common variant within the *TCF7L2* gene (rs7903146) and of a common variant within the *FTO* gene (rs9939609) on plasma metabolite concentrations. The identification of metabolites altered by these gene variants will eventually improve our understanding of the gene

functions, the effects of the gene variations, their impact on metabolism and how they relate to disease development.

As both SNPs are associated with metabolic diseases acquired by over-nutrition, we decided to challenge the metabolism by standardized nutritional challenge tests, like an oral glucose tolerance test. Research design and methods used within this study, were similar for both gene variants under investigation. Therefore, in this dissertation research design and methods are described in the following section for both gene variants. After this, the results are described and discussed separately for both gene variants; the *FTO* gene variant under section 3.3. and the *TCF7L* gene variant in section 3.4. A more detailed literature review on the gene variants is provided as introduction to these sections.

## **3.2 Research Design and Methods**

### **3.2.1 Study participants and study design**

#### **Study participants**

For the present study, 55 male participants aged between 35 and 67 years were recruited from the KORA F4 cohort, which provides an extensively phenotyped and genotyped sample from the general population. The KORA F4 cohort comprises male and female individuals aged between 35 and 84 years, who are residents of the region of Augsburg, Southern Germany. Participants for the present study were selected according to their genotype. Volunteers homozygous for the *FTO* risk variant (AA) in SNP rs9939609 were assigned to the *FTO* group, volunteers homo- or heterozygous for the *TCF7L* risk variant (TT or TC) in SNP 7903146 were assigned to the *TCF7L2* group, and volunteers not carrying either risk variant were assigned to the control group.

All subjects were phenotyped by standardized anthropometric measurements including body weight, height, waist and hip circumferences, blood pressure, heart rate and body composition measured by bioelectrical impedance analysis (Tanita BC-418 segmental body composition

analyzer, Sindelfingen, Germany). Routine clinical blood biochemistry was assessed in morning blood samples after a 12-hour over-night fasting period.

The study was conducted in accordance to the Declaration of Helsinki. All subjects gave their written informed agreement to participate. The approval for the study was obtained from the ethics committee of the Bavarian Medical Association (Bayerische Landesärztekammer).

### **Study design**

The VID-Study was designed as a randomized, double-blind intervention study to analyze clinical and metabolic differences between *FTO* risk allele carriers or *TCF7L2* risk allele carriers and control subjects. The investigators were blinded concerning the genotypes. Study participants stayed at the human study center of the Else Kröner-Fresenius-Center for Nutritional Medicine (EKFZ) of the Technische Universität München over a 2 day period under strictly controlled conditions. Within this period all subjects underwent the following three defined challenge tests:

1. Oral glucose tolerance test (OGTT): On day 1 at 8 am subjects underwent a standardized two hour oral glucose tolerance test (75g glucose; Dextro O.G.T., Roche Diagnostics, Mannheim, Germany).
2. Western diet test (WDT): On day 1 at 12 am, a representative fast food meal, containing one Big Mac burger (219g), 400 ml Fanta and 114 g french fries (Mc Donald`s, Freising, Germany) was ingested within 15 minutes.
3. Oral lipid tolerance test (OLTT): On day 2 at 8 am, a standardized oral lipid drink (35g fat/m<sup>2</sup> body surface) was prepared by mixing 3 parts Fresubin Energy drink chocolate (Fresenius Kabi, Bad Homburg, Germany) with 1 part Calogen® (Nutricia, Pfrimmer, Germany). On average, participants received a volume of 424 ml of the test drink within 5 minutes. Nutritional composition of the challenge tests are presented in Table 5.

**Table 5: Nutrient composition of the SLD, WDT and the OLTT**

CHO, carbohydrates; SFA, saturated fatty acids; MUFA, monounsaturated fatty acids; PUFA, polyunsaturated fatty acids  
 † from: <http://www.mcdonaldsmenu.info/nutrition/menucal.jsp>; 20.10.2012

	OGTT	WDT†	OLTT
	per subject (Mean ± SD)	per subject	per subject (Mean ± SD)
Amount (ml)	300	219g Burger + 114g french fries + 400 ml Softdrink	423.6±30.9
Energy (kJ)	1256	4251	3963.2±289.1
Energy (kcal)	300	1015	953.2±69.5
Protein (% energy)	0	13	7.5
CHO (% energy)	100	50	25
Fat (% energy)	0	37	67.5
Protein (g)	0	32	17.8±1.3
Carbohydrates (g)	75	126	59.7±4.4
Fat (g)	0	42	71.4±5.
SFA (g)	0	11	7.2±0.5
MUFA (g)	0	Unknown	43.9±3.2
PUFA (g)	0	Unknown	20.2±1.5
Fiber (g)	0	7	0.0

Besides the test meals, volunteers received a standardized supper on day 1, mineral water and unsweetened tea. All volunteers were asked to refrain from drinking alcohol or undertaking any undue exercise at least 12 hours before the test period started.

The study design is shown in Figure 13. 17 venous plasma samples per subject were collected at pre-defined time points, starting before each challenge (=baseline), then 15, 30, 60, 120 minutes after the OGTT and 1, 2, 4, 6, 8 hours after the WDT and OLTT. Standard biochemical parameters, including glucose, insulin, lactate, triglycerides and non-esterified fatty acids (NEFAs) were measured at all 17 time points. Metabolites were measured in plasma samples at 9 time points, which were taken at baseline (=before each challenge) and then 1 and 2 hours after the OGTT and 2 and 6 hours after the OLTT or the WDT.

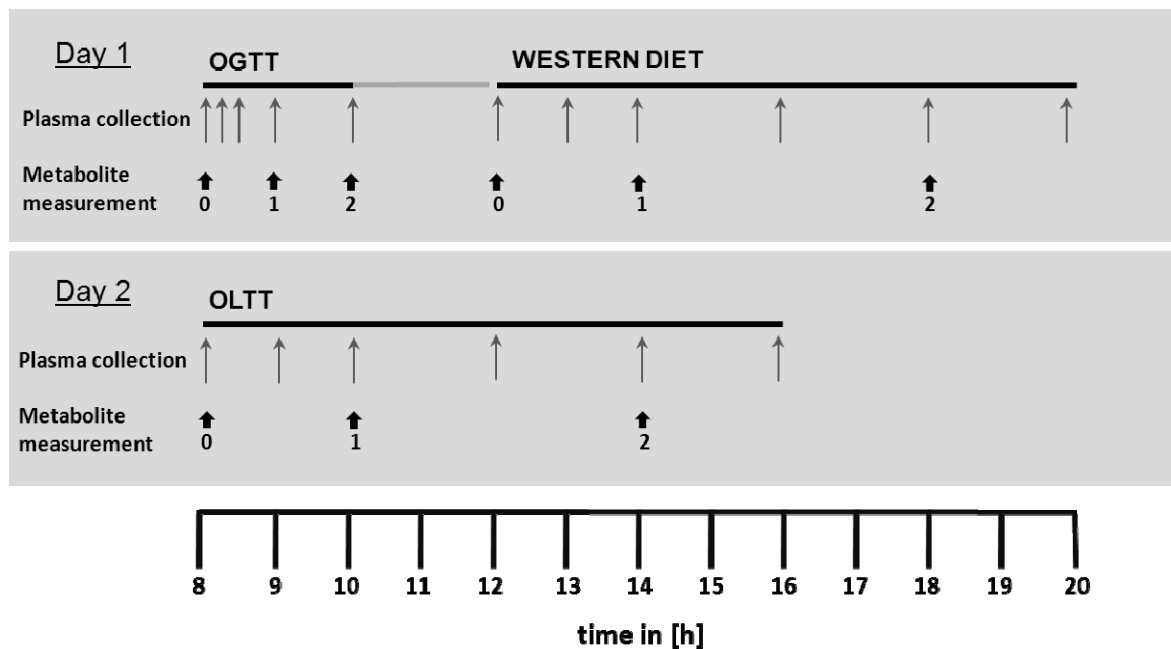


**Figure 13: Study design of the VID-study.**

Black bars indicate the duration of a challenge test. Grey arrows indicate the time points of plasma collection. Black arrows indicate the time points of metabolite analyses in plasma. These 3 time points are denoted as time point 0 (pre-challenge) and two post-challenge time points 1 and 2.

### Blood sample collection

Blood samples were drawn into 4.5 ml EDTA K<sub>2</sub>-Gel tubes (Sarstedt, Nümbrecht, Germany) using a venous cannula (18 G 1 ¼, Vasofix Braunüle, Braun, Germany) placed into a forearm vein. EDTA tubes were immediately centrifuged (Centrifuge 5702 R, Eppendorf AG, Hamburg, Germany) at 3,000 g for 10 min at 20°C. The venous plasma obtained was aliquoted using an automatic pipette (Eppendorf AG, Hamburg, Germany), immediately deep-frozen on dry ice and subsequently stored at -80°C until analysis.

### 3.2.2 Biochemical analyses

Glucose, lactate and hemoglobin levels were measured immediately in venous whole blood by enzymatic amperometric technique (Super GL easy<sup>+</sup>, Dr. Müller Geräte Bau, Freital, Germany). Insulin was measured in plasma by an enzyme-linked immunosorbent assay (ELISA) (Dako #K6219, Glostrup, Denmark). Plasma triglycerides were measured using an enzymatic colorimetric test (Fluitest TG, Analyticon Biotechnologies AG, Lichtenfels, Germany). This method uses lipoprotein lipase for the rapid and complete hydrolysis of triglycerides to glycerol and free fatty acids followed by oxidation of glycerol to dihydroxyacetone phosphate and hydrogen peroxide. Hydrogen peroxide reacts with 4-aminophenazone and 4-chlorophenol under the catalytic action of peroxidase to form a red dye. Optical density was determined at 546 nm using a spectrophotometer (DU<sup>®</sup> 800, Beckman Coulter, Fullerton, California). NEFAs were quantitatively measured in plasma by an enzymatic colorimetric assay (NEFA-HR, Wako Chemicals GmbH, Neuss, Germany). All assays were conducted according to the manufacturers' guidelines and coefficients of variation were within the accepted limits.

### 3.2.3 Metabolomics analyses

A panel of 163 different metabolites was measured and quantified on an API 4000 Q TRAP LC/MS/MS System (Applied Biosystems) using the AbsoluteIDQ kit (BIOCRATES Life Sciences AG) at the German Research Center for Environmental Health GmbH (Helmholtz Zentrum München, Munich, Germany). The metabolomics measurement technique is described in detail by US patent US 2007/0004044, in published literature (21-23) and in the manufacturer's manuals. The metabolomics data set contains 14 amino acids, hexose, free carnitine (C0), 40 acylcarnitines (Cx:y), hydroxylacylcarnitines (C(OH)x:y) and dicarboxylacylcarnitines (Cx:y-DC), 15 sphingomyelins (SM Cx:y) and *N*-hydroxylacyloylsphingosylphosphocholines (SM(OH)Cx:y), 77 diacyl (PC aa Cx:y) and acyl-alkyl (PC ae Cx:y) phosphatidylcholines and 15 *lyso*-phosphatidylcholines (LPC a Cx:y), where Cx:y abbreviates the lipid side chain composition, x and y denoting the sum of carbons and double bonds, respectively. All metabolite concentrations are reported in  $\mu\text{mol/L}$ .

Metabolite measurements were performed on six different plates. To correct for plate effects, measurements were multiplied by a metabolite- and plate-specific correction factor calculated as



the geometric mean of the six plate-specific geometric means of metabolite concentrations divided by the respective plate-specific geometric mean. We excluded 31 metabolites which met one of the following criteria: (1) The coefficient of variation (CV) of metabolite concentrations in the five reference samples was  $> 0.25$  on any of the plates, (2) Kendall's correlation p-value was  $< 0.1$  for a correlation between the sample and the reference sample means of the six plates, and (3)  $> 30\%$  of metabolite concentrations were zero for this metabolite. These criteria ensured that only metabolites with high measurement stability were considered.

### 3.2.4 Statistical analysis

All calculations were performed using the statistical environment R, version 2.13.0. 42 selected metabolite sums and ratios that were assumed to indicate a certain metabolic state or process, as proposed by Biocrates (MetaDis/IDQ™ kit), were calculated. In addition, we considered 14 metabolite ratios that were significantly associated with genetic loci in a previous genome-wide analysis study (22). Distributions of the metabolite concentrations, sums and ratios (metabolite traits) were assessed using quantile-quantile-plots. For all models, the *FTO* (rs9939609) genotype was coded as 1 for risk allele carriers (AA), *TCF7L2* (rs7903146) genotype was coded as 2 for risk allele carriers (TT or TC) and 0 for control subjects (negative for both risk SNPs). Differences in baseline anthropometric and clinical data between the two genotype groups were assessed using Wilcoxon-signed-rank-tests. To determine baseline associations between genotype groups and metabolite concentrations, sums and ratios, fasting measurements of two subsequent days were averaged and linear models were fitted for each metabolite trait adjusting for BMI and age.

Metabolite traits were determined at three time points for each challenge: At baseline, 1 and 2 hours (OGTT) or at baseline, 2 and 6 hours (OLTT; Western Diet). To identify *FTO* or *TCF7L2* genotype effects on challenge-induced changes in metabolite traits, we fitted linear mixed models with random intercept for each metabolite trait and each challenge using the R package *nlme*, modeling time point as a three-level factor:

Metabolite trait ~ genotype + time point 1 + time point 2 + genotype\*time point 1 + genotype\*time point 2 + BMI + age

In this model, the estimate of the interaction term genotype\*time point 1 can be interpreted as genotype effect on metabolite trait changes between baseline and 1 hour (OGTT) or 2 hours (OLTT; Western Diet). Similarly, the estimate of the interaction term genotype\*time point 2 reflects genotype effect on metabolite trait changes between baseline and 2 hours (OGTT) or 6 hours (OLTT; Western Diet).

### **3.3 The impact of a common *FTO* gene variant on plasma metabolite profiles during nutritional challenges**

#### **3.3.1 *FTO* – Fat Mass and Obesity Associated Gene**

Overweight and obesity are significant risk factors for the development of numerous chronic diseases, including type 2 diabetes mellitus (T2DM), cardiovascular disease and some types of cancer (50). The worldwide incidence of obesity has more than doubled since 1980 (51) and is mainly attributed to an imbalance of energy intake and expenditure. The incidence of obesity is influenced by both environmental and genetic factors, the latter accounting for a high proportion (20–80%) of BMI development (52, 53). The genetic predisposition to common forms of obesity is based on the individual polygenic build-up with each single nucleotide polymorphism (SNP) identified so far showing only a small influence on BMI. Sufficient statistical power to detect such small genetic influences is provided by large genome-wide association studies (GWAS), which yielded substantial progress in the identification of polygenic variants in the past few years. To date at least 52 gene variants have been identified which influence BMI (54). Variants in the *FTO* (fat mass and obesity associated) gene explained the largest proportion of BMI variation in the investigated populations (55). SNPs in the *FTO* gene locus were initially associated with an increased susceptibility to T2DM by a GWA in 2007 (12). Subsequent research recognized that this association with T2DM is most probably mediated by the impact of *FTO* locus SNPs on body mass index (BMI) (11). About 16% of adults with Caucasian origin are homozygous for the *FTO* risk allele in rs9939609. Adults homozygous for rs9939609 have been shown to weigh about 3 kilograms more and to have a 1.67-fold increased risk for obesity compared to subjects not inheriting a risk

allele (11). The association of this SNP in the *FTO* gene locus with an increased risk of being overweight or obese has been robustly and reproducibly associated in multiple populations (11, 55-64). Since the initial detection of common variants in the *FTO* locus as obesity risk alleles in 2007 several attempts have been made to unravel the function of the *FTO* gene. So far, a bioinformatics approach revealed, that human *FTO* has strong similarity with the DNA repair proteins AlkB, ABH2 and ABH3. These proteins belong to the Fe<sup>2+</sup> and 2-oxoglutarate-dependent dehydrogenases and are therefore implicated in various cellular processes such as DNA- and post-translational modifications (65).

Thus, until now the biological mechanism by which the obesity susceptibility variant rs9939609 increases BMI remains to be elucidated. One step forward in understanding the effects of this *FTO* gene variant on human metabolism would be the identification of metabolite alterations. The novel metabolomic approaches developed in the past years have been shown to be highly sensitive in detecting differences in the metabolic profiles between lean and obese individuals (66, 67) or to discover genotype-specific metabotypes (48). To our knowledge, so far a *FTO*-genotype specific metabotype is not yet described. All human studies analyzing metabotypes have used only plasma samples of the fasting state.

SNPs in the *FTO* gene locus influence body weight and therefore might reveal early alterations in postprandial nutrient utilization. Thus, such differences may only be revealed by a study approach, which does not rely on a single homeostatic measurement as usually performed in large cohort studies. Therefore, we conducted a study to analyze the effects on the *FTO* locus risk allele in rs9939609 on plasma metabolites under basal conditions as well as under acute metabolic regulations, induced by standardized challenge tests.

### 3.3.2 Results

#### 3.3.2.1 Genotype-specific differences in baseline measures

A comparison of the baseline anthropometric and clinical characteristics of the *FTO* and the control group is provided in Table 6. The group with the at-risk genotype (AA) at rs9939609 and the control group (TT) showed no significant differences in mean age, BMI or body composition. Both groups showed normal fasting glucose and insulin levels. Interestingly, in the *FTO* group significantly lower mean creatinine ( $p < 0.01$ ) and hemoglobin ( $p = 0.03$ ) levels than the control group.

**Table 6: Baseline anthropometric and clinical data of the *FTO* and the control group.**

All data are expressed as mean  $\pm$  SD. Controls: Group of subjects with low risk genotype (TT) at rs9939609; *FTO*: Group of subjects with high-risk genotype (AA) at rs9939609; BMI: body mass index; FM: fat mass; FFM: fat free mass; p: p-value adjusted for BMI and age

	Controls	<i>FTO</i>	P
<b>N</b>	20	19	-
<b>Age [y]</b>	51.1 $\pm$ 9.2	51.7 $\pm$ 9.7	0.77
<b>Height [m]</b>	1.80 $\pm$ 7.6	1.77 $\pm$ 5.2	0.08
<b>Weight [kg]</b>	88.9 $\pm$ 9.3	81.8 $\pm$ 11.5	0.06
<b>BMI [kg/m<sup>2</sup>]</b>	27.3 $\pm$ 2.3	26.3 $\pm$ 3.5	0.27
<b>FM [kg]</b>	21.2 $\pm$ 5.6	18.6 $\pm$ 7.8	0.57
<b>FFM [kg]</b>	67.8 $\pm$ 6.9	63.0 $\pm$ 5.9	0.06
<b>Waist circumference [cm]</b>	96.9 $\pm$ 6.9	95.8 $\pm$ 10.1	0.45
<b>Hip circumference [cm]</b>	98.8 $\pm$ 5.0	95.6 $\pm$ 7.7	0.20
<b>Heart rate [1/min]</b>	66.3 $\pm$ 6.4	70.7 $\pm$ 9.6	0.08
<b>Total cholesterol [mg/dl]</b>	214.3 $\pm$ 42.3	204.2 $\pm$ 34.8	0.4
<b>LDL cholesterol [mg/dl]</b>	134.3 $\pm$ 41.1	120.1 $\pm$ 30.5	0.24
<b>HDL cholesterol [mg/dl]</b>	50.6 $\pm$ 12.7	59.8 $\pm$ 18.6	0.13
<b>Triglycerides [mg/dl]</b>	140.4 $\pm$ 44.9	123.3 $\pm$ 48.4	0.45
<b>Creatinine [mg/dl]</b>	0.95 $\pm$ 0.11	0.83 $\pm$ 0.14	< 0.01*
<b>Hemoglobin [g/dl]</b>	14.1 $\pm$ 0.8	14.9 $\pm$ 1.2	0.03*
<b>TSH basal [<math>\mu</math>U/ml]</b>	1.6 $\pm$ 0.8	1.6 $\pm$ 0.9	0.9
<b>HbA1c [%]</b>	5.5 $\pm$ 0.3	5.6 $\pm$ 0.3	0.26
<b>Baseline glucose [mg/dl]</b>	85.5 $\pm$ 8.4	82.4 $\pm$ 8.6	0.45
<b>Baseline insulin [<math>\mu</math>U/ml]</b>	8.1 $\pm$ 3.1	7.5. $\pm$ 4.9	0.78

The metabolite traits showing significant differences between controls and at risk subjects at baseline are summarized in Table 7. After an over-night fast of 12 hours, homozygous *FTO* risk-allele carriers had significantly elevated plasma levels of C18.1 ( $p=0.04$ ) and of the sum of long-chain carnitines ( $p=0.05$ ). Moreover, the ratio of phosphatidylcholine PC ae C44:5 and PC ae C42:5 was significantly elevated in the *FTO* group ( $p = 0.01$ ). Additionally, the *FTO* risk allele carriers had higher levels of histidine ( $p=0.01$ ), tryptophan ( $p=0.03$ ), phenylalanine ( $p=0.05$ ) and the sum of aromatic amino acids ( $p=0.03$ ) in plasma.

**Table 7: Metabolite traits significantly associated with *FTO* genotype at baseline.**

The analysis was based on fasting concentrations averaged over two different days. Data is expressed as mean  $\pm$  SD;  $p$  =  $p$ -value adjusted for BMI and age.  $\beta$  =  $\beta$ -coefficient adjusted for BMI and age. The  $\beta$ -coefficient is a standardized measure for the genotype-specific difference and varies between -1 and +1. Negative values indicate a smaller metabolite concentration in the *FTO* group than in controls. Controls: Group of subjects with low risk genotype (TT) at rs9939609; *FTO*: Group of subjects with high-risk genotype (AA) at rs9939609

Metabolite trait	Controls	<i>FTO</i>	$\beta$	$p$
C18.1 [ $\mu$ M]	0.11 $\pm$ 0.02	0.13 $\pm$ 0.02	0.58	0.044
Long-chain carnitines [ $\mu$ M]	0.36 $\pm$ 0.06	0.4 $\pm$ 0.06	0.56	0.049
PC.ae.C44.5 / PC.ae.C42.5	0.8 $\pm$ 0.06	0.87 $\pm$ 0.09	0.77	0.013
Histidine [ $\mu$ M]	71.54 $\pm$ 8.72	80.21 $\pm$ 10.8	0.79	0.015
Tryptophan [ $\mu$ M]	78.6 $\pm$ 7.16	85.94 $\pm$ 11.05	0.73	0.026
Phenylalanine [ $\mu$ M]	55.36 $\pm$ 5.65	59.95 $\pm$ 8.64	0.65	0.046
Aromatic amino acids [ $\mu$ M]	202.49 $\pm$ 16.28	220.2 $\pm$ 30.56	0.72	0.022

### 3.3.2.2 Genotype-specific differences in challenge-induced metabolite dynamics

Upon nutritional challenges, the plasma glucose, insulin, NEFAs, triglycerides and lactate levels followed the expected time-curves (Figure 14). Due to the large amount of fat, the elevation of plasma glucose levels induced by the OLTT was delayed in both genotype groups if compared with the OGTT. Plasma lactate levels showed a weak, but consistent dependency on the nutritional challenges and increased levels were seen 1 hour after the OGTT and 2 hours after the OLTT in both groups (Figure 14).

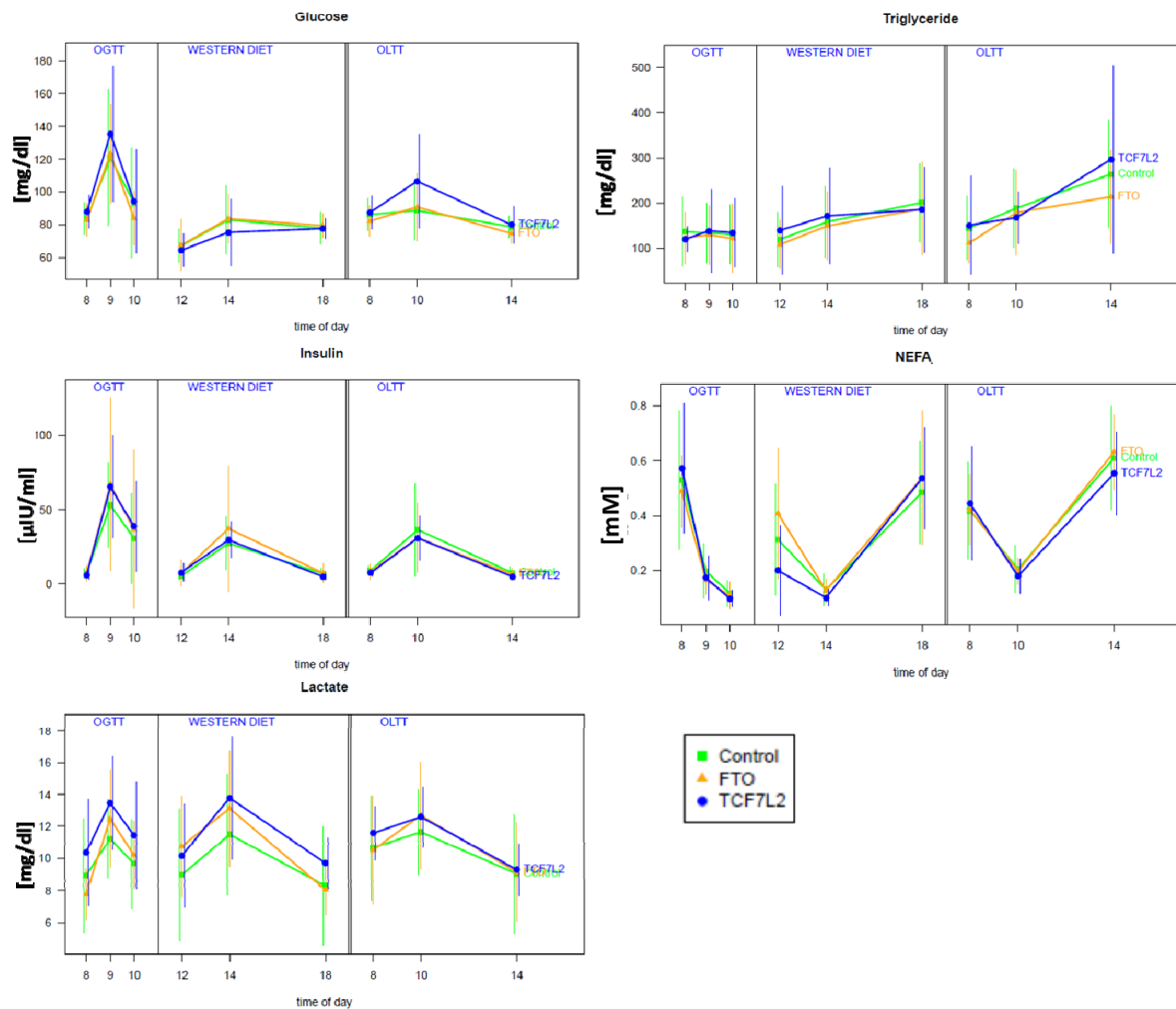


**Figure 14: Concentration profiles of 5 metabolic key parameters (glucose, insulin, lactate, NEFAs and triglycerides, color coded for the 3 genotypes investigated within the VID study.**

Volunteers stayed in the study unit for two days. They received the OGTT at 8am of the first morning and the OLTT at 8am on the second morning.

### Metabolites showing genotype-specific regulation after the OGTT

Table 8 lists all metabolites with a significant ( $p < 0.05$ ) difference between both genotypes, regarding the challenge-induced metabolite concentration changes ( $\Delta$  Change). As presented in Table 8A, 1 hour after the OGTT, the increase in plasma levels of lactate, C0 or 15 long chain PCs was significantly altered in FTO-locus risk-allele carriers compared to controls. The plasma lactate level increase within the FTO-locus risk-allele group (+4.71mg/dl) was more than twofold higher compared to the control group (+2.30mg/dl). These significant differences ( $p = 0.004$ ) in post-challenge elevation of lactate levels were still evident 2 hours after the OGTT ( $p = 0.009$ ), when

lactate levels in controls were almost reduced to baseline level (+0.75mg/dl), whereas they remained at a high level within the FTO group (+2.45mg/dl). Additionally, the FTO group showed a greater increase in C0 levels ( $p=0.03$ ) 1 hour after the OGTT and one hour after glucose intake, the average decline in plasma concentrations of PCs and plasmalogen/plasmogen species containing long-chain fatty acids (PC.aa.C38.1, PC.aa.C38.3, PC.aa.C38.6, PC.aa.C40.6, PC.aa.C42.1, PC.ae.C36.4, PC.ae.C38.3, PC.ae.C40.3, PC.ae.C40.5, PC.ae.C44.5) was significantly smaller ( $p<0.05$ ) in the FTO-locus risk-allele carriers than in the control group (Table 8A). 2 hours after the OGTT, this difference in output of the respective PCs was not significant anymore.

#### **Metabolites showing genotype-specific regulation after the WDT**

1 hour after the WDT no metabolites showed genotype-specific regulation. 6 hours after the WDT, insulin and glucose levels have already returned to their baseline values. At this time point, high concentrations of triglycerides and NEFAs were measured in both groups (Figure 14) however the increase was not significantly different between genotypes. In this metabolic state *FTO*-locus risk-allele carriers showed a significantly ( $p<0.05$ ) stronger decrease in C5, Valine and the sum of BCAAs compared to control subjects (Table 8B).

#### **Metabolites showing genotype-specific regulation after the OLTT**

Due to the high amount of fat, peak values of plasma glucose and insulin after intake of the lipid drink were delayed and lower in both groups if compared with the OGTT (Figure 14). 1 hour after the lipid intake one metabolite (lysoPC.a.C18.2) showed a significant ( $p=0.047$ ) group specific difference in the reaction to the challenge (Table 8C): While lysoPC.a.C18.2 remained stable in the control group, its concentration increased from  $30.89\pm 7.25\mu\text{M}$  to  $33.89\pm 7.18\mu\text{M}$  in the FTO group. 6 hours after the lipid drink, the ingested fat resulted in high values of triglycerides and NEFAs in both groups (Figure 14). In this metabolic state, *FTO* risk allele carriers showed a significantly stronger ( $p<0.05$ ) decrease in C3 ( $\Delta$  Change *FTO* = -0.08 vs.  $\Delta$  Change Control = -0.03) and the sum of odd chain carnitines than control subjects ( $\Delta$  Change *FTO* = -0.07 vs.  $\Delta$  Change Control = -0.02) (Table 8C).

**Table 8: Metabolite traits with significant ( $p < 0.05$ ) effect of the *FTO* SNP rs9939609 on (A) OGTT-induced changes after 1 and 2 hours, (B) on WDT-induced changes after 2 and 6 hours and (C) on OLTT-induced changes after 2 and 6 hours.**

Linear mixed models were adjusted for BMI and age. Units: Lactate in [mg/dl], all other presented metabolites in [ $\mu$ M]; Controls: Group of subjects with low risk genotype (TT) at rs9939609; *FTO*: Group of subjects with high-risk genotype (AA) at rs9939609;  $\beta$ -coefficient = a standardized measure of the genotype-specific difference in change and varies between -1 and +1. Negative values indicate a stronger decline in metabolite concentration in the *FTO* group than in controls, occurring between baseline and the post-challenge time points.

**(A) OGTT**

Metabolite trait			Controls			<i>FTO</i>		
	$\beta$	<i>p</i> -value	baseline (mean $\pm$ SD)	$\Delta$ Change at 1 hour	$\Delta$ Change at 2 hours	baseline (mean $\pm$ SD)	$\Delta$ Change at 1 hour	$\Delta$ Change at 2 hours
Significant genotype effect on changes between baseline and 1 hour								
Lactate	0.80	0.004	8.92 $\pm$ 3.55	2.30	0.75	7.75 $\pm$ 1.59	4.71	2.45
C0	0.38	0.033	38.67 $\pm$ 6.71	0.37	2.35	40.93 $\pm$ 5.60	3.17	4.04
PC.ae.C36.4	0.32	0.032	20.67 $\pm$ 5.14	-2.28	-1.57	21.32 $\pm$ 4.61	-0.67	-0.76
PC.aa.C38.1	0.48	0.035	1.45 $\pm$ 0.40	-0.13	-0.10	1.35 $\pm$ 0.33	0.06	-0.02
PC.aa.C38.3	0.30	0.046	56.39 $\pm$ 14.93	-5.03	-3.10	55.61 $\pm$ 8.56	-1.53	-1.91
PC.ae.C38.3	0.37	0.028	3.81 $\pm$ 0.84	-0.38	-0.24	3.82 $\pm$ 0.70	-0.12	-0.05
PC.aa.C38.6	0.19	0.050	101.46 $\pm$ 35.91	-8.29	-4.84	85.24 $\pm$ 28.33	-2.01	-1.72
PC.ae.C40.3	0.39	0.033	1.10 $\pm$ 0.24	-0.10	-0.07	1.06 $\pm$ 0.16	-0.03	-0.03
PC.ae.C40.5	0.34	0.025	3.54 $\pm$ 0.66	-0.35	-0.22	3.70 $\pm$ 0.76	-0.11	-0.10
PC.aa.C40.6	0.20	0.023	32.77 $\pm$ 12.92	-2.86	-1.52	26.72 $\pm$ 9.02	-0.57	-0.39
PC.aa.C42.1	0.30	0.049	0.26 $\pm$ 0.07	-0.02	-0.02	0.25 $\pm$ 0.08	0.00	0.00
PC.ae.C44.5	0.22	0.029	1.72 $\pm$ 0.40	-0.19	-0.10	2.02 $\pm$ 0.59	-0.08	-0.07
long.PCs	0.25	0.043	72.63 $\pm$ 20.79	-6.57	-3.88	68.04 $\pm$ 14.27	-2.14	-1.64
long.PC.aa	0.23	0.040	52.87 $\pm$ 17.70	-4.71	-2.69	47.35 $\pm$ 11.89	-1.27	-0.89
Significant genotype effect on changes between baseline and 1 hour								
Lactate	0.56	0.009	8.92 $\pm$ 3.55	2.30	0.75	7.75 $\pm$ 1.59	4.71	2.45



**(B) WDT**

Metabolite trait			Controls			FTO		
			baseline (mean±SD)	Δ Change at 2 hours	Δ Change at 6 hours	baseline (mean±SD)	Δ Change at 2 hours	Δ Change at 6 hours
Significant genotype effect on changes between baseline and 2 hours								
Significant genotype effect on changes between baseline and 6 hours								
C5.1	-0.67	0.029	0.04±0.01	0.00	0.00	0.05±0.01	0.00	-0.01
Val	-0.42	0.043	237.24±34.22	45.06	53.68	236.94±39.05	55.83	35.24
BCAAs	-0.44	0.045	392.88±58.95	120.07	152.24	394.08±65.73	139.61	111.79

**(C) OLTT**

Metabolite trait			Controls			FTO		
			baseline (mean±SD)	Δ Change at 1 hours	Δ Change at 6 hours	baseline (mean±SD)	Δ Change at 1 hour	Δ Change at 6 hours
Significant genotype effect on changes between baseline and 2 hours								
lysoPC.a.C18.2	0.34	0.047	30.06±12.45	-0.39	7.14	30.89±7.25	3.12	8.44
Significant genotype effect on changes between baseline and 6 hours								
C3	-0.47	0.04	0.42±0.07	0.044	-0.03	0.44±0.1	0.03	-0.08
odd.carn	-0.50	0.05	0.62±0.08	0.045	-0.02	0.65±0.1	0.03	-0.07

### 3.3.3 Discussion

The A variant in the *FTO* SNP rs9939609, within the first intron of the *FTO*-gene, has been robustly associated with obesity. However, previous reports state that this *FTO*-locus genotype is not associated with BMI in an older population not living in an obesogenic environment (68) or in young people who meet the recommended levels of daily physical activity (69). This implies that the *FTO*-genotype acts as a susceptibility locus for obesity affecting the response or adaptation to changes in energy supply and expenditure. The metabolite responses to a nutritional challenge might reveal altered regulatory mechanism of energy metabolism, which is important for obesity development and helps to learn more about possible metabolic effects of the *FTO* gene. Therefore, in this study we analyzed metabolite levels in the fasting state and during the response to a nutritional challenge in non-obese *FTO*-locus risk allele carriers.

#### **Metabolites showing genotype-specific differences at baseline**

In this study we observed significantly elevated plasma levels of the essential aromatic amino acids histidine, tryptophan, phenylalanine and the sum of all aromatic amino acids in the *FTO* risk allele carriers at baseline, but they were not regulated differently after our dietary challenges. Based on this result, a genotype-specific difference in amino acid uptake from food contents is not likely. The genotype-specific differences may rather be due to a genotype-specific effect on storage, degradation or conversion of the respective metabolites. The enzyme aromatic L-amino acid decarboxylase (AAAD) catalyzes both, the degradation of histidine and phenylalanine, and the conversion of tryptophan to serotonin. An altered activity of this enzyme might explain the observed elevation in histidine, tryptophane and phenylalanine in the *FTO* group. While in an older study fasting plasma concentrations of phenylalanine have been positively correlated with obesity (70), more recently plasma tryptophan levels have been shown to be below normal in obese subjects (71). Serotonin neurons function in neuronal circuits that diminish food intake (72, 73) and the synthesis of serotonin in the brain is partially depending on the availability of L-tryptophan. Therefore, the finding of higher tryptophan levels in the *FTO*-locus risk allele carriers could promote higher satiety. Previous studies have demonstrated that *FTO* gene expression in the arcuate nucleus is regulated by fasting (65, 74). These data imply the potential contribution of the *FTO* gene in the regulation of energy homeostasis. The *FTO* SNP might affect *FTO* expression and thereby result in

an impaired control in eating behavior, which leads to eating in the absence of hunger as observed by Tanofsky-Kraff et al. (75). Additionally, the results of from our study may also imply other mechanisms affecting eating behavior, like lower tryptophan to serotonin conversion or a reduced tryptophan brain uptake rate. Depending on a replication of the here observed results, the differences in the plasma levels of histidine, phenylalanine and tryptophan, their degradation products and the enzyme aromatic L-amino acid decarboxylase are interesting targets for further studies regarding metabolic effects of the *FTO* risk allele.

Several PC species have been reported to be positively associated with obesity (32, 76). Our non-obese *FTO* group showed no significant differences in baseline PC levels compared to the control group. However, after glucose intake, the decline in several long chain PCs was more pronounced in plasma of controls than in plasma of *FTO* risk allele carriers. Plasma PCs as components of circulating blood lipoproteins, have been shown to associate with HDL and total cholesterol levels, while phosphatidylethanolamine (PE) species associate with triglyceride levels (31). Therefore, the stronger reduction of plasma PC levels in controls might indicate that lipid metabolism in *FTO* risk allele carriers reacts less flexible to the glucose and insulin increase after an OGTT.

In this study, all baseline levels of metabolites were measured after fasting for 12 hours overnight. The metabolic adaptation to this fasting is reflected in both groups by elevated NEFA levels as a consequence of the increased lipolysis. Plasma NEFA levels were not affected by the genotype. Therefore, we conclude that the *FTO* risk allele does not alter lipolysis or fatty acid entry into cells. Carnitine as the substrate for carnitine palmitoyltransferase 1 (CPT1) plays an essential role in the translocation of long-chain fatty acyl groups into the mitochondrial matrix for subsequent  $\beta$ -oxidation (77). Another important function of carnitine is to buffer an intracellular acyl-CoA overload, which occurs due to incomplete  $\beta$ -oxidation (78). An increased availability of substrates for  $\beta$ -oxidation leads to an accumulation of acyl-CoAs, if TCA (tricarboxylic acid)-cycle capacity is exceeded. In contrast to acyl-CoAs, the respective acylcarnitines can cross the mitochondrial membrane and cytosolic acylcarnitines are further released into the blood stream (35). Therefore, plasma acylcarnitine profiles reflect intra-mitochondrial acyl-CoA levels derived during the specific steps of  $\beta$ -oxidation. Consequently, they are well established standard diagnostic markers for inborn fatty acid oxidation disorders (39) and have been shown to increase during fasting (7, 79,

80). Correspondingly we also found higher acylcarnitine levels in plasma collected during fasting than under postprandial conditions in both groups. However, the fasting samples of the *FTO* group showed significantly higher concentrations of C18.1 and the sum of long-chain carnitines. Such even-chain carnitines with chain length between C6 to C22 arise in plasma from incomplete  $\beta$ -oxidation (78). Elevated levels of these acylcarnitines were present in fasting plasma samples of animal models of obesity and diabetes (78, 81). Moreover, elevated plasma levels of acylcarnitines of different chain length, including C18.1 have been observed in fasting plasma samples in obese adults (81). Therefore, under fasting conditions even non-obese *FTO* risk allele carriers show similarities in their lipid-derived acylcarnitine profiles with obese subjects.

### **Metabolites showing genotype-specific variation during challenges**

In contrast to the fasting condition, after carbohydrate intake, insulin decreases lipolysis. After the OGTT all participants showed an increase in plasma glucose and insulin levels and a decrease in plasma NEFAs and lipid-derived acylcarnitines. The decrease in lipolysis after carbohydrate intake was accompanied by an increase in plasma free carnitine levels, which might result from lower binding of acetyl- or acyl-groups (78, 82). In the present study, induction of anabolic states by oral glucose intake increased plasma levels of free carnitine (C0) in both groups (see Table 8A). However, 1 hour after the OGTT, when  $\beta$ -oxidation is suppressed by peak insulin levels, the postprandial increase in C0 plasma levels ( $\Delta$  change at 1 hour after the OGTT) was significantly ( $p=0.033$ ) and almost 10 fold higher in the *FTO* risk allele carriers than in the control group (Table 8A). More than 95% of the body's carnitine is present in skeletal muscle (83). Therefore, the rapid increase observed for C0 plasma levels probably originates from C0 release from muscle tissue. Lower intracellular C0 levels might imply lower rates of  $\beta$ -oxidation because less C0 is available for the import of fatty acids into the mitochondria. Stephens et al. showed that under conditions of high carbohydrate availability skeletal muscle carnitine levels increased, followed by decreased muscle lactate content (84). After glucose intake we observed a higher increase of C0 and lactate in plasma of the *FTO* group compared to controls. Assuming that higher plasma C0 concentration entails lower intramuscular C0 levels, the increased plasma levels of lactate in the *FTO* group are the consequence of the biological energy regulatory processes:

The significantly higher lactate output in *FTO* risk allele carriers was observed 1 and 2 hours after glucose ingestion. Under states of high plasma glucose and insulin levels, high levels of acetyl-CoA from glycolysis or NADH from the TCA cycle would exert feed-back inhibition of the pyruvate dehydrogenase complex (PDC). The mitochondrial PDC catalyzes the oxidative decarboxylation of pyruvate to acetyl-CoA. Under conditions of high glycolytic flux, PDC inhibition consequently leads to anaerobic conversion of pyruvate to lactate (85), which could explain the higher plasma lactate output within our *FTO* risk allele carriers. A schematic overview of metabolic alterations induced by the *FTO* genotype is presented in Figure 15.

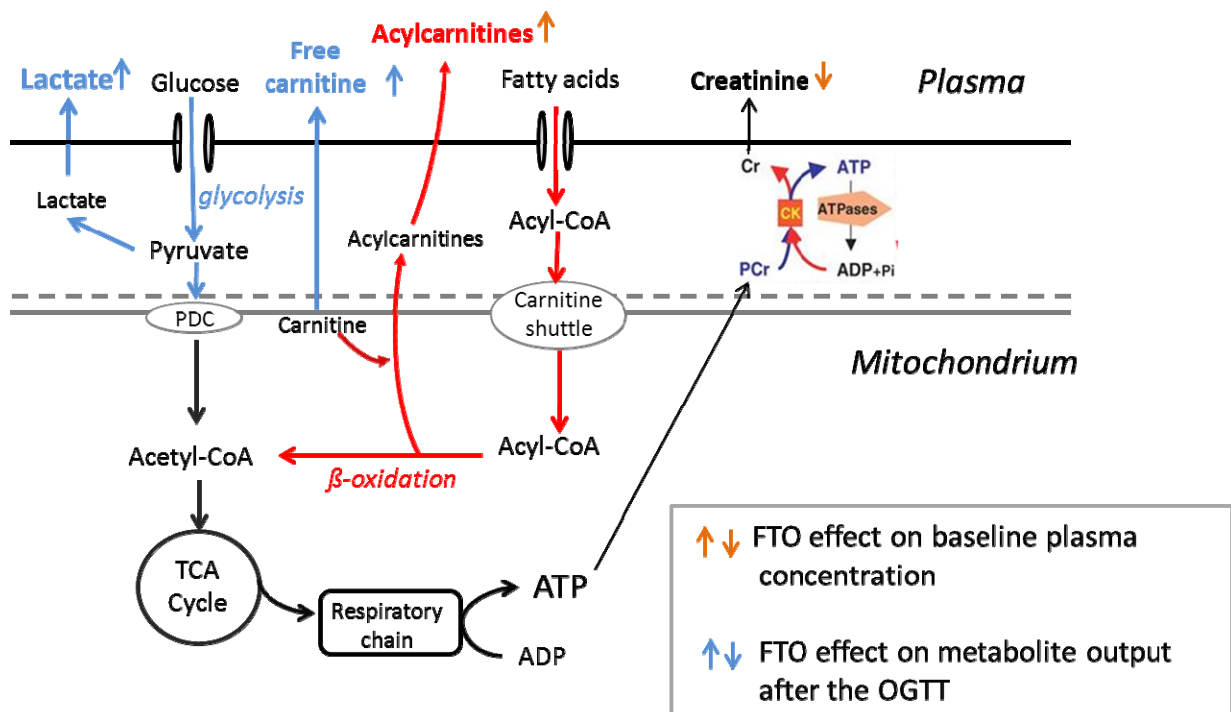


**Figure 15: Schematic illustration of metabolites changed within the *FTO* risk allele carriers in the context of cellular energy metabolism.**

The *FTO* risk variant significantly altered plasma concentrations of acylcarnitine and creatinine in our study at baseline (orange arrows) and the concentration change of lactate and free carnitine after glucose intake (blue arrows). These plasma metabolites are interconnected via the presented intracellular metabolic pathways.

Concluding, on the one hand, we observed higher levels of long chain acylcarnitines in the fasting state, a finding, which has been interpreted to demonstrate higher rates of incomplete fat oxidation (36, 78). On the other hand, we observed higher CO release into plasma 1 hour after glucose ingestion paralleled by higher lactate release. These findings could result from inhibitory

mechanisms on glycolytic or  $\beta$ -oxidative enzymes which may be mediated by intra-cellular accumulation of acetyl-CoA (85) or by high NADH from the tricarboxylic acid (TCA)-cycle. Nevertheless, an intracellular accumulation of acetyl-CoA would lead to higher plasmatic C2 levels, which were not observed in our *FTO* group and are therefore unlikely.

Therefore, the *FTO* risk allele might rather lead to a greater accumulation of energy equivalents like NADH, which also inhibits  $\beta$ -oxidation and PDC (85) or faster ATP generation and subsequent NADH accumulation. Indeed, a higher capacity for aerobic ATP generation in *FTO* risk allele carriers has been suggested by Grunnet et al (86). They observed higher phosphocreatinine recovery rates in oxidative muscle fibers (m. tibialis) of homozygous carriers of the *FTO* risk allele (rs9939609), which were supposed to result from faster ATP generation during oxidative phosphorylation. They further suggested that increased ATP generation in *FTO* risk allele carriers occurs due to an increased coupling of oxidative phosphorylation. Therefore, a reduced substrate usage for heat production might contribute to the higher obesity risk in carriers of the risk allele of the *FTO*-SNP (86). Our results support this hypothesis, as higher ATP levels could result in the observed metabolite alterations by increasing the NADH levels. Moreover, we observed lower levels of plasma creatinine in the *FTO* subjects. Creatinine, the degradation product of creatine and phosphocreatine is formed by a non-enzymatic process depending on temperature and pH. Creatinine is membrane permeable, diffuses into the blood and is subsequently excreted by the kidneys into the urine (87). Therefore, it is tempting to speculate that the observed lower plasma levels of creatinine imply a lower phosphocreatine degradation rate in muscle tissue. Nevertheless, experimental approaches are essential to clarify, if an increased efficacy of ATP generation or other alterations like decreased glycogen synthesis rates occur within *FTO* risk allele carriers.

### 3.3.4 Conclusion

Additional work is needed to further understand the metabolite alterations observed within this study and the altered regulation of fuel substrate in *FTO* carriers. Due to the small sample size, the results of this proof-of-principle study have to be considered as preliminary, which will need either verification by replication in studies of larger cohort size or by complementation with functional data. In addition, the here presented results are not adjusted for multiple testing. Therefore the results should only be regarded as hints to create further hypotheses concerning the effects of the *FTO* risk SNP on fasting and postprandial metabolism. However, to our knowledge this is the first study demonstrating genotype-specific metabolite alterations of the *FTO* gene. In contrast to most GWAS, the here presented study concept can reveal regulatory alterations associated with a specific genetic factor, therefore providing a more functional read-out. Overall, the metabolite alterations observed in this study indicate that the *FTO* risk allele alters substrate regulation and utilization under fasting and postprandial conditions, most strikingly one hour after intake of pure carbohydrates. The intake of a mixed western diet or a high-fat liquid drink did not reveal convincing genotype-specific metabolite alterations.

## **3.4 The impact of the T risk variant in rs7903146 of the *TCF7L2* gene on plasma metabolite profiles during nutritional challenges**

### **3.4.1 Transcription factor 7 like 2 - *TCF7L2***

Type 2 Diabetes Mellitus (T2DM) has reached epidemic scale and by 2030 its incidence is expected to increase up to 366 million worldwide (88) or even up to 439 million as stated by a more recent study (89). This increase is strongly driven by the changes in population body weight (90), reduced activity level (91, 92) and age structure (93). Nevertheless, a genetic component to T2DM is undeniable given the results of family- and twin-studies (94, 95) or the high prevalence in particular ethnic groups (96). Furthermore, genetic studies including linkage analysis, candidate gene approaches, and genome-wide association studies have identified more than 60 loci associated with T2DM or related traits (12, 97-104). Among all, so far identified loci, the variants within the transcription factor 7-like 2 (*TCF7L2*) gene showed the strongest effect on T2DM risk (12, 98, 105). *TCF7L2* has been associated with T2DM for the first time (106) in 2006. Up to now, this association has been confirmed by genome-wide association studies in multiple populations (107, 108). In a meta-analysis, *TCF7L2* was suggested to be implicated in 1/5 of all T2DM cases (108). Interestingly, no *TCF7L2* variant associated to T2DM is located in a coding gene-region (109). The C to T transposition in rs7903146 has repeatedly shown the strongest association with T2DM with a per T allele odds ratio of approximately 1.4 (108). This supports that rs7903146 might be the causal single nucleotide polymorphism (SNP), even though rs7903146 and all its correlated polymorphisms are not within any coding region (109). Rather than altering *TCF7L2* structure, the T risk allele most likely acts by altering *TCF7L2* expression as observed in human islets (110).

The *TCF7L2* gene product is a high mobility box containing a transcription factor, which in conjunction with  $\beta$ -catenin regulates gene transcription downstream of the WNT signaling cascade. 19 different WNT ligands are secreted by different cells, demonstrating the complexity of this signaling pathway (111). Figure 16 provides a mechanistic overview of WNT signaling.



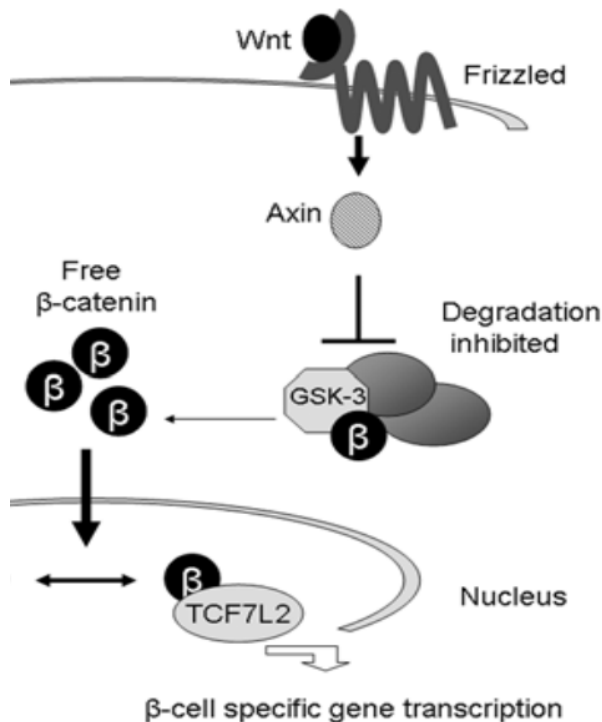


**Figure 16: Schematic representation of the canonical WNT signaling pathway.** Secreted WNTs bind to Frizzled (FZD) receptors, which then inactivate the protein complex effecting the degradation of β-catenin. β-catenin then binds to the nuclear *TCF7L2* receptors, activating more than 60 different genes.

From: Loder et al. (112)

As a consequence of the numerous functions of WNT signaling it might not be possible to pin down to only one underlying mechanism, by which *TCF7L2* variants increase the risk of diabetes. Metabolomics allow the simultaneous measurement of multiple metabolites produced along various interconnected pathways of metabolism and therefore provides a comprehensive read-out of the metabolic condition of at-risk individuals. Metabolite profiles have been shown to be highly characteristic for every individual and can help to understand the effects of diet, lifestyle or genes on metabolism and disease development. Therefore, in this study we investigated the metabolic profile of non-diabetic subjects carrying the risk allele (TT and TC) in rs7903146 compared to BMI and age-matched controls heterozygous for the low-risk allele (CC). Additionally, we investigated concentration changes between genotypes after nutritional interventions, including an oral glucose load and a western diet test meal. We expected that the concept of disturbing metabolic

homeostasis by defined challenge tests unmasks early deregulations not observable in the fasting condition and that genotype-specific differences in the metabolite response profile are of value for understanding the effects of *TCF7L2* on metabolic regulation. To our knowledge, this is the first study reporting the effects of the risk allele in rs7903146 on gene-diet responsiveness with a comprehensive set of metabolites.

## **3.4.2 Results**

### **3.4.2.1 Genotype-specific differences in baseline measures**

Each subject was characterized in a clinical examination, which included measurement of anthropometric and routine blood parameters. A comparison of the baseline characteristics of the *TCF7L2* and the control groups is provided in Table 9. The group with the at-risk genotype (TT or TC) at rs7903146 and the control group (CC genotype) showed no significant differences in mean age, BMI or in body composition, as demonstrated by the similar body fat or lean mass percentages (Table 9). Both groups showed normal fasting glucose levels. Mean baseline insulin levels of the at-risk group were 6.6% lower in comparison to the control group, however, this difference did not reach significance ( $p=0.06$ ). Nevertheless, the *TCF7L2* group had significantly higher HbA1c [%] levels than the controls. Additionally, the *TCFL2* group actually showed a tendency for a beneficial lipid-profile, including lower triglyceride and LDL levels and significantly ( $p=0.05$ ) higher plasma HDL levels.

**Table 9: Baseline values of anthropometric and routine blood parameters of the *TCF7L2* and the control group.**

Data is expressed as mean  $\pm$  SD; routine blood parameters are measured after 12h-overnight fast; p = p-value adjusted for BMI and age.  $\beta$  =  $\beta$ -coefficient adjusted for BMI and age. The  $\beta$ -coefficient is a standardized measure for the genotype-specific difference and varies between -1 and +1. Negative values indicate a smaller metabolite concentration in the *TCF7L2* group than in controls.

	Controls	<i>TCF7L2</i>	$\beta$	p
N	20	16		
Age [y]	51.05 $\pm$ 9.21	53.56 $\pm$ 10.24	0.26	0.45
BMI [kg/m <sup>2</sup> ]	27.30 $\pm$ 2.32	27.36 $\pm$ 2.85	0.02	0.94
WHR	0.98 $\pm$ 0.05	0.97 $\pm$ 0.04	-0.32	0.30
Fat whole body [%]	23.56 $\pm$ 5.17	23.73 $\pm$ 4.51	-0.05	0.86
Fat trunk [%]	25.99 $\pm$ 6.46	25.91 $\pm$ 5.51	-0.08	0.75
FFM [%]	0.76 $\pm$ 0.05	0.76 $\pm$ 0.04	0.07	0.79
Creatinine [mg/dl]	0.95 $\pm$ 0.11	0.91 $\pm$ 0.18	-0.31	0.39
Urea [mg/dl]	20.47 $\pm$ 8.09	17.38 $\pm$ 9.32	-0.43	0.26
ALT [U/l]	36.47 $\pm$ 24.31	26.53 $\pm$ 8.75	-0.43	0.19
Triglycerides [mg/dl]	140.93 $\pm$ 67.41	131.53 $\pm$ 52.53	-0.20	0.57
Cholesterol [mg/dl]	214.32 $\pm$ 42.26	209.00 $\pm$ 24.21	-0.10	0.78
LDL [mg/dl]	134.26 $\pm$ 41.13	127.80 $\pm$ 16.50	-0.16	0.65
HDL [mg/dl]	50.63 $\pm$ 12.76	61.67 $\pm$ 18.06	0.71	0.05*
LDL/HDL-ratio	2.78 $\pm$ 1.05	2.24 $\pm$ 0.70	-0.56	0.12
HbA1c [%]	5.51 $\pm$ 0.25	5.72 $\pm$ 0.33	0.68	0.05*
TSH basal [ $\mu$ U/ml]	1.56 $\pm$ 0.81	1.57 $\pm$ 1.30	-0.02	0.95
Haemoglobin [mg/dl]	14.13 $\pm$ 0.77	13.71 $\pm$ 0.81	-0.42	0.22
Glucose [mg/dl]	84.99 $\pm$ 8.58	86.98 $\pm$ 8.26	0.16	0.63
Insulin [U/L]	8.09 $\pm$ 3.09	6.41 $\pm$ 2.62	-0.63	0.06
Lactate [mg/dl]	9.79 $\pm$ 3.22	10.91 $\pm$ 1.82	0.36	0.30
NEFA [mmol/l]	0.47 $\pm$ 0.19	0.55 $\pm$ 0.23	0.31	0.36

We investigated the metabolic profiles of the *TCF7L2* and the control group in the baseline fasting condition. For this analysis, we included the two plasma samples collected at 8 am after a 12-hour overnight fasting period. All metabolites and metabolite traits revealing genotype-specific differences in their plasma concentration after an overnight fast are provided in Table 10. In accordance with the increased diabetes risk, plasma concentration of hexoses was higher in *TCF7L2* subjects (p=0.04). Other metabolites with genotype-specific concentration differences belong to the group of (i) amino acids, (ii) acylcarnitines or (iii) phosphatidylcholines.

Amongst 14 measured amino acids, the three amino acids glutamine, histidine and methionine were elevated in plasma of *TCF7L2* risk allele carriers when compared to controls. Additionally, the sum of all measured amino acids was 6.9% higher ( $p=0.022$ ) and the sum of all non-essential amino acids was 8.3% higher ( $p=0.008$ ) in the *TCF7L2* group than in controls.

Furthermore, the plasma concentrations of the acylcarnitines C3 and C16.2.OH were with  $0.52\pm 0.14$   $\mu\text{M}$  and  $0.011\pm 0.001$   $\mu\text{M}$  significantly ( $p<0.05$ ) higher in plasma of *TCF7L2* risk allele carriers, whereas concentration of C16.OH was significantly lower ( $p=0.03$ ). Moreover, the sum of all odd-chain carnitines, including C3 and C5, was significantly ( $p<0.05$ ) higher in the *TCF7L2* group. Additionally, two long chain phosphatidylcholines (PC.aa.C40.1 and PC.ae.C42.0) were significantly elevated in the *TCF7L2* group (Table 10).

**Table 10: Metabolite traits significantly associated with *TCF7L2* genotype at baseline.**

The analysis was based on fasting concentrations averaged over two different days. All models were adjusted for BMI and age.  $\beta$ -coefficient = a standardized measure of the genotype-specific difference and varies between -1 and +1. Negative values indicate a smaller metabolite concentration in the *TCF7L2* group than in controls.

Metabolite trait in $\mu\text{M}$	<i>TCF7L2</i>	Controls	$\beta$	P
Hexose	5634.20 $\pm$ 536.22	5285.35 $\pm$ 365.22	0.69	0.038
Glutamine	622.42 $\pm$ 71.43	577.44 $\pm$ 51.31	0.62	0.049
Histidine	78.11 $\pm$ 8.58	71.54 $\pm$ 8.72	0.71	0.035
Methionine	37.07 $\pm$ 4.10	33.65 $\pm$ 3.90	0.77	0.020
Non.Ess.Aas	1309.82 $\pm$ 109.00	1209.37 $\pm$ 92.66	0.85	0.008
Aas	2324.20 $\pm$ 186.10	2175.16 $\pm$ 155.43	0.76	0.022
C3	0.52 $\pm$ 0.14	0.43 $\pm$ 0.09	0.76	0.026
C16.OH	0.008 $\pm$ 0.001	0.009 $\pm$ 0.001	-0.66	0.029
C16.2.OH	0.011 $\pm$ 0.002	0.009 $\pm$ 0.002	0.92	0.004
odd.carn	0.74 $\pm$ 0.15	0.64 $\pm$ 0.10	0.77	0.024
PC.aa.C40.1	0.37 $\pm$ 0.034	0.42 $\pm$ 0.08	-0.79	0.020
PC.ae.C42.0	0.49 $\pm$ 0.07	0.56 $\pm$ 0.08	-0.80	0.017

### 3.4.2.2 Genotype-specific differences in challenge-induced metabolite dynamics

#### Metabolic adaption and genotype-specific regulation after the OGTT

After glucose intake we observed the well-known metabolic adaptations of increased plasma glucose/hexose and insulin levels accompanied by decreased NEFA levels in both groups (Figure 14). Despite the finding, that insulin was lower ( $p=0.06$ ) and hexose was significantly higher ( $p=0.04$ ) in fasting plasma samples of *TCF7L2* risk allele carriers, both groups showed equal quantities of concentration change in those two diabetes-associated parameters, 1 and 2 hours after glucose intake (Figure 14).

All metabolites, which showed a group-specific concentration change, are presented in Table 11. This analysis revealed that two groups of metabolites, the amino acids and the phosphatidylcholines, showed genotype-specific concentration changes after glucose intake.

The amino acids revealed a genotype-specific regulation at both time points (1 hour and 2 hours after the OGTT). After glucose ingestion, the summarized amino acid concentration decreased in both groups (Table 11A). Within one hour after glucose intake, the summarized concentration of all amino acids dropped from  $2160.3 \pm 230.8$  to  $1896.7 \pm 321.3$   $\mu\text{M}$  ( $\Delta = -263.65 \mu\text{M}$ ) in controls and from  $2332.1 \pm 203.4$  to  $1866.5 \pm 200.3$   $\mu\text{M}$  ( $\Delta = -465.63 \mu\text{M}$ ) in the *TCF7L2* group. The respective change ( $\Delta$ ) is therefore significantly ( $p < 0.05$ ) stronger in the *TCF7L2* group compared to controls and this trend is still evident 2 hours post glucose intake. Regarding single amino acids; glutamine, glycine, threonine, serine, methionine and ornithine showed significant ( $p < 0.05$ ) stronger concentration decrease in the *TCF7L2* group (Table 11A). Therefore, these individual amino acids profoundly contributed to the trend observed for the sum of amino acid. One hour after the OGTT, some metabolite traits, such as the ratio ornithine/arginine and the ratio branched-chain amino acids/aromatic amino acids, showed a distinct difference between genotypes. Both ratios decrease stronger in the subjects at-risk.

1 hour after the OGTT, 7 phosphatidylcholines (Table 11A) were regulated differentially in the *TCF7L2* group compared to controls. The phosphatidylcholines uniformly showed a positive  $\beta$ -coefficient. Therefore, between baseline and 1 hour after glucose intake these

phosphatidylcholines significantly decreased within the control group. However, these phosphatidylcholines showed no significant declines in the *TCF7L2* group.

#### **Metabolites showing genotype-specific regulation after the WDT**

The WDT was performed at 12 noon. Plasma samples collected immediately before food-intake were defined as WDT-baseline samples. Due to the day time of sampling and the precedent OGTT the metabolic condition cannot be compared with the baseline samples taken at 8 am. Therefore, the results on metabolite concentrations and genotype-specific differences of the WDT-baseline are included in Table 11B under “Effect before WDT”. At this timepoint, we observed significantly ( $p < 0.05$ ) higher plasma concentrations of C0 (*TCF7L2* vs. Controls;  $46.7 \pm 7.1 \mu\text{M}$  vs.  $40.7 \pm 7.2 \mu\text{M}$ ), C3 (*TCF7L2* vs. Controls;  $0.45 \pm 0.1 \mu\text{M}$  vs.  $0.36 \pm 0.08 \mu\text{M}$ ) and C4 (*TCF7L2* vs. Controls;  $0.21 \pm 0.11 \mu\text{M}$  vs.  $0.14 \pm 0.01 \mu\text{M}$ ) and higher concentration of the summarized concentrations of all odd-chain carnitines (*TCF7L2* vs. Controls;  $0.65 \pm 0.11 \mu\text{M}$  vs.  $0.56 \pm 0.09 \mu\text{M}$ ) in the *TCF7L2* group as compared to the control group. Furthermore, two phosphatidylcholines (PC.aa.C34.4 and PC.aa.C40.4) showed significantly ( $p < 0.05$ ) higher concentrations in the *TCF7L2* than in the control group.

In the period between baseline and 2 hours post-challenge no genotype-specific regulation was observed. However, while insulin showed an equal increase in the *TCF7L2* and the control group between baseline and two hours, the subsequent decrease was enhanced by the risk allele in *TCF7L2*. Consequently, 6 hours after the WDT, *TCF7L2* risk allele carriers showed a decrease of insulin levels when compared with baseline values, while insulin levels in the control group were still elevated at this time point (Figure 14 and Table 11B). NEFA levels decreased in both groups equally between baseline and 2 hours post-ingestion and then increased 6 hours after the WDT (Figure 14). However, as shown in Table 11B, between baseline and 6 hours after food-intake, the observed increase of non-esterified fatty acids (NEFA) was with  $+0.17 \text{ mM}$  significantly ( $p = 0.02$ ) lower in plasma of *TCF7L2* risk variant carriers than in controls ( $+0.34 \text{ mM}$ ).

#### **Metabolites showing genotype-specific regulation after the OLTT**

All 20 controls, but only 12 of 14 *TCF7L2* risk allele carriers completed the OLTT. One volunteer in the *TCF7L2* group disagreed staying for two days, the other volunteer was sent home before completing the OLTT, because blood draws with the intravenous canula were not possible on day 2. Due to this lower subject number, statistical power was decreased. For this study, this might

explain the low number of metabolites, which showed significant genotype-specific differences in their concentration changes (Table 11C). 2 hours after intake of the lipid-containing drink, the hexose increase was significantly ( $p < 0.05$ ) higher in the *TCF7L2* group ( $\Delta = +1466.13 \mu\text{M}$ ) than in controls ( $\Delta = +407.28 \mu\text{M}$ ). Additionally, in this period, the concentration of Glutaryl-L-carnitine (C5.DC) or Hydroxyhexanoyl-L-carnitine (C6.OH) was increased in the *TCF7L2* group ( $+0.018 \mu\text{M}$ ), but decreased in the control group ( $-0.001 \mu\text{M}$ ), resulting in a significant ( $p = 0.01$ ) difference between both groups.

**Table 11: Metabolite traits with significant ( $p<0.05$ ) effect of the TCF7L2 risk allele (T) in rs7903146 on (A) OGTT-induced changes after 1 and 2 hours and (B) on WDT- and (C) on OLTT-induced changes after 2 and 6 hours.**

Linear mixed models were adjusted for BMI and age. Units: Insulin in [ $\mu\text{U/ml}$ ], NEFA in [ $\text{mM}$ ], all other presented metabolites in [ $\mu\text{M}$ ]. C5.DC and C6.OH cannot be distinguished by our method.  $\beta$ -coefficient = a standardized measure of the genotype-specific difference in change and varies between -1 and +1. Negative values indicate a stronger decline in metabolite concentration in the TCF7L2 group than in controls, occurring between baseline and the post-challenge time points.

**(A) OGTT**

Metabolite	$\beta$	P	TCF7L2			Control		
			baseline (mean $\pm$ SD)	$\Delta$ Change at 1 hour	$\Delta$ Change at 2 hours	baseline (mean $\pm$ SD)	$\Delta$ Change at 1 hour	$\Delta$ Change at 2 hours
<b>Significant effect between baseline and 1 hour</b>								
<b>C18</b>	-0.62	0.022	0.051 $\pm$ 0.01	-0.004	-0.01	0.046 $\pm$ 0.01	0.002	-0.003
<b>PC.aa.C32.0</b>	0.37	0.041	13.47 $\pm$ 2.64	-0.37	-0.81	13.76 $\pm$ 2.87	-1.53	-1.38
<b>PC.aa.C40.1</b>	0.40	0.039	0.37 $\pm$ 0.04	-0.004	-0.01	0.44 $\pm$ 0.09	-0.04	-0.02
<b>PC.aa.C42.5</b>	0.34	0.019	0.37 $\pm$ 0.10	-0.002	-0.02	0.40 $\pm$ 0.10	-0.04	-0.02
<b>PC.ae.C32.2</b>	0.59	0.012	0.60 $\pm$ 0.13	0.0002	-0.01	0.61 $\pm$ 0.11	-0.07	-0.04
<b>PC.ae.C40.1</b>	0.32	0.033	1.60 $\pm$ 0.43	-0.06	-0.15	1.71 $\pm$ 0.41	-0.21	-0.16
<b>PC.ae.C40.5</b>	0.38	0.033	3.42 $\pm$ 0.61	-0.11	-0.15	3.54 $\pm$ 0.66	-0.35	-0.22
<b>PC.ae.C42.0</b>	0.46	0.012	0.49 $\pm$ 0.08	-0.001	-0.01	0.56 $\pm$ 0.10	-0.04	-0.01
<b>Gln</b>	-0.89	0.018	623.36 $\pm$ 84.90	-115.66	-122.24	568.58 $\pm$ 72.10	-35.55	-53.61
<b>Gly</b>	-0.64	0.041	246.43 $\pm$ 41.41	-50.98	-49.85	228.46 $\pm$ 35.75	-23.34	-24.21
<b>Thr</b>	-0.46	0.003	107.57 $\pm$ 24.16	-22.83	-32.42	94.49 $\pm$ 25.77	-10.85	-20.76
<b>Ser</b>	-0.53	0.008	93.04 $\pm$ 14.46	-19.17	-26.82	81.84 $\pm$ 16.32	-9.96	-17.30
<b>Met</b>	-0.52	0.044	35.64 $\pm$ 4.57	-8.16	-12.31	31.72 $\pm$ 5.25	-4.82	-8.87
<b>Orn</b>	-0.69	0.015	62.60 $\pm$ 11.57	-15.05	-19.20	59.35 $\pm$ 11.19	-7.03	-12.44
<b>Orn / Arg</b>	-0.58	0.022	0.61 $\pm$ 0.13	-0.03	-0.02	0.63 $\pm$ 0.13	0.04	0.02
<b>BCAA/ aromatic AAs</b>	-0.23	0.045	2.56 $\pm$ 0.28	-0.25	-0.32	2.68 $\pm$ 0.30	-0.16	-0.31
<b>Non.Ess.AAs</b>	-0.73	0.024	1293.57 $\pm$ 122.95	-235.33	-278.40	1169.19 $\pm$ 128.69	-111.67	-156.56
<b>Glucog.AAs</b>	-0.66	0.023	339.47 $\pm$ 51.046	-70.15	-76.67	310.30 $\pm$ 44.14	-33.30	-41.51
<b>AAs</b>	-0.64	0.027	2332.10 $\pm$ 203.39	-465.63	-606.43	2160.33 $\pm$ 230.79	-263.65	-413.91



Significant effect between baseline and 2 hours								
<b>Gln</b>	-0.77	0.012	623.36±84.90	-115.66	-122.24	568.58±72.10	-35.55	-53.61
<b>Gly</b>	-0.63	0.012	246.43±41.41	-50.98	-49.85	228.46±35.751	-23.34	-24.21
<b>Thr</b>	-0.44	0.004	107.57±24.16	-22.83	-32.42	94.49±25.77	-10.85	-20.76
<b>Ser</b>	-0.56	0.022	93.04±14.46	-19.17	-26.82	81.84±16.32	-9.96	-17.30
<b>Met</b>	-0.53	0.029	35.67±4.57	-8.16	-12.31	31.72± 5.25	-4.82	-8.87
<b>Orn</b>	-0.57	0.018	62.60±11.57	-15.05	-19.20	59.35±11.19	-7.03	-12.44
<b>Non.Ess.AAs</b>	-0.73	0.007	1293.57±122.95	-235.33	-278.40	1169.19±128.69	-111.67	-156.56
<b>Glucog.AAs</b>	-0.67	0.010	339.47±51.05	-70.15	-76.67	310.30±44.14	-33.30	-41.51
<b>AAs</b>	-0.60	0.020	2332.10±203.39	-465.63	-606.43	2160.33±230.79	-263.65	-413.91

**(B) WDT**

Metabolite	β	P	TCF7L2			Control		
			baseline (mean±SD)	Δ Change at 2 hours	Δ Change at 6 hours	baseline (mean±SD)	Δ Change at 2 hours	Δ Change at 6 hours
<b>Significant effect before WDT</b>								
<b>C0</b>	0.67	0.03	46.76±7.12	-0.41	-3.3	40.7±7.2	0.75	-2.16
<b>C3</b>	0.7	0.01	0.45±0.1	0.06	0.06	0.36±0.08	0.07	0.04
<b>C4</b>	0.77	0.01	0.21±0.11	-0.01	0.03	0.14±0.04	0.01	0.01
<b>odd.carn</b>	0.71	0.02	0.65±0.11	0.04	0.06	0.56±0.09	0.05	0.05
<b>PC.aa.C34.4</b>	0.72	0.05	2.04±0.65	-0.17	-0.15	1.63±0.51	-0.11	-0.07
<b>PC.aa.C40.4</b>	0.71	0.03	4.48±1.23	-0.16	0.05	3.63±0.87	-0.01	0.03
<b>PC.aa.C44.5/ PC.aa.C42.5</b>	0.82	0.02	0.83±0.07	0.003	-0.01	0.77±0.07	0.01	0.01
<b>Significant effect between baseline and 6 hours</b>								
<b>Insulin</b>	-0.32	0.004	7.76±6.08	21.74	-2.96	5.33±2.68	21.95	1.52
<b>NEFA</b>	0.73	0.02	0.2±0.16	-0.1	0.34	0.31±0.2	-0.18	0.17
<b>PC.aa.C40.3/ PC.aa.C42.5</b>	-0.44	0.04	1.83±0.29	-0.09	-0.12	1.76±0.27	0.03	-0.002
<b>PUFA.PC./ SFA.PC</b>	-0.28	0.05	51.96±4.39	1.23	2.38	51.82±6.64	1.55	4

### (c) OLTT

Metabolite	$\beta$	P	TCF7L2			Control		
			baseline (mean $\pm$ SD)	$\Delta$ Change at 2 hours	$\Delta$ Change at 6 hours	baseline (mean $\pm$ SD)	$\Delta$ Change at 2 hours	$\Delta$ Change at 6 hours
<b>Significant effect between baseline and 2 hours</b>								
H1	0.99	0.04	5545.89 $\pm$ 529.79	1466.13	-694.64	7012.02 $\pm$ 1886.81	407.28	-339.25
C5.DC or C6.OH	0.88	0.01	0.018 $\pm$ 0.003	0.003	0.002	0.021 $\pm$ 0.01	-0.001	-0.0001
<b>Significant effect between baseline and 6 hours</b>								
PC.aa.C36.3/ PC.aa.C36.4	-0.20	0.001	0.67 $\pm$ 0.119	0.01	0.05	0.67 $\pm$ 0.13	0.01	0.08
PC.aa.C44.4	-0.44	0.04	0.38 $\pm$ 0.06	-0.0020	-0.02	0.38 $\pm$ 0.06	0.01	0.02

### 3.4.3 Discussion

T2DM is a multifactorial metabolic disease and its development is depending on the inheritance of susceptibility genes combined with the presence of certain environmental risk factors, such as obesity. Metabolites as the products of metabolism reflect the final outcome of gene-environment interactions. The metabolites we measured in our study are involved in amino acid, fatty acid or carbohydrate metabolism and therefore could relate the *TCF7L2* genomic alteration to a broad metabolic outcome.

Under fasting conditions, *TCF7L2* risk allele carriers showed insignificantly lower ( $p=0.06$ ) plasma insulin levels than controls in this study. Lower insulin levels in subjects carrying the *TCF7L2* rs7903146 risk variant have been reported before (113, 114). The effect of the *TCF7L2* gene locus on insulin secretion has been discussed to be mediated most probably by the implication of the *TCF7L2* gene in the WNT signaling pathway, which plays a critical role in pancreatic growth and  $\beta$ -cell mass development (115) and influences synthesis of the insulinotropic incretin GLP-1 in intestinal L-cells (116). We observed that subjects in the *TCF7L2* group had significantly higher HbA1c levels, underscoring the significant disadvantageous effects of the *TCF7L2* risk allele per se on glucose metabolism even in healthy subjects. HbA1c is a routine clinical parameter used to

evaluate the average blood glucose concentration over the previous 8 to 12 weeks (117). Higher levels in the subdiabetic range (4.8 - 5.9%) have been shown to be predictive of type 2 diabetes risk (118) and therefore demonstrate the increased diabetes risk in our subjects carrying the *TCF7L2* rs7903146 risk allele. In parallel, Franklin et al. (119) and Karns et al. (120) reported significant associations of the risk variant in the *TCF7L2* gene (rs7903146) with HbA1c levels of healthy individuals. Higher levels in hemoglobin glycation normally result from higher incessant glucose levels. Baseline and postprandial glucose levels were slightly, but insignificantly elevated in our *TCF7L2* group, but our metabolite analysis of fasting plasma samples revealed significantly higher hexose levels. The main proportion of plasma hexose levels is provided by glucose. D-Mannose and D-fructose are found in human plasma, however in very low concentration (121). Nevertheless, higher plasma mannose (122, 123) and fructose (123) concentrations have been found in T2DM. As the here used MS-technique does not distinguish between the hexoses, it is not possible to compare plasma mannose or fructose levels between controls and *TCF7L2* risk variant carriers within this study.

In addition to the here observed changes in glucose/insulin plasma levels, we showed changes in lipid levels with the T allele being associated with significantly higher levels of HDL cholesterol ( $p = 0.05$ ) and a tendency for lower levels of LDL cholesterol and triglycerides. These findings suggest a lower risk lipid profile in our T allele carriers in rs7903146. A similar lipid profile for the T allele has been observed in a previous population based study which included 944 older diabetic and non-diabetic subjects (125).

Our metabolite analysis of plasma samples taken after over-night fasting period, revealed in addition to the higher levels of hexose, increased concentrations of (i) certain acylcarnitines and (ii) of numerous amino acids in the *TCF7L2* risk allele carriers.

#### **(i) Plasma acylcarnitine alterations**

As described in chapter 2 of this thesis, acylcarnitines accumulate in plasma during fasting. This effect has been proposed to result from high lipid oxidation, when inadequate capacity of the TCA cycle relative to fuel delivery results in a build-up of intra-cellular acyl-CoAs (78). Plasma acylcarnitines therefore reflect the intracellular acyl-CoA pool (78) and, consequently, C3 reflects

the intracellular levels of propionyl-CoA. Propionyl-CoA is either formed by beta-oxidation of odd-chain fatty acids or by degradation of isoleucine and valine or from  $\alpha$ -ketobutyrate, which in turn is a degradation product of threonine and methionine. Propionyl-CoA is converted to succinyl-CoA before entering the TCA-cycle (126). In states of high beta-oxidation rates, which include the samples taken after an overnight fast and the samples taken at 12 am before the WDT, our *TCF7L2* group showed higher concentrations of plasma acylcarnitines, especially C3 and the concentration of summarized odd-chain acylcarnitines. While higher concentrations of acylcarnitines in fasting plasma have been reported in subjects with T2DM (78, 127, 128), no reports on elevated C3 or C5 concentrations exist. In contrary, reduced propionylcarnitine levels have been reported in T2DM (127). The authors hypothesized that anaplerotic propionyl-CoA increases TCA-cycle activity in mitochondria. The increased plasma C3 levels therefore might be explained by a compensatory mechanism occurring in our healthy *TCF7L2* risk-allele carriers. It is possible, that the selected study group of male *TCF7L2* risk-allele carriers, still healthy at an average age of  $54\pm 19$  years, promoted the inclusion of individuals with compensatory mechanisms which reduced their diabetes risk. Therefore, further studies will be required to evaluate if similar changes in plasma propionylcarnitine also occur in diabetics carrying the *TCF7L2* risk allele.

According to our results, the *TCF7L2* risk allele does not alter acylcarnitine concentration changes after glucose or food-intake, except for C18 and C5:DC, 1 hour after the OGTT and 2 hours after the lipid-drink, respectively.

Metabolite changes after glucose intake are reflective of the well-known effects of insulin on glycolysis, lipolysis and proteolysis (129). According to this metabolic adaption we observed increases in plasma glucose and insulin or decreases in NEFA levels in both groups. Historically, the defining characteristic of T2DM is disrupted glucose homeostasis and up to now glucose metabolism is the main target for research reports on metabolic effects of *TCF7L2*. However, after intake of oral glucose, our non-diabetic, non-obese risk allele carriers, showed similar challenge-induced changes on the two most common parameters plasma glucose and insulin levels if compared with the control group. Instead, two distinct classes of metabolites comprising (ii) the plasma amino acids and (iii) the long chain phosphatidylcholines were differentially regulated between genotypes. Indeed, there is growing appreciation, that insulin resistance involves changes

in amino acid and lipid metabolism in addition to glucose metabolism. Additionally, the involvement of TCF7L as final transcription factor of the WNT signaling cascade provides a connection to multiple metabolic pathways that go beyond regulation of insulin secretion.

### **(ii) Amino acid alterations in *TCF7L2* risk variants**

Disturbed amino acid metabolism has been found in insulin resistance and T2DM in various studies (130). General hyperaminoacidemia was shown to be a characteristic manifestation in obesity (70) or diabetes (131), probably caused by insulin resistance or low insulin levels. In line with these findings, at baseline the overall amino acid plasma levels were significantly higher in our *TCF7L2* risk allele carriers when compared with controls. However, while our at-risk subjects showed significantly elevated plasma levels of glutamine, methionine and histidine, previous research reports repeatedly described elevated blood concentrations of BCAAs (leucine, isoleucine, valine) in obese and/or T2DM human subjects (132, 133). Even if less often, elevated plasma concentrations of other amino acids including glutamine (134), methionine (70, 134, 135) and histidine (136) were also reported as indicators of insulin resistance and/or predictors of T2DM risk. To this end, a body of literature exists, which supports the idea of modest changes in amino acid concentrations as a very early alteration towards T2DM development. It is possible, that the amino acids found to be altered in our study provide a typical feature in *TCF7L2*-associated T2DM development. However, publications analyzing the genetic associations of metabolite profiles in large cohort studies did not describe metabolites associated with *TCF7L2* (22, 48, 49).

On the one hand, these findings could be of distinct value in terms of personalized nutritional recommendations: For example dietary methionine restriction, with subsequent decreases in plasma methionine levels, was reported to increase insulin sensitivity (137). Therefore, our finding of elevated methionine levels in *TCF7L2* carriers might indicate a particular beneficial effect of nutritional methionine restriction in subjects predisposed to T2DM by the T allele as in rs7903146.

On the other hand, the presented findings might reveal new targets of metabolic pathways influenced by the *TCF7L2* gene locus: For example, glutamine provides an efficient substrate for gluconeogenesis (138) and plasma levels are increased after an overnight fasting period due to muscle proteolysis. The *TCF7L2* gene has been shown to be an important regulator of

gluconeogenic genes and subsequently of hepatic glucose production in cultured hepatocytes (139). However, *in vitro* experiments (140) and net balance studies in humans (138, 141, 142) provided evidence, that alanine and glutamine are selective gluconeogenic precursors metabolized in liver and kidney, respectively. In our study glutamine, but not alanine levels were elevated in *TCF7L2* risk allele carriers. These results suggest that the impact of *TCF7L2* on renal gluconeogenesis should be investigated in further studies.

After glucose intake, increased insulin levels inhibit proteolysis and stimulate amino-acid uptake resulting in a decreased plasma amino acid pool (142). This decrease in plasma amino acid levels was evident in both groups. Notably, we observed a significantly stronger decrease of amino acid levels in the *TCF7L2* risk allele carriers if compared to the control subjects. This steeper decline was present between baseline and both post-challenge time points after the OGTT for glutamine, glycine, threonine, serine, methionine, ornithine, the sum of non-essential AAs, of glucogenic AAs and of all AAs.

Insulin is necessary for the transport of certain amino acid into hepatocytes, skeletal muscle, and fibroblasts, explaining, at least partially, the clinical observation that insulin reduces the plasma pool of amino acids. At least four amino acid transport systems were shown to be insulin sensitive and those insulin sensitive systems were reported to mainly transport nonessential amino acids (143). Compared to controls, assimilation of pure glucose equally increased plasma insulin levels in our *TCF7L2* group, accompanied by a significantly stronger reduction in the overall plasma concentration of non-essential amino acids. This observation indicates a higher insulin sensitivity of amino acid transport into cells in the *TCF7L2* group. In line with this, previous studies already stated that insulin sensitivity was either not altered (110, 144) or even increased (145, 146) in *TCF7L2* variants.

Additionally, the transport system of BCAAs is not sensitive to insulin action (143). These amino acids have often been described to be altered in insulin resistant states (130, 133), but were not differentially regulated between our *TCF7L2* risk allele carriers and controls.

To this end, a body of literature exists, which supports the idea of modest changes in amino acid concentration as a very early alteration towards T2DM development. Our findings suggest that

*TCF7L2* variants alter multiple intermediary metabolic pathways including amino acid metabolism. *TCF7L2*-associated alterations in amino acid metabolism might play a potential key role early in the pathogenesis of *TCF7L*-associated T2DM and follow-up studies on amino acid profiles should be attempted to elucidate the significance of either of these changes.

### **(iii) Plasma phosphatidylcholine alterations**

PCs are the predominant phospholipids in cell membranes and of the circulating blood lipoproteins. Dyslipidemia, comprising increased plasma TG and LDL concentrations and lowered HDL levels, is a common feature in humans with type 2 diabetes. These lipid changes have been proposed to result from an increased free fatty acid flux secondary to insulin resistance (147). Particularly phosphatidylcholines are prominent components of all plasma lipoproteins. PC species have been shown to be associated with HDL and total cholesterol levels, while phosphatidylethanolamine (PE) species are associated with triglyceride levels (31). Suhre et al. reported lower PC and higher PE concentration in T2DM patients, treated with lipid-lowering medication, accompanied with lower HDL and total cholesterol levels and higher triglyceride levels in this group (40). Here, we report lower concentrations of phosphatidylcholines (PC.aa.C40.1, PC.ae.C42.0) in the *TCF7L2* group at baseline, which might reflect the observed lower cholesterol and TG levels in the *TCF7L2* group. Additionally, in the *TCF7L2* risk allele carriers we observed differences in postprandial regulation of plasma PC concentrations compared to the control group. Especially, 1 hour after glucose intake PC concentrations decreased stronger in controls than in the at-risk group. This might indicate that lipid metabolism in *TCF7L2* risk allele carriers adapts less flexible to the altered energy availability after an OGTT.

### **3.4.4 Conclusion**

In this study, we observed modest metabolic alterations in the *TCF7L2* risk allele carriers like lower insulin and higher HbA1c levels at baseline, as previously reported in literature (119, 148, 149). After the OGTT, we found differences in the postprandial regulation of amino acids and phosphatidylcholines. The metabolite alterations observed in this study indicate that the *TCF7L2* risk allele alters amino acid and lipid metabolism under conditions of high glucose and high insulin concentrations. Due to the small sample size, results of this proof-of-principle study can only be considered as preliminary findings, which need verification by studies of larger sample size. Furthermore, the results were not adjusted for multiple testing, which bears the risk of false positive results. After verification, additional work must be conducted to further understand the metabolite alterations observed within this study.



## LIST OF FIGURES

Figure 1: Study design of the HuMet-study .....	8
Figure 2: Time courses of glucose (A), hexose (B), insulin (C) and lactate (D) concentrations over all 56 time-points measured within the HuMet-study. ....	20
Figure 3: Cluster analysis classifies plasma carnitines into two main clusters. ....	22
Figure 4: Mean values of free carnitine, acetylcarnitine, cluster 1 and 2 over all time points. ....	23
Figure 5: Time courses of PC.aa.32.2 (A), PC.aa.32.1 (B), lysoPC.a.C14 (C) and (D) lysoPC.a.C18.2 concentrations over all 56 time -points measured within the HuMet-study. ....	25
Figure 6: Time courses of 11 amino acids, with significant concentration changes over all 56 time points measured within the HuMet-study.....	27
Figure 7: Cluster dendrogram of 11 amino acids, C2 and acylcarnitines over all time points. ....	28
Figure 8: Concentration changes of selected catabolic marker metabolites during the fasting period. ....	29
Figure 9: Correlations in metabolite trends. ....	30
Figure 10: Metabolic response to challenges. ....	31
Figure 11: Inter-individual variation of metabolite concentrations in the context of challenges and sample types. ....	34
Figure 12: Comparison of baseline metabolite, challenge metabolite and metabolite ratio levels with glucose concentration.....	36
Figure 13: Study design of the VID-study.....	48
Figure 14: Concentration profiles of 5 metabolic key parameters (glucose, insulin, lactate, NEFAs and triglycerides, color coded for the 3 genotypes investigated within the VID study. ....	55

Figure 15: Schematic illustration of metabolites changed within the FTO risk allele carriers in the context of cellular energy metabolism. .... 62

Figure 16: Schematic representation of the canonical WNT signaling pathway. .... 66

## LIST OF TABLES

Table 1: Nutrient composition of the SLD and the OLTT .....	10
Table 2: Presentation of all metabolites revealing significant concentration changes over time. ....	18
Table 3: Baseline characteristics of the study cohort. ....	32
Table 4: Model-derived metabolite ratios improve correlation with metabolic parameters. ....	37
Table 5: Nutrient composition of the SLD, WDT and the OLTT .....	47
Table 6: Baseline anthropometric and clinical data of the <i>FTO</i> and the control group. ....	53
Table 7: Metabolite traits significantly associated with <i>FTO</i> genotype at baseline. ....	54
Table 8: Metabolite traits with significant ( $p<0.05$ ) effect of the <i>FTO</i> SNP rs9939609 on (A) OGTT-induced changes after 1 and 2 hours, (B) on WDT-induced changes after 2 and 6 hours and (C) on OLTT-induced changes after 2 and 6 hours. ....	57
Table 9: Baseline values of anthropometric and routine blood parameters of the <i>TCF7L2</i> and the control group.....	68
Table 10: Metabolite traits significantly associated with <i>TCF7L2</i> genotype at baseline. ....	69
Table 11: Metabolite traits with significant ( $p<0.05$ ) effect of the <i>TCF7L2</i> risk allele (T) in rs7903146 on (A) OGTT-induced changes after 1 and 2 hours and (B) on WDT- and (C) on OLTT-induced changes after 2 and 6 hours.....	73

## ABBREVIATIONS

ADP	Adenosine diphosphate
ALT	Alanin-Aminotransferase
AST	Aspartat-Aminotransferase
ATP	Adenosine triphosphate
AUC	Area under the curve
BIA	Bioelectrical impedance analysis
BMI	Body mass index
CRP	C-reactive protein
CV	Coefficient of variance
Cx:y	Acylcarnitine with x denoting the chain length and y denoting the number double-bonds
DBP	Diastolic blood pressure
EBC	Exhaled breath condensate
EDTA	Ethylenediaminetetraacetic acid
<i>FTO</i>	Fat mass and obesity associated
GOT	Glutamat-oxalacetat-transaminase
GPT	Glutamat-pyruvat-transaminase
GWAS	Genome wide association study
HbA1c	Hemoglobin A1c
HC	Hip circumference
HDL	High - density lipoprotein
HOMA	Homeostasis model assessment
HSC	Human study center

LC	Liquid chromatography
LDL	Low - density lipoprotein
MCH	Mean corpuscular hemoglobin
MCHC	Mean corpuscular hemoglobin concentration
MCV	Mean corpuscular volume
mRNA	Messenger Ribonucleic acid
MS	Mass spectrometry
MS/MS	Tandem Mass spectrometry
MUFA	Mono unsaturated fatty acid
NADH	Nicotinamide adenine dinucleotide hydrogen
NEFA	Non-esterified fatty acid
OGTT	Oral glucose tolerance test
OLTT	Oral lipid tolerance test
PAT	Physical activity test
PC	Phosphatidylcholine
PCA	Principal component analysis
PDC	Pyruvate dehydrogenase complex
PE	Phosphatidylethanolamine
PUFA	Poly unsaturated fatty acid
QUICKI	Quantitative insulin-sensitivity check index
RMR	Resting metabolic rate
SBP	Systolic blood pressure
SD	Standard deviation
SFA	Saturated fatty acids
SLD	Standard liquid Diet

SNP	Single nucleotide polymorphism
T2DM	Type 2 diabetes mellitus
TCA	Tricarboxylic acid
<i>TCF7L2</i>	Transcription factor 7-like 2
TG	Triglycerides
TSH	Thyroid-stimulating hormone
V13	Volunteer 13
V14	Volunteer 14
WC	Waist circumference
WHO	World Health Organization
WHR	Waist-to-hip-ratio
Wnt	Wingless-type MMTV integration site family member

## REFERENCES

1. Kell DB (2006) Systems biology, metabolic modelling and metabolomics in drug discovery and development. *Drug Discov. Today* 11:1085–1092.
2. Pohmann R (2011) Physical basics of NMR. *Methods Mol Biol* 771:3–21.
3. Villas-Boas S, Mas S, Akesson M, Smedsgaard J, Nielsen J (2005) Mass spectrometry in metabolome analysis. *Mass Spectrom Rev* 24:613–646.
4. Kühn O (2008) *Phosphorus-31 NMR spectroscopy. A concise introduction for the synthetic organic and organometallic chemist* (Springer, Berlin, London).
5. Dunn WB, Bailey NJC, Johnson HE (2005) Measuring the metabolome: current analytical technologies. *Analyst* 130:606–625.
6. Hoffmann E de, Stroobant V (2011) *Mass spectrometry. Principles and applications* (Wiley, Chichester).
7. Krug S *et al.* (2012) The dynamic range of the human metabolome revealed by challenges. *FASEB J* 26:2607–2619.
8. Martins AM (1999) Inborn errors of metabolism: a clinical overview. *Sao Paulo Med J* 117:251–265.
9. Garrod AE (1975) The Lancet. The incidence of alkaptonuria: a study in chemical individuality. *Nutr. Rev.* 33:81–83.
10. Peltonen L, McKusick VA (2001) Genomics and medicine. Dissecting human disease in the postgenomic era. *Science* 291:1224–1229.
11. Frayling TM *et al.* (2007) A common variant in the *FTO* gene is associated with body mass index and predisposes to childhood and adult obesity. *Science* 316:889–894.
12. Frayling TM (2007) Genome-wide association studies provide new insights into type 2 diabetes aetiology. *Nat. Rev. Genet.* 8:657–662.
13. Garrod AE (1902) The incidence of alkaptonuria: a study in chemical individuality. *Yale J Biol Med* 75 (4):221-231.
14. Levy PA (2010) An overview of newborn screening. *J Dev Behav Pediatr* 31:622–631.
15. Jansson J *et al.* (2009) Metabolomics reveals metabolic biomarkers of Crohn's disease. *PLoS ONE* 4:e6386.
16. Bogdanov M *et al* (2008) Metabolic profiling to develop blood biomarkers for Parkinson's disease. *Brain* 131:389-396.
17. Gowda GA *et al* (2008) Metabolomics-based methods for early disease diagnostics. *Expert Rev. Mol. Diagn.* 8:617-633.

18. Shaham O *et al.* (2008) Metabolic profiling of the human response to a glucose challenge reveals distinct axes of insulin sensitivity. *Mol. Syst. Biol.* 4:214.
19. Wopereis S *et al.* (2009) Metabolic profiling of the response to an oral glucose tolerance test detects subtle metabolic changes. *PLoS ONE* 4:e4525.
20. Rubio-Aliaga I *et al.* (2010) Metabolomics of prolonged fasting in humans reveals new catabolic markers. *Metabolomics*: 1–13.
21. Altmaier E *et al.* (2008) Bioinformatics analysis of targeted metabolomics--uncovering old and new tales of diabetic mice under medication. *Endocrinology* 149:3478–3489.
22. Illig T *et al.* (2010) A genome-wide perspective of genetic variation in human metabolism. *Nat. Genet.* 42:137–141.
23. Römisch-Margl W *et al.* (2011) A procedure for tissue sample preparation and metabolite extraction for high-throughput targeted metabolomics, *Metabolomics*: 1-10.
24. Weljie AM *et al.* (2006) Targeted profiling: quantitative analysis of 1H NMR metabolomics data. *Anal. Chem.* 78:4430-4442.
25. Lindinger W, Hansel A, Jordan A (1998) On-line monitoring of volatile organic compounds at pptv levels by means of proton-transfer-reaction mass spectrometry (PTR-MS): medical applications, food control and environmental research. *Int. J. Mass Spectrom.* 173:191-241.
26. Lucio M *et al.* (2010) Insulin sensitivity is reflected by characteristic metabolic fingerprints--a Fourier transform mass spectrometric non-targeted metabolomics approach. *PLoS ONE* 5:e13317.
27. Suhre K, Schmitt-Kopplin P (2008) MassTRIX: mass translator into pathways. *Nucleic Acids Res* 36:W481-4.
28. Benjamini Y, Hochberg Y (1995) Controlling the false discovery rate: a practical and powerful approach to multiple testing. *J. Royal Stat. Soc. B (Methodological)* 57:289–300.
29. Luck JM, Morrison G, Wilbur LF (1928) The effect of insulin on the amino acid content of blood. *Journal of Biological Chemistry* 77:151–156.
30. Rhee EP *et al.* (2011) Lipid profiling identifies a triacylglycerol signature of insulin resistance and improves diabetes prediction in humans. *J. Clin. Invest.* 121:1402–1411.
31. Wiesner P, Leidl K, Boettcher A, Schmitz G, Liebisch G (2009) Lipid profiling of FPLC-separated lipoprotein fractions by electrospray ionization tandem mass spectrometry. *J Lipid Res* 50:574–585.
32. Pietiläinen KH *et al.* (2007) Acquired obesity is associated with changes in the serum lipidomic profile independent of genetic effects--a monozygotic twin study. *PLoS ONE* 2:e218.
33. Bartlett K, Eaton S (2004) Mitochondrial beta-oxidation. *Eur. J. Biochem.* 271:462–469.
34. Eaton S (2002) Control of mitochondrial beta-oxidation flux. *Prog. Lipid Res.* 41:197–239.



35. Ramsay RR (2000) The carnitine acyltransferases: modulators of acyl-CoA-dependent reactions. *Biochem. Soc. Trans.* 28:182–186.
36. Noland RC *et al.* (2009) Carnitine insufficiency caused by aging and overnutrition compromises mitochondrial performance and metabolic control. *J. Biol. Chem.* 284:22840–22852.
37. Maher AD, Zirah SFM, Holmes E, Nicholson JK (2007) Experimental and analytical variation in human urine in <sup>1</sup>H NMR spectroscopy-based metabolic phenotyping studies. *Anal. Chem.* 79:5204–5211.
38. Begriche K *et al.* (2008) [beta]-Aminoisobutyric Acid Prevents Diet-induced Obesity in Mice With Partial Leptin Deficiency. *Obesity* 16:2053–2067.
39. Rashed MS (2001) Clinical applications of tandem mass spectrometry: ten years of diagnosis and screening for inherited metabolic diseases. *J. Chromatogr. B Biomed. Sci. Appl.* 758:27–48.
40. Suhre K *et al.* (2011) Human metabolic individuality in biomedical and pharmaceutical research. *Nature* 477:54–60.
41. Zhao X *et al.* (2010) Metabonomic fingerprints of fasting plasma and spot urine reveal human pre-diabetic metabolic traits. *Metabolomics* 6:362–374.
42. Gall WE *et al.* (2010) alpha-hydroxybutyrate is an early biomarker of insulin resistance and glucose intolerance in a nondiabetic population. *PLoS ONE* 5:e10883.
43. Wang TJ *et al.* (2011) Metabolite profiles and the risk of developing diabetes. *Nat. Med.* 17:448–453.
44. Kettunen J *et al.* (2012) Genome-wide association study identifies multiple loci influencing human serum metabolite levels. *Nat. Genet* 44:269–276.
45. Van Dongen J, Slagboom PE, Draisma HHM, Martin NG, Boomsma DI (2012) The continuing value of twin studies in the omics era. *Nat. Rev. Genet* 13:640–653.
46. Nicholson G *et al.* (2011) Human metabolic profiles are stably controlled by genetic and environmental variation. *Mol. Syst. Biol* 7:525.
47. Shah SH *et al.* (2009) High heritability of metabolomic profiles in families burdened with premature cardiovascular disease. *Mol Syst Biol* 5.
48. Gieger C *et al.* (2008) Genetics meets metabolomics: a genome-wide association study of metabolite profiles in human serum. *PLoS Genet.* 4:e1000282.
49. Suhre K *et al.* (2011) A genome-wide association study of metabolic traits in human urine. *Nat. Genet.* 43:565–569.
50. Kopelman P (2007) Health risks associated with overweight and obesity. *Obes Rev.* 1:13-27.
51. WHO (2011) WHO| Obesity and overweight. <http://www.who.int/mediacentre/factsheets/fs311/en/>.

52. Maes HH, Neale MC, Eaves LJ (1997) Genetic and environmental factors in relative body weight and human adiposity. *Behav Genet.* 27(4):325-351. Review.
53. Hjelmborg JV *et al.* (2008) Genetic influences on growth traits of BMI: a longitudinal study of adult twins. *Obesity (Silver Spring)* 16(4):847-52.
54. Loos, R.J. (2012) Genetic determinants of common obesity and their value in prediction. *Best Pract. Res. Clin. Endocrinol. Metab.* 26:211–226.
55. Speliotes EK *et al.* (2010) Association analyses of 249,796 individuals reveal 18 new loci associated with body mass index. *Nat Genet.* 42(11):937-48.
56. Cha SW *et al.* (2008) Replication of genetic effects of *FTO* polymorphisms on BMI in a Korean population. *Obesity (Silver Spring)* 16:2187–2189.
57. González-Sánchez JL *et al.* (2009) Variant rs9939609 in the *FTO* gene is associated with obesity in an adult population from Spain. *Clinical Endocrinology* 70:390–393.
58. Chauhan G *et al.* (2011) Common variants of *FTO* and the risk of obesity and type 2 diabetes in Indians. *J Hum Genet.* 2011 56:720-6.
59. Fang H *et al.* (2010) Variant rs9939609 in the *FTO* gene is associated with body mass index among Chinese children. *BMC Med Genet.* 22: 136.
60. Okuda M *et al.* (2011) Association between the *FTO* gene and overweight in Japanese children and adolescents. *Pediatr Diabetes.* 12(5):494-500.
61. Peeters A *et al.* (2008) Variants in the *FTO* gene are associated with common obesity in the Belgian population. *Mol Genet Metab.* 93(4):481-4.
62. Scuteri A *et al.* (2007) Genome-Wide Association Scan Shows Genetic Variants in the *FTO* Gene Are Associated with Obesity-Related Traits. *PLoS Genet.* 3 (7): e115.
63. Villalobos-Comparán M *et al.* (2008) The *FTO* gene is associated with adulthood obesity in the Mexican population. *Obesity (Silver Spring)* 16:2296-2301.
64. Hubacek JA *et al.* (2008) The *FTO* gene and obesity in a large Eastern European population sample: the HAPIEE study. *Obesity (Silver Spring)* 16:2764-2766.
65. Gerken T *et al.* (2007) The obesity-associated *FTO* gene encodes a 2-oxoglutarate-dependent nucleic acid demethylase. *Science* 318:1469–1472.
66. Kim JY *et al.* (2010) Metabolic Profiling of Plasma in Overweight/Obese and Lean Men using Ultra Performance Liquid Chromatography and Q-TOF Mass Spectrometry (UPLC-Q-TOF MS). *Journal of Proteome Research* 9:4368–4375.
67. Wang C *et al.* (2011) Metabolic profiling of urine in young obese men using ultra performance liquid chromatography and Q-TOF mass spectrometry (UPLC/Q-TOF MS). *J Chromatogr B Analyt Technol Biomed Life Sci.* 879:2871-2876.
68. Jacobsson JA *et al.* (2009) The common *FTO* variant rs9939609 is not associated with BMI in a longitudinal study on a cohort of Swedish men born 1920-1924. *BMC Med Genet.* 10:131.

69. Ruiz JR *et al.* (2010) Attenuation of the Effect of the *FTO* rs9939609 Polymorphism on Total and Central Body Fat by Physical Activity in Adolescents: The HELENA Study. *Arch Pediatr Adolesc Med* 164:328–333.
70. Felig P, Marliss E, Cahill GF (1969) Plasma Amino Acid Levels and Insulin Secretion in Obesity. *New England Journal of Medicine. N Engl J Med* 281:811–816.
71. Breum L, Rasmussen MH, Hilsted J, Fernstrom JD (2003) Twenty-four-hour plasma tryptophan concentrations and ratios are below normal in obese subjects and are not normalized by substantial weight reduction. *The American Journal of Clinical Nutrition* 77:1112–1118.
72. Sugrue MF (1987) Neuropharmacology of drugs affecting food intake. *Pharmacol. Ther* 32:145–182.
73. Blundell JE (1984) Serotonin and appetite. *Neuropharmacology* 23:1537–1551.
74. Fredriksson R *et al.* (2008) The obesity gene, *FTO*, is of ancient origin, up-regulated during food deprivation and expressed in neurons of feeding-related nuclei of the brain. *Endocrinology* 149:2062–2071.
75. Tanofsky-Kraff M *et al.* (2009) The *FTO* gene rs9939609 obesity-risk allele and loss of control over eating. *American Journal of Clinical Nutrition* 90:1483–1488.
76. Graessler J *et al.* (2009) Top-Down Lipidomics Reveals Ether Lipid Deficiency in Blood Plasma of Hypertensive Patients. *PLoS ONE* 4:e6261.
77. Fritz IB, McEwen B (1959) Effects of carnitine on fatty-acid oxidation by muscle. *Science* 129:334–335.
78. Koves TR *et al.* (2008) Mitochondrial overload and incomplete fatty acid oxidation contribute to skeletal muscle insulin resistance. *Cell Metab.* 7:45–56.
79. Frohlich J, Secombe DW, Hahn P, Dodek P, Hynie I (1978) Effect of fasting on free and esterified carnitine levels in human serum and urine: correlation with serum levels of free fatty acids and beta-hydroxybutyrate. *Metab. Clin. Exp* 27:555–561.
80. Costa CC, Almeida IT de, Jakobs C, Poll-The BT, Duran M (1999) Dynamic changes of plasma acylcarnitine levels induced by fasting and sunflower oil challenge test in children. *Pediatr. Res* 46:440–444.
81. Mihalik S *et al.* (2010) Increased levels of plasma acylcarnitines in obesity and type 2 diabetes and identification of a marker of glucolipototoxicity. *Obesity (Silver Spring)* 18:1695–1700.
82. Hoppel CL, Genuth SM (1980) Carnitine metabolism in normal-weight and obese human subjects during fasting. *Am. J. Physiol* 238:E409-15.
83. Brass EP (1995) Pharmacokinetic considerations for the therapeutic use of carnitine in haemodialysis patients. *Clin Ther* 1995:176–185.

84. Stephens FB, Constantin-Teodosiu D, Laithwaite D, Simpson EJ, Greenhaff PL (2006) An Acute Increase in Skeletal Muscle Carnitine Content Alters Fuel Metabolism in Resting Human Skeletal Muscle. *Journal of Clinical Endocrinology & Metabolism* 91:5013–5018.
85. Weber G (2002) *Advances in enzyme regulation, volume 42. Proceedings of the Forty-Second International Symposium on Regulation of Enzyme Activity and Synthesis in Normal and Neoplastic Tissues, held at Indiana University School of Medicine Indianapolis, Indiana, September 24-25, 2001* (Pergamon, Oxford).
86. Grunnet LG *et al.* (2009) Increased Recovery Rates of Phosphocreatine and Inorganic Phosphate after Isometric Contraction in Oxidative Muscle Fibers and Elevated Hepatic Insulin Resistance in Homozygous Carriers of the A-allele of *FTO* rs9939609. *Journal of Clinical Endocrinology & Metabolism* 94:596–602.
87. Wyss M, Kaddurah-Daouk R (2000) Creatine and Creatinine Metabolism. *Physiological Reviews* 80:1107–1213.
88. Wild S (2004) Global prevalence of diabetes: estimates for the year 2000 and projections for 2030. *Diabetes Care*. 27(5):1047-53.
89. Shaw J, Sicree R, Zimmet P (2010) Global estimates of the prevalence of diabetes for 2010 and 2030. *Diabetes Research and Clinical Practice* 87:4–14.
90. Lazar MA (2005) How obesity causes diabetes: not a tall tale. *Science*. 307(5708):373-5.
91. Bassuk SS, Manson JE (2005) Epidemiological evidence for the role of physical activity in reducing risk of type 2 diabetes and cardiovascular disease. *J Appl Physiol*. 99(3):1193-204. Review.
92. Manson JE *et al.* (1991) Physical activity and incidence of non-insulin-dependent diabetes mellitus in women. *Lancet*. 338(8770):774-8.
93. Lönnroth P, Smith U (1986) Aging enhances the insulin resistance in obesity through both receptor and postreceptor alterations. *J Clin Endocrinol Metab*. 62(2):433-7.
94. Groop LC, Tuomi T (1997) Non-insulin-dependent diabetes mellitus--a collision between thrifty genes and an affluent society. *Ann Med* 29:37–53.
95. Newman B *et al.* (1987) Concordance for type 2 (non-insulin-dependent) diabetes mellitus in male twins. *Diabetologia*. 30(10):763-8.
96. Dabelea D, Pettitt DJ, Jones KL, Arslanian SA (1999) TYPE 2 DIABETES MELLITUS IN MINORITY CHILDREN AND ADOLESCENTS: An Emerging Problem. *Endocrinology & Metabolism Clinics of North America* 28:709–729.
97. Travers ME, McCarthy MI (2011) Type 2 diabetes and obesity: genomics and the clinic. *Hum. Genet* 130:41–58.
98. Zeggini E *et al.* (2007) Replication of genome-wide association signals in UK samples reveals risk loci for type 2 diabetes. *Science* 316:1336–1341.

99. Bonnefond A *et al.* (2010) Molecular diagnosis of neonatal diabetes mellitus using next-generation sequencing of the whole exome. *PLoS ONE* 5:e13630.
100. Ntzani EE, Kavvoura FK (2012) Genetic risk factors for type 2 diabetes: insights from the emerging genomic evidence. *Curr Vasc Pharmacol.* 10(2):147-55.
101. Ridderstråle M, Groop L (2009) Genetic dissection of type 2 diabetes. *Mol Cell Endocrinol.* 297(1-2):10-7.
102. Billings LK, Florez JC. The genetics of type 2 diabetes: what have we learned from GWAS? *Ann N Y Acad Sci.* 2010;1212:59–77.
103. Voight BF, *et al.* Twelve type 2 diabetes susceptibility loci identified through large-scale association analysis. *Nat Genet.* 2010;42:579–89.
104. Zeggini E, Ioannidis JPA (2009) Meta-analysis in genome-wide association studies. *Pharmacogenomics* 10:191–201.
105. Sladek R, *et al.* A genome-wide association study identifies novel risk loci for type 2 diabetes. *Nature.* 2007;445:881–885. Grant SFA *et al.* (2006) Variant of transcription factor 7-like 2 (*TCF7L2*) gene confers risk of type 2 diabetes. *Nat. Genet.* 38:320–323.
106. Grant SFA *et al.* (2006) Variant of transcription factor 7-like 2 (*TCF7L2*) gene confers risk of type 2 diabetes. *Nat. Genet.* 38:320–323.
107. Cauchi S *et al.* (2007) *TCF7L2* is reproducibly associated with type 2 diabetes in various ethnic groups: a global meta-analysis. *J Mol Med (Berl).* 85:777-82.
108. Tong Y *et al.* (2009) Association between *TCF7L2* gene polymorphisms and susceptibility to type 2 diabetes mellitus: a large Human Genome Epidemiology (HuGE) review and meta-analysis. *BMC Med. Genet.* 10:15.
109. Weedon MN (2007) The importance of *TCF7L2*. *Diabet Med.* 24:1062-6. Review.
110. Lyssenko V *et al.* (2007) Mechanisms by which common variants in the *TCF7L2* gene increase risk of type 2 diabetes. *J. Clin. Invest.* 117:2155–2163.
111. Smith U (2006) *TCF7L2* and type 2 diabetes—we WNT to know. *Diabetologia* 50:5–7.
112. Loder M, da S, McDonald A, Rutter G (2008) *TCF7L2* controls insulin gene expression and insulin secretion in mature pancreatic beta-cells. *Biochem Soc Trans* 36:357–359.
113. McCaffery JM *et al.* (2011) *TCF7L2* Polymorphism, Weight Loss and Proinsulin:Insulin Ratio in the Diabetes Prevention Program. *PLoS ONE* 6:e21518.
114. Florez JC *et al.* (2007) A 100K genome-wide association scan for diabetes and related traits in the Framingham Heart Study: replication and integration with other genome-wide datasets. *Diabetes* 56:3063–3074.
115. Papadopoulou S, Edlund H (2005) Attenuated Wnt signaling perturbs pancreatic growth but not pancreatic function. *Diabetes* 54:2844–2851.

116. Yi F, Brubaker P, Jin T (2005) TCF-4 mediates cell type-specific regulation of proglucagon gene expression by beta-catenin and glycogen synthase kinase-3beta. *J Biol Chem* 280:1457–1464.
117. Mortensen HB, Christophersen C (1983) Glucosylation of human haemoglobin a in red blood cells studied in vitro. Kinetics of the formation and dissociation of haemoglobin A1c. *Clin Chim Acta*. 134(3):317-26.
118. Pradhan A (2007) Obesity, metabolic syndrome, and type 2 diabetes: inflammatory basis of glucose metabolic disorders. *Nutr Rev*. 65:152-6. Review.
119. Franklin CS *et al.* (2010) The *TCF7L2* Diabetes Risk Variant is Associated with HbA1C Levels: a Genome-Wide Association Meta-Analysis. *Annals of Human Genetics* 74:471–478.
120. Karns R *et al.* (2011) Replication of genetic variants from genome-wide association studies with metabolic traits in an island population of the Adriatic coast of Croatia. *Eur J Hum Genet*. 19:341-6.
121. Pitkänen E, Kanninen T (1994) Determination of mannose and fructose in human plasma using deuterium labelling and gas chromatography/mass spectrometry. *Biol. Mass Spectrom* 23:590–595.
122. Akazawa S, Metzger BE, Freinkel N (1986) Relationships between glucose and mannose during late gestation in normal pregnancy and pregnancy complicated by diabetes mellitus: concurrent concentrations in maternal plasma and amniotic fluid. *J. Clin. Endocrinol. Metab* 62:984–989.
123. Taguchi T *et al.* (2005) Hepatic glycogen breakdown is implicated in the maintenance of plasma mannose concentration. *Am. J. Physiol. Endocrinol. Metab* 288:E534-40.
124. Kawasaki T, Akanuma H, Yamanouchi T (2002) Increased Fructose Concentrations in Blood and Urine in Patients With Diabetes. *Diabetes Care* 25:353–357.
125. Melzer D *et al.* (2006) Effects of the diabetes linked *TCF7L2* polymorphism in a representative older population. *BMC Med*. 4:34.
126. Halarnkar PP, Blomquist GJ (1989) Comparative aspects of propionate metabolism. *Comparative Biochemistry and Physiology Part B: Comparative Biochemistry* 92:227–231.
127. Adams SH *et al.* (2009) Plasma Acylcarnitine Profiles Suggest Incomplete Long-Chain Fatty Acid  $\hat{1}^2$ -Oxidation and Altered Tricarboxylic Acid Cycle Activity in Type 2 Diabetic African-American Women. *The Journal of Nutrition* 139:1073–1081.
128. Inokuchi T, Imamura K, Nomura K, Nomoto K, Isogai S (1995) Changes in carnitine metabolism with ketone body production in obese glucose-intolerant patients. *Diabetes Res Clin Pract* 30:1–7.
129. Bilous R, Donnelly R (2010) in *Handbook of Diabetes*. (Wiley-Blackwell), pp 22–34.

130. Adams SH (2011) Emerging Perspectives on Essential Amino Acid Metabolism in Obesity and the Insulin-Resistant State. *Advances in Nutrition: An International Review Journal* 2:445–456.
131. Mans AM, DeJoseph MR, Davis DW, Hawkins RA (1987) Regional amino acid transport into brain during diabetes: effect of plasma amino acids. *Am J Physiol.* 253:E575-83.
132. Wang TJ *et al.* (2011) Metabolite profiles and the risk of developing diabetes. *Nat. Med.* 17:448–453.
133. Newgard CB *et al.* (2009) A branched-chain amino acid-related metabolic signature that differentiates obese and lean humans and contributes to insulin resistance. *Cell Metab* 9:311–326.
134. Tai ES *et al.* (2010) Insulin resistance is associated with a metabolic profile of altered protein metabolism in Chinese and Asian-Indian men. *Diabetologia* 53:757–767.
135. Huffman KM *et al.* (2009) Relationships between circulating metabolic intermediates and insulin action in overweight to obese, inactive men and women. *Diabetes Care.* 32:1678-83.
136. Fiehn O *et al.* (2010) Plasma metabolomic profiles reflective of glucose homeostasis in non-diabetic and type 2 diabetic obese African-American women. *PLoS One.* 5(12):e15234.
137. Plaisance EP *et al.* (2011) Dietary Methionine Restriction Increases Fat Oxidation in Obese Adults with Metabolic Syndrome. *Journal of Clinical Endocrinology & Metabolism* 96:E836.
138. Stumvoll M, Perriello G, Meyer C, Gerich J (1999) Role of glutamine in human carbohydrate metabolism in kidney and other tissues. *Kidney Int* 55:778–792.
139. Norton L *et al.* (2011) Chromatin occupancy of transcription factor 7-like 2 (TCF7L2) and its role in hepatic glucose metabolism. *Diabetologia.* 54:3132-42.
140. Wirthensohn G, Guder WG (1986) Renal substrate metabolism. *Physiol Rev.* 66(2):469-97.
141. Marliss EB *et al.* (1971) Muscle and splanchnic glutamine and glutamate metabolism in postabsorptive and starved man. *J Clin Invest.* 50:814-7.
142. Felig P (1975) Amino acid metabolism in man. *Annu Rev Biochem.* 44:933-55.
143. LeRoith D, Taylor SI, Olefsky JM (2004) Diabetes mellitus. A fundamental and clinical text (Lippincott Williams & Wilkins, Philadelphia).
144. Rasmussen-Torvik LJ, Pankow JS, Jacobs DR, Sinaiko AR (2009) Preliminary report: No association between *TCF7L2* rs7903146 and euglycemic-clamp-derived insulin sensitivity in a mixed-age cohort. *Metab. Clin. Exp* 58:1369–1371.
145. Wegner L *et al.* (2008) Impact of *TCF7L2* rs7903146 on insulin secretion and action in young and elderly Danish twins. *J. Clin. Endocrinol. Metab* 93:4013–4019.
146. Schäfer SA *et al.* (2007) Impaired glucagon-like peptide-1-induced insulin secretion in carriers of transcription factor 7-like 2 (*TCF7L2*) gene polymorphisms. *Diabetologia* 50:2443–2450.

147. Mooradian AD (2009) Dyslipidemia in type 2 diabetes mellitus. *Nat Clin Pract Endocrinol Metab* 5:150–159.
148. Kimber CH *et al.* (2007) *TCF7L2* in the Go-DARTS study: evidence for a gene dose effect on both diabetes susceptibility and control of glucose levels. *Diabetologia* 50:1186–1191.
149. Pilgaard K *et al.* (2009) The T allele of rs7903146 *TCF7L2* is associated with impaired insulinotropic action of incretin hormones, reduced 24 h profiles of plasma insulin and glucagon, and increased hepatic glucose production in young healthy men. *Diabetologia* 52:1298–1307.



## PUBLICATIONS AND PRESENTATIONS

Krug S, Kastenmüller G, Stückler F, Rist MJ, Skurk T, Sailer M, Raffler J, Römisch-Margl W, Adamski J, Prehn C, Frank T, Engel KH, Hofmann T, Luy B, Zimmermann R, Moritz F, Schmitt-Kopplin P, Krumsiek J, Kremer W, Huber F, Oeh U, Theis FJ, Szymczak W, Hauner H, Suhre K and Daniel H (2012) The dynamic range of the human metabolome revealed by challenges. *FASEB J* .26 (6): 2607-19

Wahl S, Krug S, Then C, Kirchhofer A, Kastenmüller G, Brand T, Skurk T, Claussnitzer M, Huth C, Heier Margit, Meisinger C, Peters A, Thorand B, Gieger C, Prehn C, Römisch-Margl W, Adamski J, Suhre K, Illig T, Grallert H, Laumen H, Seissler J, Hauner H (2013) Comparative analysis of plasma metabolomics response to metabolic challenge tests in healthy subjects and influence of the FTO obesity risk allele. *Metabolomics* :1573-3882

Petersen AK, Stark K, Musameh MD, Nelson CP, Römisch-Margl W, Kremer W, Raffler J, Krug S, Skurk T, Rist MJ, Daniel H, Hauner H, Adamski J, Tomaszewski M, Döring A, Peters A, Wichmann HE, Kaess BM, Kalbitzer HR, Huber F, Pfahlert V, Samani NJ, Kronenberg F, Dieplinger H, Illig T, Hengstenberg C, Suhre K, Gieger C and Kastenmüller G (2012) Genetic associations with lipoprotein subfractions provide information on their biological nature. *Hum Mol Genet*. 21 (6): 1433-43

Krug S, Skurk T, Rist MJ, Kastenmüller G, Suhre K, Daniel H, Hauner H. The HuMet (Human Metabolome)-study: Analysis of plasma metabolites in healthy males during six standardized metabolic challenges. Abstract/Poster 82. *Metabolomics&More international Symposium, Freising-Weihenstephan, 10–12 March 2010.*

Krug S, Skurk T, Rist MJ, Kastenmüller G, Suhre K, Sonntag D, Scandurra F, Kremer W, Huber F, Daniel H, Hauner H. The HuMet (Human Metabolome)-study: Profiling of plasma metabolites and hormones during an oral lipid tolerance test. Abstract/Poster 29. European Nutrigenomics Organisation (NuGO) week, Glasgow, 31 August- 3 September 2010.

Wahl S, Krug S, Then C, Brand T, Ehlers K, Claussnitzer M, Skurk T, Lechner A, Wichmann H, Huth C, Meisinger C, Prehn C, Stückler F, Kastenmüller G, Adamski J, Suhre K, Illig T, Grallert H, Laumen H, Seissler J, Hauner H. Metabolic characterization of common variants of the *FTO* and *TCF7L2* loci by nutritional challenge tests. Abstract/Poster P13.09. European Human Genetics Conference, Nürnberg, 23-26 June 2012.

Krug S, Zhang Y, Mori TA, Croft KD, Vickers JJ, Langton LK, Whitworth JA (2008) N-Acetylcysteine prevents but does not reverse dexamethasone-induced hypertension. *Clin Exp Pharmacol Physiol.* 35(8):979-81.

# CURRICULUM VITAE

## Personal Details

Name: Susanne Gabriele Krug  
Date of birth: October 4, 1982  
Place of birth: Munich/Germany  
Address: Rappstrasse 20, 20146 Hamburg, Germany  
Phone: + 49 (0) 40 20917007  
Email: krug\_susanne@yahoo.de

## Academic Education

03/2008 until 12/2011: Ph.D. (Dr. rer. nat) at the Department for Nutritional Medicine, Technische Universität München, Germany.  
04/2006 until 11/2007: Master of Science (M.Sc.) in Nutritional Science; Technische Universität München, Germany.  
10/2002 until 07/2005: Bachelor of Science (B.Sc.) in Nutritional Science; Technische Universität München, Germany.

## Work experience

01/2012 to present: Clinical Research Associate on behalf of Novartis Pharma GmbH.  
03/2007 until 08/2007: Research scholar at the John Curtin School of Medical Research, Australian National University, Canberra, Australia.  
07/2006 until 12/2006: Assistant at the Department for Nutritional Medicine; University hospital Rechts-der-Isar, TU München.  
12/2005 until 02/2006: Internship at Institute of Food, Nutrition and Human Health, Massey University, Albany Campus, Auckland, New Zealand.